The Physics of Metals and Metallography, Vol. 76, No. 4, 1993.

THEORY OF METALS

Localized and Itinerant Behavior of Electrons in Metals: II

S. V. Vonsovskii*, M. I. Katsnel'son*, and A. V. Trefilov**

**Institute of Metal Physics, Ural Division, Russian Academy of Sciences, ul. Kovalevskoi 18, Ekaterinburg, 620219 Russia*

***Kurchatov Institute Russian Scientific Center, ploshchad' Kurchatova 1, Moscow, 123182 Russia*

Received May 25, 1993

CONTENTS

"Slow is the life of all deep well-springs: they have to wait for a long time before they know what has gone into their depths."

F.W. Nietzsche, "Thus Spake Zarathustra"

5. STRONGLY CORRELATED *d* SYSTEMS: MOTT INSULATORS AND NARROW-BAND FERROMAGNETS

This chapter examines a range of phenomena related in one way or another to the metal–insulator transition and the properties of Mott insulators. Main emphasis is placed on a description of the approaches based on the atomic representation and many-electron X operators. Detailed consideration is given to ferro- and antiferromagnets with narrow energy bands. Matters that are related to phase separation, high-temperature superconductivity, and low-dimensional systems are briefly touched upon. Compared with the other chapters, the presentation is one of a debate because the issues involved are complicated and rather entangled.

5.1. Mott Insulators Defined: A Historical Overview and the State of the Art

Thus far we have rigorously classified the electronic states into localized and delocalized (itinerant), regarding the former as states of the atomic type and the latter as Bloch states filled by electrons according to the Fermi statistics. Then, Wilson's metal–nonmetal criterion must be satisfied. More specifically, a semiconductor (or insulator) is a material which has only completely filled and empty energy bands, and a metal is a material

which has partially filled bands [1].[1] However, as early as the 1930s, it became known that there were crystals to which the Wilson criterion did not apply. De Boer and Verwey [2] demonstrated that NiO crystals and some other transition-metal oxides were insulators, although, according to their crystalline structure, they must have partially filled bands and be metals. In his unpublished report at a conference in Bristol in 1937, Peierls came up with the view that Wilson's criterion could break down because of the correlations associated with Coulomb interaction [3]. Later, this view was developed by Landau and Zel'dovich [4]. In 1949, Mott [5] clearly formulated the problem of the metal–insulator criterion for compounds of the NiO type, that is, the transition-metal monoxides. Following that, the term "Mott insulators" became a generally adopted one for substances that are nonmetals in violation of Wilson's criterion of the conventional band theory. Actually, the first attempt to define the metal–insulator criterion with allowance for Coulomb interaction (practically equivalent to Mott's reasoning in [5]) had been made by Schubin and Vonsovskii [6 - 9] well before de Boer and Verwey. The first quantitative calculation in the quasiclassical approximation advanced in [6 - 9] was made by Svirskii and Vonsovskii [10] and a more consistent quantum-mechanical calculation by Vonsovskii *et al.* in [11 - 13].

In the 1950s it was realized, however, that the question as to whether or not Wilson's criterion was violated was not so simple as it had appeared previously. The point is that all "Mott insulators" are antiferromagnets and, as Slater demonstrated for the first time in 1951 [14], antiferromagnetic order leads to a further splitting of energy bands – an occurrence that might, generally, account for the nonmetallic nature of NiO, MnO, and other similar substances. The fact that they remain insulators even in the paramagnetic phase (that is, above the Néel temperature T_N) might be attributed to the preservation of local magnetic moments (and, possibly, antiferromagnetic short-range order as well [15]). However, the quantitative calculation undertaken by Terakura *et al.* [16] using the local spin density functional method for the 3*d* metal monoxides demonstrated that Slater's hypothesis was inadequate to resolve the problem. According to the calculation and in contrast to experiment, FeO and CoO in the antiferromagnetic phase turned out to be metals and the energy gap in MnO and NiO was found to be too small; moreover, it tended to diffuse strongly upon transition to the paramagnetic state. Thus, the problem of the violation of Wilson's criterion of the band theory still exists, even if by the band theory one means a present-day approach based on the local spin density functional method and allowing in part for correlation effects (see Ch. 4).

Recent years have seen a surge of interest in the problem of Mott insulators in the wake of the hypothesis (now almost generally accepted) advanced by Anderson [17], who maintains that the "base" compounds for high-temperature superconductivity (such as La_2CuO_4 and $YBa_2Cu_3O_6$) likewise fall in this class of substances.

Thus far, we have not actually explained what Coulomb interaction has to do with the metal-insulator criterion. We will discuss the matter in this chapter. Importantly, it is not limited to the appearance of additional bandgaps in the energy spectrum – the very character of the electronic states and even their occupancy (statistics!) may be drastically changed.

It is convenient to begin our discussion of this range of matters by setting forth the fundamentals of the polar model first advanced by Schubin and Vonsovskii [6 - 9].

5.2. The Atomic Representation and the Polar Model of a Solid

As stressed in the Introduction, the main difficulty in a theoretical study of transition-metal compounds lies in the necessity to take into account both the band effects and the traits of the atomlike behavior of the *d* and *f* states, notably strong interactions within the atom. For the first time, a similar problem arose in the theory of the hydrogen molecule [18]. Consider this very simple example. Each hydrogen atom has an electron in the nondegenerate 1*s* orbital state. The excited states of the atom are rather distant from the 1*s* state in terms of energy, and may be excluded from consideration in the simplest approximation. Then, each atom can exist in any one of four states. Notably, it can have one electron with rightward or leftward spin (such states will be designated as $|\uparrow\rangle$ and $|\downarrow\rangle$ or as $|+\rangle$ and $|-\rangle$), two electrons with antiparallel spins (a $|2\rangle$ state or a "couple"), or no electrons at all (the $|0\rangle$ state or a "hole"). If one proceeds from the condition for a minimal energy of interactions within the atom, one may disregard the so-called polar states, that is, couples and holes. Such an approximation corresponds to the Heitler–London method [18]; it is applicable in the case of a large internuclear distance *R*, when interatomic interactions may be taken to be small and allowed for in terms of the perturbation theory. In the Heitler–London approximation, each hydrogen atom is assumed to have a well-defined spin moment; exchange interaction between them leads to antiparallel order.

This state (called "homopolar") is unfavorable as regards the kinetic energy of electrons, each of which is "locked" on its own atom and, by virtue of the Heisenberg uncertainty relation, has a large mean-square momentum. On neglecting electron–electron interaction, it would be more favorable energetically for both electrons to be uniformly distributed between two atoms. True, each atom would then be occupied with a probability of 1/4 by a couple, and this would increase the energy of electron–electron Coulomb repulsion. With small *R*, one may expect that the "kinetic" factor will tilt the balance in its favor, and the hydrogen molecule can be adequately described in the language of molecular orbitals, whose analogs for the crystal are Bloch states [18]. By the molecular orbital method, not only all of the molecule but also each of its atoms have no definite magnetic moment.

By extending this reasoning to a crystal composed of identical atoms, one may conclude that, with large *R*, metallic conduction is unfeasible in the ground state because each electron will be locked on some atom, thus giving rise to a local magnetic moment. As *R* decreases, the overlap of the wave functions at different sites will increase, until at some critical value R_c the electrons will change to the Bloch state, that is, a metal–insulator transition will occur [5]. Of course, this holds for atoms with unfilled shells (that is, the transition elements). For filled shells, the Heitler–London and molecular-orbital methods are equivalent, and whether one uses the Bloch or the atomic states is a matter of convenience.

The polar model of a solid [6 - 9] is a generalization of the hydrogen molecule theory to the crystal case. One considers a crystal lattice of identical atoms with a number *N* of sites, equal to the number of electrons, each of which can exist in one nondegenerate orbital state (in the single-electron approximation, this corresponds to the tight-binding approximation [1]). The second-quantized Hamiltonian of the system in question takes the form [19]

$$\hat{H} = \sum_{ij\sigma}{}' t_{ij} c_{i\sigma}^{+} c_{i\sigma} + \frac{1}{2}\sum_{\substack{ijkl\\ \sigma\sigma'}} F(ij, kl) c_{i\sigma}^{+} c_{j\sigma'} c_{i\sigma'}^{+} c_{k\sigma}, \quad (5.1)$$

where $c_{i\sigma}^{+}$ and $c_{i\sigma}$ are the operators of the creation and annihilation of an electron on the *i*th site with spin projection $\sigma = \uparrow, \downarrow (+, -)$; t_{ij} and $F(ij, kl)$ are the matrix elements of the one-electron Hamiltonian and the pairwise interaction Hamiltonian, respectively; and $\sum'$ is the sum with $i \neq j$. Here, in (5.1), account will be taken of only the terms that describe the direct Coulomb interaction $F(ii, ii) = U$ between a pair of electrons on the same site (in the couple state), and $F(ij, ij) = V_{ij}$ on different sites

$$\hat{H}_c = U\sum_i n_{i\uparrow} n_{i\downarrow} + \frac{1}{2}\sum_{ij}{}' V_{ij} n_i n_j, \quad (5.2)$$

where $n_{i\sigma} = c_{i\sigma}^{+} c_{i\sigma}$, $n_i = n_{i\uparrow} + n_{i\downarrow}$, and the term that takes care of electron transfer is

$$\hat{H}_t = \sum_{ij\sigma}{}' \{ t_{ij} c_{i\sigma}^{+} c_{j\sigma} + \sum_l F(il, jl) c_{i\sigma}^{+} n_l c_{j\sigma} \}. \quad (5.3)$$

The remaining terms in (5.1) contain the matrix elements $F(ij, kl)$ with two pairs of overlapping functions of different sites ($i \neq j$, $k \neq l$). Such matrix elements are small [19] and, apparently, immaterial with regard to the matters in question.[2]

In the polar model, the state of the system is completely described by the labels of the sites that are in a $|2\rangle$ state, a $|0\rangle$ state, a $|+\rangle$ state, and a $|-\rangle$ state. Taken together, such labels will be designated as *f*, *g*, *h*, and *k*, respectively, and the probability amplitude of such a distribution of electrons will be denoted by *a*(*fghk*). In this representation, the Schrödinger equation takes the form

$$\sum_{f'g'h'k'} \langle f'g'h'k' | \hat{H}_c + \hat{H}_t | fghk \rangle a(f'g'h'k') = Ea(fghk). \quad (5.4)$$

In finding the matrix elements that enter into (5.4), it is convenient to change from the operators $c_{i\sigma}^{+}$ and $c_{i\sigma}$ to Hubbard's *X* operators [20]

$$X_i^{\alpha\beta} = |i\alpha\rangle\langle i\beta|, \quad (5.5)$$

where $\alpha, \beta = 2, +, -, 0$ is the complete set of many-electron states on the *i*th site. Any operator A_i acting on the *i*th site can be written as

$$A_i = \sum_{\alpha\beta} \langle\alpha| A_i |\beta\rangle X_i^{\beta\alpha}. \quad (5.6)$$

By making the operator A_i more specific in terms of the operators $c_{i\sigma}$, one obtains from (5.6)

$$\begin{aligned} c_{i\uparrow} &= X_i^{0+} + X_i^{-2}, \quad c_{i\uparrow}^{+} = X_i^{+0} + X_i^{2-}, \\ c_{i\downarrow} &= X_i^{0-} - X_i^{+2}, \quad c_{i\downarrow}^{+} = X_i^{-0} - X_i^{2+}, \\ n_{i\uparrow} n_{i\downarrow} &= X_i^{22}, \quad n_i = X_i^{22} - X_i^{00} + 1. \end{aligned} \quad (5.7)$$

By virtue of (5.7), the operators (5.2) and (5.3) take the form

$$\begin{aligned} \hat{H}_c &= U\sum_i X_i^{22} \\ &+ \frac{1}{2}\sum_{ij}{}' V_{ij} (X_i^{22} - X_i^{00})(X_j^{22} - X_j^{00}) + \text{const}; \end{aligned} \quad (5.8)$$

$$\begin{aligned} \hat{H}_t = \sum_{ij}{}' \Big[t_{ij} + \sum_l F(il, jl)(n_l - \delta_{il}) \Big] \\ \times \Big[\sum_\sigma (X_i^{2\sigma} X_j^{\sigma 2} - X_j^{0\sigma} X_i^{\sigma 0}) + X_i^{+0} X_j^{-2} - X_i^{-0} X_j^{+2} \\ + X_i^{2-} X_j^{0+} - X_i^{2+} X_j^{0-} \Big], \end{aligned} \quad (5.9)$$

where we took into account the anticommutativity of the operators $X_j^{0\sigma}$ and $X_i^{\sigma 0}$ for $i \neq j$. The matrix elements of the *X* operators on amplitudes *a*(*fghk*) are calculated in a trivial way. Therefore, subject to equations (5.8)

[1] This holds with an odd number of electrons per atom or when the bands overlap with any number of electrons per atom.

[2] One also drops from the Hamiltonian (5.1) all terms with exchange integrals, which are essential when one considers the magnetic properties of the system.

and (5.9) and to the approximations of the Schubin–Vonsovskii equation [6, 9], we obtain

$$\left[E - sU - \frac{1}{2}\sum_{ff'}{}'V_{ff'} - \frac{1}{2}\sum_{gg'}{}'V_{gg'} + \sum_{fg}V_{fg}\right]a(fghk)$$
$$= \sum_{fp}\beta'_{fp}a(T_{fp}|fghk) + \sum_{gp}\beta''_{gp}a(T_{gp}|fghk) \quad (5.10)$$
$$+ \sum_{hk}\gamma_{hk}\,[a(S_{h\to f,k\to g}|fghk) - a(S_{k\to f,h\to g}|fghk)]$$
$$+ \sum_{fg}\gamma_{fg}\,[a(S_{f\to h,g\to k}|fghk) - a(S_{f\to k,g\to h}|fghk)]\,,$$

where s is the number of couples in the state $a(fghk)$, equal to the number of holes; β'_{fp} is the integral of the transfer of a couple f to a simple site p

$$\beta'_{ij} = t_{ij} + \sum_{l\neq i,j}F(il,jl)n_l^{(0)} + 2F(ii,ji), \quad (5.11a)$$

($n_l^{(0)}$ are the occupation numbers of the sites, which remain unchanged upon the transition $i \to j$); β''_{gp} is the integral for the transport of a hole g to a simple site p

$$\beta''_{ij} = -t_{ij} - \sum_{l\neq i,j}F(il,jl)n_l^{(0)}, \quad (5.11b)$$

γ_{fg} and γ_{hk} are the integrals for the transformation of a pair of simple sites to a couple–hole pair and back

$$\gamma_{ij} = t_{ij} + \sum_{l\neq i,j}F(il,jl)n_l^{(0)} + F(ii,ji). \quad (5.11c)$$

The symbol T_{ij} in (5.10) stands for interchanging the labels i and j, and the symbol $S_{i\to j,i'\to j'}$ stands for the substitution of j, j' for i, i'.

The Hubbard model (4.36) is a special case of the polar model: it neglects (i) the interaction between electrons of different sites ($V_{ij} = 0$, $i \neq j$), (ii) the many-electron contribution to the transfer integrals ($\beta'_{ij} = -\beta''_{ij} = \gamma_{ij} = t_{ij}$), and (iii) the exchange integrals.

Ignoring (i) deprives one of the possibility to consider matters associated with charge ordering, but this is apparently not very essential when one takes up phenomena related to magnetism. In any case, it is assumed that Coulomb interaction is shielded by the outer electrons of the atom and is therefore effective only over a short range. The Coulomb-like drop of the V_{ij} integrals at long distances would significantly change the character of the metal–insulator transition (the formation of Wannier–Mott exciton) [3, 1]. Neglecting the many-electron contributions to the transfer integrals (5.11a) - (5.11c) may likewise be important, e.g., when one considers nonphonon mechanisms of superconductivity [21]. The same can be said for ignoring exchange integrals [see Footnote 2 on p. 345 and also later comments in connection with equation (5.15)].

The atomic representation, first introduced in [6], may be generalized to any many-particle system. In general, the states of the latter can be specified in several ways. One is the configurational representation, in which the state vector is written as a wave function dependent on the coordinates of all particles. Another is second quantization, in which case the state vector is specified by giving a set of occupation numbers for the eigenstates of some single-particle operator. Still another way is atomic representation. With it, a many-particle system is divided into blocks. Within each block, the interaction can be accounted for exactly; the interaction between blocks is written on the basis of exact eigenfunctions of each block. How adequate such a description is when one is to define the state of electrons as atomlike or itinerant was discussed earlier.

In the case of narrow bands, where the characteristic energies of the model are such that

$$|\beta'|, |\beta''|, |\gamma| \ll U, V, \quad (5.12)$$

one obtains from (5.10) for the energy of a system

$$E = sU + \frac{1}{2}\sum_{ff'}{}'V_{ff'} + \frac{1}{2}\sum_{gg'}{}'V_{gg'} - \sum_{fg}V_{fg}. \quad (5.13)$$

Let the number of electrons be equal to the number of lattice sites, $N_e = N$. Then, if the interaction between electrons falls off with distance rather rapidly, so that the main contribution to (5.13) comes from the first term, a homopolar state, $s = 0$, will correspond to the energy minimum. If, on the other hand, V is fairly great so that in, for example, the nearest-neighbor approximation

$$U < zV, \quad (5.14)$$

where z is the number of nearest neighbors, then the ground state will correspond to a charge order of the "couple–hole–couple–hole..." type [6] (the maximum polarity state, investigated in detail in [22]). In nature, however, this case occurs very seldom, if at all, and we will not discuss it any longer. If one takes into account second-order perturbations in the transport integrals, then excitations near the homopolar ground state for $N_e = N$ will be described by the effective Heisenberg Hamiltonian with antiferromagnetic exchange (demonstrated for the first time by Bogolyubov [19]). In Hubbard's approximation it takes the form

$$\hat{H}_{ex} = \frac{2}{U}\sum_{ij}{}'|t_{ij}|^2\,(\hat{\mathbf{S}}_i\hat{\mathbf{S}}_j - \frac{1}{4}). \quad (5.15)$$

Thus, for $N_e = N$ and $U \gg W$ (where W is the energy band width) and in accordance with the qualitative reasoning set forth above, we have an antiferromagnetic insulator state. Whether or not the Heisenberg model (5.15) has an antiferromagnetic long-range order depends on the space dimensionality and lattice type, and this poses a very complicated question [23]. Here, when

referring to an "antiferromagnetic insulator," we will mean either long-range or short-range magnetic order.

What happens with an increase in W is a question that has a direct bearing on the nature and character of the Mott transition [5]. It will be discussed in the following sections, and we will give here only the simplest estimates in the quasiclassical Schubin–Vonsovskii approximation [6]. We replace the X operators in (5.8) and (5.9) by c-numbers, which are the numerical functions that characterize the probability of the creation and annihilation of couples, holes, etc. on one site. That is, we put $X_i^{20} \to \Phi_i^*\Psi_i^*$, $X_i^{2+} \to \Phi_i^*\varphi_i$, and $X_i^{0-} \to \Psi_i^*\psi_i$ etc., where Φ_i, Ψ_i, φ_i, and ψ_i are the amplitudes of the annihilation of a couple, a hole, a spin up, or a spin down, respectively, on the ith site. Moreover, all of these events are treated as independent. This corresponds to the determination of energy E from the variational principle

$$E = \min_{|\psi\rangle}(\langle\Psi|\hat{H}|\Psi\rangle/\langle\Psi|\Psi\rangle) \quad (5.16)$$

with a trial function $|\psi\rangle$ of the form

$$|\psi\rangle = \prod_i(\Phi_i^*\,X_i^{20} + \Psi_i^*\,+\varphi_i^*\,X_i^{+0} + \psi_i^*\,X_i^{-0})|\text{vacuum}\rangle, \quad (5.17)$$

which corresponds to the physical significance of the parameters Φ_i, Ψ_i, φ_i, and ψ_i described above. The function (5.17) mixes the "Bose-like" excitations at the site (those proportional to X_i^{20}) with the "Fermi-like" excitations (those proportional to $X_i^{\sigma 0}$). For this reason, it does not possess the necessary permutation properties, nor does it obey even the Pauli exclusion principle. However, it takes care of the classical Coulomb repulsion of electrons in a couple and may in this sense be regarded as an analog of the Hartree (but not the Hartree–Fock) trial function. In estimating the condition for a metal–insulator transition to a very rough approximation, this appears quite acceptable.

The X operators at different sites are either commutative or anticommutative [20]. In factorizing the normalization integral $\langle\psi|\psi\rangle$ with respect to i, however, the anticommutative operators change sign an even number of times. Taking advantage of the property of X operators that

$$X_i^{\alpha\beta}X_i^{\gamma\varepsilon} = \delta_{\beta\gamma}X_i^{\alpha\varepsilon}, \quad (5.18)$$

which stems from the very definition of the X operators by (5.5), we find

$$\langle\psi|\psi\rangle = \prod_i[|\Phi_i|^2 + |\Psi_i|^2 + |\varphi_i|^2 + |\psi_i|^2] = 1. \quad (5.19)$$

We also find that

$$\langle\psi|\hat{H}|\psi\rangle \equiv H(\Phi\Psi\varphi\psi, \Phi^*\Psi^*\varphi^*\psi^*)$$
$$= U\sum_i|\Phi_i|^2 + \frac{1}{2}\sum_{ij}{}'V_{ij}\,(|\Phi_i|^2 - |\Psi_i|^2)\,(|\Phi_j|^2 - |\Psi_i|^2)$$
$$+ \sum_{ij}{}'t_{ij}\,\{(\varphi_i\varphi_j^* + \psi_i\psi_j^*)\,(\Phi_j\Phi_i^* - \Psi_j\Psi_i^*) \quad (5.20)$$
$$+ \frac{1}{2}(\varphi_i\psi_j - \psi_i\varphi_j)\,(\Phi_i^*\,\Psi_j^* - \Psi_i^*\,\Phi_j^*)$$
$$+ \frac{1}{2}(\varphi_i^*\,\psi_j^* - \psi_i^*\,\varphi_j^*)\,(\Phi_i\Psi_j - \Psi_i\Phi_j)\,\}$$

(where, for simplicity, we put $\beta'_{ij} = -\beta''_{ij} = \gamma_{ij} = t_{ij}$).

Equation (5.20), which we just derived, is the same as the quasiclassical Hamiltonian postulated in [6].

Equation (5.20) was minimized by Oertel [24]. We seek the solution of the variational problem in the forms (see [6])

$$\varphi_i = \varphi\exp(i\mathbf{k}_1\mathbf{R}_i), \quad \psi_i = \psi\exp(i\mathbf{k}_2\mathbf{R}_i),$$
$$\Phi_i = \Phi\exp(i\mathbf{k}_3\mathbf{R}_i), \quad \Psi_i = \Psi\exp(i\mathbf{k}_4\mathbf{R}_i), \quad (5.21)$$

where for $N_e = N$, $|\Phi| = |\Psi|$ and the nonferromagnetic case, to which we limit ourselves, $|\varphi| = |\psi| = (1/2 - |\Phi|^2)^{1/2}$. Then, the terms with V_{ij}, which describe the interaction between electrons of different sites, disappear automatically, and we obtain

$$H = UN|\Phi|^2 + N|\Phi|^2\,(\frac{1}{2} - |\Phi|^2)$$
$$\times\,\{t(\mathbf{k}_1 - \mathbf{k}_3) + t(\mathbf{k}_2 - \mathbf{k}_3) - t(\mathbf{k}_1 - \mathbf{k}_4) - t(\mathbf{k}_2 - \mathbf{k}_4)$$
$$+ 2\delta_{\mathbf{k}_1-\mathbf{k}_3,\,\mathbf{k}_4-\mathbf{k}_2}t(\mathbf{k}_1 - \mathbf{k}_3) - 2\delta_{\mathbf{k}_1-\mathbf{k}_4,\,\mathbf{k}_3-\mathbf{k}_2}t(\mathbf{k}_1 - \mathbf{k}_4)\,\}\,, \quad (5.22)$$

where $t(\mathbf{k}) = \frac{1}{N}\sum_{ij}{}'t_{ij}\exp[i\mathbf{k}\,(\mathbf{R}_i - \mathbf{R}_j)]$ is the band energy. The expression in the braces in (5.22), minimized with respect to $\mathbf{k}_1$, $\mathbf{k}_2$, $\mathbf{k}_3$, and $\mathbf{k}_4$ [which depends on the specific dispersion law $t(k)$] is $-\lambda W$, where $W = \max t(\mathbf{k}) - \min t(\mathbf{k})$ is the band width and λ is a numerical factor on the order of unity. Minimizing (5.22) with respect to $|\Phi|^2 = s/N$ yields

$$\frac{s}{N} = \begin{cases} 0, & U > \lambda W/2, \\ \frac{1}{2}(\frac{1}{2} - \frac{U}{\lambda W}), & U < \lambda W/2. \end{cases} \quad (5.23)$$

Because when $N_e = N$ the only charge carriers are couples and holes, then for $U > U_c = \lambda W/2$ the system will be an insulator and for $U < U_c$ it will be a metal with a

number of charge carriers proportional to $[(U - U_c)/U_c]N$ for U tending to U_c.

At first glance, the quasiclassical approximation given by (5.16) and (5.17) may appear unduly simplified.[3] However, the result (5.23) is the same as yielded by some present-day, more sophisticated approaches. For example, a result of the form (5.23) for the average number of couples can, according to [35], be obtained if one represents the X operators in terms of the Fermi and Bose operators acting in some limited space (the auxiliary boson method) and then applies continual integration and the mean-field approximation over boson fields.

The metal–insulator transition itself at $U \approx W$ is described by the above expression. On the other hand, there is, generally, no ground for identifying the number of charge carriers with the number of couples s (which is equal to the number of holes). The point is that couples and holes can be coupled pairwise into zero-charge excitations. It will be shown in the next section that this does happen at sufficiently high U and, at the same time, $s \neq 0$ for no finite U. The existence of coupled (virtual) couples and holes in the insulator phase leads to the antiferromagnetism of Mott insulators. That is what we now proceed to discuss.

5.3. The Slater Picture of an Antiferromagnetic Insulator

As noted in Section 5.1, all "Mott" insulators are antiferromagnets at low temperatures (although many of them remain insulators even in the paramagnetic state). According to Slater's idea [14], this fact, which leads to the appearance of an antiferromagnetic gap in the energy spectrum even in the Hartree–Fock approximation, is enough to explain their insulating nature. Such an approach seems very natural, although how well it fits reality calls for special consideration (see [25] and also Section 5.4). For the time being, we will basically follow the same lines as those in [26] and consider the Slater picture of an antiferromagnetic insulator within the Hubbard model.

The formation of antiferromagnetic order with a wave vector $\boldsymbol{\kappa}$ has as a corollary the fact that the operators $c^+_{\mathbf{k}\uparrow}$ and $c^+_{\mathbf{k}+\boldsymbol{\kappa},\uparrow}$ (where $c^+_{\mathbf{k}\sigma}$ is the operator of the creation of an electron with a quasimomentum $\mathbf{k}$ and spin projection σ) are mixed, and the operators $\alpha^+_{\mathbf{k}}$ and $\beta^+_{\mathbf{k}}$ generate new band states that can be introduced by applying the Bogolyubov transformations

$$\alpha^+_{\mathbf{k}} = u_{\mathbf{k}} c^+_{\mathbf{k}\uparrow} + v_{\mathbf{k}} c^+_{\mathbf{k}+\boldsymbol{\kappa},\downarrow},$$
$$\beta^+_{\mathbf{k}} = -v_{\mathbf{k}} c^+_{\mathbf{k}\uparrow} + u_{\mathbf{k}} c^+_{\mathbf{k}+\boldsymbol{\kappa},\downarrow}, \tag{5.24}$$

$$u^2_{\mathbf{k}} + v^2_{\mathbf{k}} = 1. \tag{5.25}$$

We assume that the energy band generated by the operators $\alpha^+_{\mathbf{k}}$ is completely filled and by the operators $\beta^+_{\mathbf{k}}$ is empty. Then, in the generalized Hartree–Fock approximation [14], the trial function of the ground state will be sought in the form

$$|\Phi\rangle = \prod_{\mathbf{k}} \alpha^+_{\mathbf{k}} |\text{vacuum}\rangle. \tag{5.26}$$

Here, the product is taken over all k of the Brillouin zone; $u_{\mathbf{k}}$ and $v_{\mathbf{k}}$ are variational parameters. We then find the average $\langle\Phi|\hat{H}|\Phi\rangle$ with Hubbard's Hamiltonian (4.36), minimize it with respect to $v_{\mathbf{k}}$ and $u_{\mathbf{k}}$ subject to the auxiliary condition (5.25), and obtain the estimate of the ground-state energy

$$E = \frac{NU}{4}(1 + S^2) + \frac{1}{2}\sum_{\mathbf{k}} \varepsilon_{\boldsymbol{\kappa}}(\mathbf{k}); \tag{5.27}$$

$$\varepsilon_{\boldsymbol{\kappa}}(\mathbf{k}) = [U^2 S^2 + b^2_{\boldsymbol{\kappa}}(\mathbf{k})]^{1/2}, \quad b_{\boldsymbol{\kappa}}(\mathbf{k}) = t(\mathbf{k}+\boldsymbol{\kappa}) - t(\mathbf{k}),$$

where

$$S = \frac{2}{N}\sum_{\mathbf{k}} u_{\mathbf{k}} v_{\mathbf{k}} = 2\langle S^+_{\boldsymbol{\kappa}}\rangle$$

is the sublattice magnetization defined by the equation

$$\frac{U}{N}\sum_{\mathbf{k}} \frac{1}{\varepsilon_{\boldsymbol{\kappa}}(\mathbf{k})} = 1. \tag{5.28}$$

In the limiting case of narrow bands $|t| \ll U$, equations (5.27) and (5.28) yield

$$E = -\frac{1}{4U}\sum_{\mathbf{k}} [t(\mathbf{k}+\boldsymbol{\kappa}) - t(\mathbf{k})]^2. \tag{5.29}$$

In the nearest-neighbor approximation, for the bcc and simple cubic (sc) lattices this gives

$$E = -\frac{Nzt^2}{U}, \tag{5.30}$$

where z is the number of nearest neighbors. As Anderson [27] proved, an exact estimate for the ground-state energy of alternating lattices (that is, those which permit partitioning into two sublattices) in the case of the Heisenberg Hamiltonian (5.15) can be obtained in the form of the inequalities

$$-\frac{N(z+1)t^2}{U} < E_0 < -\frac{Nzt^2}{U}. \tag{5.31}$$

This proves that the estimate (5.30) is quite accurate for high z. Note that the concentration of holes in the limit

[3] Such quasiclassical calculations have been done by many investigators for quite some time. They have yielded different estimates for the parameter λ. For the first time, such an estimate appears to have been proposed by Oertel [24] upon a suggestion from Heisenberg. Later, after Hubbard's works, such calculations were performed within his model (see Ch. 4 in [3]). Within the polar model, this issue was discussed in detail by Svirskii and Vonsovskii [10]. See also the Editor's note to the Russian translation of Mott's book, [3, pp. 329 - 342], and [11 - 13].

of large U can be found by the Hellman–Feynman parameter differentiation theorem [compare with (4.36) and (5.31)]

$$s = \frac{1}{N}\sum_i \langle n_{i\uparrow} n_{i\downarrow}\rangle = \frac{1}{N}\left\langle\frac{\partial\hat{H}}{\partial U}\right\rangle = \frac{1}{N}\frac{\partial E_0}{\partial U} = \frac{\alpha t^2}{U^2}, \tag{5.32}$$

where $z < \alpha < (z+1)$. Thus, contrary to the result given by the quasiclassical approximation, $s \neq 0$ in the insulator phase. This quantity is related to the virtual creation of couple–hole pairs from spin-up–spin-down pairs, as described by the transfer integrals γ_{hk} in the general equations (5.10) of the polar model. However, the generation of couples and holes does not, of course, imply a transition to the metallic state at large U; in such a case, they can only form a coupled zero-charge state. These reasons lie at the basis of the exciton approach to the problem of Mott insulators set forth in [28]. At first glance, it might appear quite different from the Slater picture. Nevertheless, as demonstrated in [26], it yields physically equivalent results. However, the physical picture proposed in [26, 28] enables one to look at the nature of Mott insulators from another angle and might prove useful for further generalizations [26, 29]. For these reasons, it appears beneficial to present the basic idea and results of this approach.

First, we consider the ferromagnetic saturation state $|\Phi_0\rangle$ (all spins down), which is, of course, far from the ground antiferromagnetic state in the Hubbard model, and investigate various paths for its decomposition [28]. As argued in [28], among the states with one spin up

$$|\Phi\rangle = \sum_{ij} a(i,j) c^+_{i\uparrow} c_{j\downarrow} |\Phi_0\rangle, \tag{5.33}$$

there are states both of the exciton type (a superposition of bound couple–hole states and spin-wave states) and of the type corresponding to the independent propagation of a couple and a hole. The "exciton" states correspond to a lower energy at large U; in the two- and one-dimensional cases, this will also be true even at any U. One may therefore assume that in the Hubbard model the ground state is approximated by a condensate of excitons, and in the three-dimensional case at low U by a state corresponding to the creation of unbound couples and holes in large numbers. This metal–nonmetal criterion is in qualitative agreement with the exact solution reported by Lieb and Wu [30]. According to them, in the one-dimensional Hubbard model with $N_e = N$, the ground state is always that of an insulator. Accordingly, Katsnel'son and Irkhin [26] used a ground-state trial function of the form

$$|\Phi\rangle = \left(\sum_{\mathbf{k}} \varphi(\mathbf{k}) c^+_{\mathbf{k}+\boldsymbol{\kappa},\uparrow} c_{\mathbf{k}\downarrow}\right)^{N/2} |\Phi_0\rangle \tag{5.34}$$

(an exciton condensate with a wave vector $\boldsymbol{\kappa}$) and developed a calculation procedure using this function on the basis of the graph enumeration theory [31]. In the thermodynamic limit of N tending to infinity the variational estimate for the ground-state energy with a function of the form (5.34) turned out to be the same as (5.27) and (5.28). Note that, although in the state (5.34) $\langle\Phi|S^{\pm}_{\boldsymbol{\kappa}}|\Phi\rangle$, the function (5.34) describes an antiferromagnetic state owing to the δ-function contributions from $q - \kappa$ in the corresponding paired correlators (for more detail see [32]).

In a straightforward manner, the insulator nature of the state described by a function of the form (5.26) or (5.34) can be demonstrated by calculating the polarizability $\alpha_{ij}(\omega)$ in these states $(i, j) = (x, y, z)$.

In [26], this quantity was calculated in the nonstationary state Hartree–Fock approximation. The Hubbard Hamiltonian $\hat{H}$ from (4.36) was extended to include the term $eF_i\hat{x}_i\cos\omega t$, where F and ω are the strength and frequency of the external electric field, $\hat{x}_i$ is the coordinate operator, and e is the electron charge. The trial function was sought in the form (5.34), with φ dependent on $\mathbf{k}$ and time t from the variational principle

$$\frac{\delta}{\delta\varphi^*(\mathbf{k}, t)} \frac{\langle\Phi|\, i\frac{\partial}{\partial t} - \hat{H} + eF_i\hat{x}_i\cos\omega t\,|\Phi\rangle}{\langle\Phi|\Phi\rangle} = 0. \tag{5.35}$$

Next, the average dipole moment $e\langle\hat{x}_i\rangle = \alpha_{ij}F_j$ was calculated in an approximation linear in F. The result for $\alpha_{ij}(\omega)$ is

$$\alpha_{ij}(\omega) = \frac{e^2(US)^2}{2N\Omega_0} \times \sum_{\mathbf{k}} \frac{\partial b_{\boldsymbol{\kappa}}(\mathbf{k})}{\partial k_i}\frac{\partial b_{\boldsymbol{\kappa}}(\mathbf{k})}{\partial k_j}\frac{1}{\varepsilon^3_{\boldsymbol{\kappa}}(\mathbf{k})[\varepsilon^2_{\boldsymbol{\kappa}}(\mathbf{k}) - (\omega + i\delta)^2]}, \tag{5.36}$$

where Ω_0 is the volume of the unit cell. From equation (5.36) it is seen that the product US takes the form of the direct energy gap, that is, a minimal distance between the states in the filled and empty bands having the same $\mathbf{k}$, ($\mathrm{Im}\,\alpha_{ij}(\omega) \neq 0$ for $\omega > US$). For large U ($U > W$), we have $S \approx 1$, and the gap width is equal to the Coulomb repulsion energy per atom, U, which is in full agreement with the qualitative considerations set forth in Section 5.2. By virtue of (5.32), the number of couples then tends to zero.

For low U, the system remains an antiferromagnetic insulator and does not change to the metallic state if subject to a nesting condition

$$t_{\mathbf{k}+\boldsymbol{\kappa}} = -t_{\mathbf{k}}, \tag{5.37}$$

which holds in the tight-binding and nearest-neighbor approximations for the simple cubic lattice [$\kappa = (\pi, \pi, \pi)$], the bcc lattice [$\kappa = (\pi, \pi, 0)$], a linear chain ($\kappa = \pi$), and some other cases. With antiferromagnetic order, the energy gap in such a case occurs over the entire Fermi surface at once [25, 33], thus lowering the energy of all occupied states and, consequently, the total energy. Similar considerations were first formulated by Peierls [34] when proving the instability of the metallic state in a one-dimensional chain. An expression for the energy

gap can then be readily derived from (5.28). As an example, for a one-dimensional chain it takes the form

$$US = |t| \exp\left(-\frac{2\pi|t|}{U}\right), \qquad (5.38)$$

and differs from the exact solution of Lieb and Wu [30] solely by the preexponential factor. According to this result, the ground state in the one-dimensional Hubbard model considered in the nearest-neighbor approximation and for the number of electrons equal to the number of lattice sites is one characteristic of an insulator for any relative values of U and t.

Thus, the Slater picture of the ground state of an antiferromagnetic insulator in the Hubbard model is quite satisfactory and is in qualitative agreement both with physical considerations in the limit of large U and with the exact solution in the one-dimensional case of small U. Two important questions remain open however: (1) Does this description apply to real systems?, and (2) Why is it that the insulator state is preserved in the paramagnetic phase? They are dealt with in Sections 5.4 and 5.5 that follow.

5.4. The Band-Theoretic Approach to the Problem of Mott Insulators

As noted in Section 5.1, attempts to describe the antiferromagnetic insulator state of 3*d*-metal monoxides from MnO to NiO within the standard band-theoretic approach and the local-spin-density-functional (LSDF) formalism have proved, on the whole, to be not very successful. The findings set forth in Section 5.3 offer an insight into the cause of the failure. As we observed in Section 5.3, the description of the antiferromagnetic insulator state within the Hartree–Fock approximation is quite reasonable. With it, the key factors such as the small number of couples and the formation of an energy gap in the limit of large U are determined by Coulomb effects, rather than by the intra-atomic Hund exchange, which the nondegenerate Hubbard model does not take into account at all. This is best demonstrated by the exciton approach [26] [with a trial function of the form of (5.34)]. With this approach, the antiferromagnetic insulator state is formed as electrons and holes are coupled into "excitons" of a special type [28], that is, as a result of an obvious Coulomb effect.

In the LSDF method, the formation of an antiferromagnetic energy gap is ascribed to the difference between exchange-correlation spin-up and spin-down potentials, that is, to the effects of the Hund-exchange type, as explained in detail in Ch. 4. The standard band-theoretic approach is unable to detect changes in the character of electronic states with increasing U, that is, a transition from the Bloch to the atomic picture (see Section 5.2) because, by definition, it deals with Bloch states.

In contrast to the LSDF method, the Hartree–Fock approximation with a nonlocal exchange potential directly dependent on the state on which it acts allows the possibility of localized states (as demonstrated in [25] with reference to simple examples). Unfortunately, this method is too complicated for use in calculating the electronic structure of real solids (see, however, a recent paper by Massido *et al.* [105]). Of the approaches available at present for describing real Mott insulators, what we see as most promising and fitting is the self-interaction-corrected (SIC) [38] density-functional formalism used by Svane and Gunnarsson [36, 37]. Its rationale may be summed up as follows.

In the Hartree–Fock method, an electron existing in the quantum state $|\nu\rangle$ is not acted upon, as should be, by the contribution to the self-consistent field from this state because the corresponding Hartree and Fock contributions cancel out completely [15]. In the LSDF formalism, the self-consistent potential is determined by the total charge and spin density, including the contribution from the density $|\psi_\nu(\mathbf{r})|^2$ of the $|\nu\rangle$ states. In the SIC density-functional formalism, the corresponding contribution is simply subtracted, and the potential acting on the $|\nu\rangle$ state takes the form [compare with (4.15)]

$$V_{\nu\sigma}^{SIC}(\mathbf{r}) = V_\sigma(n_\uparrow(\mathbf{r}), n_\downarrow(\mathbf{r})) - \frac{1}{2}\int d\mathbf{r}' \frac{|\psi_\nu(\mathbf{r}')|^2}{|\mathbf{r}-\mathbf{r}'|} - V_\uparrow^{xc}(|\psi_\nu(\mathbf{r})|^2, 0), \qquad (5.39)$$

where $|e| = \hbar = m = 1$; V_σ is the self-consistent potential in the LSDF method, including the Hartree and exchange-correlation contributions; and $n_\sigma(\mathbf{r})$ is the total electronic density with spins $\sigma = \uparrow, \downarrow$. The physical significance of the self-interaction corrections [the last two terms in the right-hand side of (5.39), i.e., electrostatic and exchange-correlation] is that they account for the attraction of an electron by the field of its own hole.

Two important things are worthy of note. First, the self-interaction corrections are exactly zero for delocalized (notably, Bloch) states because for them the density $|\psi_\nu(\mathbf{r})|^2$ is "spread" over an infinite volume. If one places the system in a "box" $L \times L \times L$ in size, then, for the itinerant electrons, the density $|\psi_\nu(\mathbf{r})|^2$ at every point $\mathbf{r}$ will be on the order of L^{-3} (and $n(\mathbf{r})$ is finite because it contains the sum L^3 of contributions from the individual states). Then $V^{xc}[|\psi_\nu(\mathbf{r})|^2] \to 0$ will tend to zero for L tending to infinity because $|\psi_\nu(\mathbf{r})|^2$ vanishes at every given point $\mathbf{r}$ and the electrostatic potential [the second term in (5.39)] tends to zero as L^{-1}. Therefore, any solution obtained by the LSDF formalism for the crystal is automatically a solution in the SIC density-functional formalism as well. If, however, the total width of the energy band is sufficiently small (or, equivalently, if the interaction is sufficiently strong), additional (except Bloch) localized solutions can appear, which may be qualitatively interpreted as the bound states of an electron in the field of its own hole. Second, because, by virtue of (5.39), different states are acted upon by different potentials, a single Hamiltonian that would be common to all states is nonexistent, and $\{\psi_\nu(\mathbf{r})\}$ are not the eigenfunctions of one Hermitian operator and are not orthogonal (same as in the exact Hartree–Fock method). Therefore, when one uses the SIC density-functional formalism, one has to handle the problem of

Table 5.1. Energy gaps ΔE (eV) and spin magnetic moments M_0 (μ_B) calculated for transition-metal monoxides [37]

Compound	ΔE			M_0		
	LSD	SIC–LSD	Experiment	LSD	SIC–LSD	Experiment
VO	0	0	0	0	0	0
CrO	0	1.01	–	2.59	3.45 (3.44)	–
MnO	0.8	3.98	3.6 – 3.8	4.39	4.49 (4.49)	4.79 - 4.58
FeO	0	3.07	–	3.42	3.54 (4.55)	3.32
CoO	0	2.81	2.4	2.33	2.53 (3.72)	3.35; 3.8
NiO	0.2	2.54	4.0; 4.3	1.04	1.53 (1.80)	1.64; 1.77; 1.90

Note: LSD stands for calculation in the local spin-density functional approximation; SIC–LSD denotes the self-interaction-corrected local spin-density functional formalism. For experimental data, see the references in [37]. The values of M_0 given in parentheses allow for the orbital contributions. In the case of a discrepancy between different experimental sources, several values are given.

nonorthogonality; failure to take into account the nonorthogonality of the functions $\{\psi_\nu(\mathbf{r})\}$ will significantly affect the end results [36 - 38].

In [36], this formalism was applied to model systems such as a one-dimensional Hubbard chain (in the discrete analog of the LSDF formalism) and a CuO_2 plane (a fragment of the high-temperature semiconductor structure); in [37], it was applied to 3*d*-metal monoxides. As it turned out, the self-interaction corrections enable one to bring the energy of the ground state and the width of the energy gap in the one-dimensional Hubbard model in good agreement with the exact results [30], to ascertain the antiferromagnetic insulating state for the CuO_2 plane in keeping with experimental data (which cannot be done in the usual LSDF formalism), and to improve the description of Mott MeO insulators considerably in comparison with the LSDF formalism (see Table 5.1 borrowed from Svane and Gunnarsson [37]). In quantitative terms, however, a noticeable discrepancy between the theoretical and experimental energy gap width for NiO does remain. Note that, according to Svane and Gunnarsson [37], NiO is not, in the strict sense of the word, a Mott insulator that could be described by the Hubbard model. The point is that the 3*d* states of Ni are significantly hybridized with the 2*p* states of O and that the energy gap is not a purely "intra-site" type; it also involves the *p–d* hybridization at different sites. For VO, the condition for the formation of localized states is not satisfied, all solutions in the SIC DF formalism are the same as Bloch solutions, and VO turns out to be a metal. For all other monoxides under study, the equations of the SIC LSDF formalism have localized solutions, and this corresponds to a transition from the Bloch picture to the atomic representation.

Although it is inapplicable in describing the electronic structure of Mott insulators, the conventional density functional formalism can be useful in, for example, calculating the effective Hubbard parameter U. Such a procedure has been proposed by Anisimov and Gunnarsson [39]. To determine U, one calculates the change in the total energy of the system caused by a change in the occupation number of the *d* orbitals at the selected lattice site, and then applies an appropriate procedure to obtain self-consistency. In keeping with the ideology of the Hubbard model, when doing calculations one "locks out" the hybridization of the *d* states with states of another symmetry and disregards spin polarization. This yields a U on the order of 6 eV for FeO, 7 eV for NiO and CoO, and 10.3 eV for MnO, which is quite reasonable for these systems [40]. Additionally, for the metallic VO and TiO [40] and bcc Fe [39], one similarly obtains $U \simeq 6$ eV, which is an obvious overestimate (with such U, these systems cannot remain metals). This seems to indicate that the Hubbard model is inapplicable in the latter case. Instead, one should use a model with several selected groups of *d* electrons that stands midway between the Hubbard model and the *s–d* exchange model [41].

5.5. Mott Insulators and the Metal–Insulator Transition in the Paramagnetic Phase

As noted in Section 5.1, most Mott insulators, including typical species such as NiO and MnO, remain insulators even in the paramagnetic phase (above the Néel temperature T_N). One should bear in mind, however, that, according to the diffraction analysis of spin-polarized electrons [42], MnO retains a strong short-range antiferromagnetic order over a very wide temperature range. For other 3*d*-metal monoxides, no such evidence is reported. However, one may presume that the situation is the same in their case as well, because they have the same magnetic and crystal structures and, possibly, the same exchange interactions (a case that stands all by itself is CoO, in which orbital degeneracy is observed for every ion; this degeneracy can be removed by the interaction between ions, thus leading to orbital order. This case has been described in detail by Brandow [25]).

A wide temperature range with short-range antiferromagnetic order obviously exists above T_N in quasi-two-dimensional (layered) Mott insulators, such as La_2CuO_4 and $YBa_2Cu_3O_6$. Whether an electronic structure has or does not have a short-range order is a vital issue that deserves a more detailed discussion.

We will first recapitulate some known properties of a two-dimensional Heisenberg insulator (see [43, 44]).

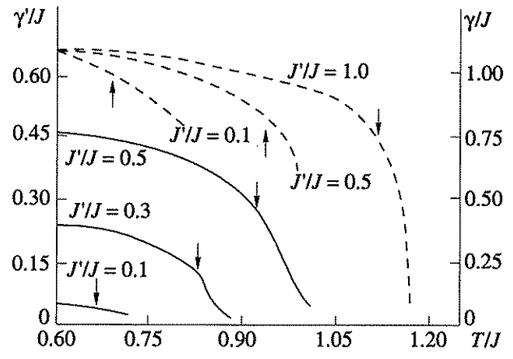

Fig. 5.1. Short-range-order parameters in the layer, γ (dashed curves), and between layers, γ' (solid lines), for different values of interaction parameters between layers, J'/J. The arrows label Néel points [52].

At finite temperatures, the magnetization of the sublattice is zero because of the divergence of longwave fluctuations of the antiferromagnetic order parameter (the Mermin–Wagner theorem [45]). This assertion also holds in the case of anisotropy of the "easy plane" type, where the energy spectrum has a gap at a wave vector $q = 0$. In the latter case, long-range order exists in some finite temperature range $T < T_N$. In an isotropic Heisenberg antiferromagnet, as in an antiferromagnet with anisotropy of the "easy axis" type, $T_N = 0$, although they significantly differ in state at $T \neq 0$. In the anisotropic case of the easy axis type one observes topologically nontrivial defects, such as Kosterlitz–Thouless vortices (see [43, 44]), and a semblance of long-range order associated with their ordering. By contrast, the Heisenberg model displays no long-range order at finite temperatures but has a finite correlation length ξ. This important result was obtained for the first time by Polyakov [46], who used the renormalization-group method. He found that $\xi \sim a\exp(\text{const}(J/T))$ for $T \ll J$, where J is the exchange integral and a is the lattice parameter (this matter is discussed in more detail in [47]). For the wave vectors $q \gtrsim \xi^{-1}$, spin excitations do not "feel" the difference between short- and long-range order. Because of this, and despite the fact that the latter is nonexistent, antiferromagnons with a linear dispersion law (for $q \ll a^{-1}$) exist. Recently, a fairly simple self-consistent spin-wave theory was developed for the two-dimensional Heisenberg antiferromagnet for $T \neq 0$ through the use of Schwinger bosons [48, 49] or the Dyson–Maleev representation [50]. By applying this theory to the effects of electron-spin interaction within the Hubbard and s–d exchange models, Irkhin and Katsnel'son [51] were able to demonstrate that, on the energy scale $|E| \gtrsim Ja/\xi$, the electron spectrum for $T \neq 0$ has the same structure as in the ordered state for $T = 0$, that is, the antiferromagnetic gap is preserved, and electron-magnon scattering appears, as if long-range order exists.

We now consider the antiferromagnetic exchange interaction J' between layers. For $J' \ll J$, the Néel temperature is low in comparison with J and, according to explicit calculations within the self-consistent spin-wave theory [52], its estimate is

$$T_N \sim \frac{J}{\ln(J/J')} \tag{5.40}$$

(the explicit expression is given in [52]), whereas short-range order exists as far as $T \sim J \gg T_N$. As the ratio J/J' increases, the region of developed short-range order decreases, mainly because of the rise in T_N. The degree of short-range order can be described by the parameter γ, which characterizes the tendency of spins at neighboring sites to form a singlet state (a triplet state in the ferromagnetic case). Its temperature dependence, calculated by the nonlinear spin-wave theory, is given in Fig. 5.1 [52], which demonstrates a short-range order region above T_N for $J' \ll J$. For the isotropic case ($J' \approx J$) and a simple cubic lattice, the width of this region decreases to about $10^{-2}T_N$ [52]. It may, however, broaden if one allows for the interaction with the next-nearest neighbors, as this leads to frustrations [53] (that is, a situation where interactions with the nearest and next-nearest neighbors are competing in the sense that they favor the formation of different magnetic structures). One may therefore think that in MnO an important thing is that the cation fcc sublattice (of the NaCl type structure) is partly frustrated or, possibly, a significant exchange interaction takes place with the next-nearest neighbors. Thus, for most known Mott insulators, one has either direct experimental evidence or a theoretical consideration that allows one to speak of a sufficiently strong short-range order above T_N. For this reason, their electronic structure in the paramagnetic phase is apparently close to that of the ground antiferromagnetic state. Nevertheless, the description of Mott insulators in a "deeply paramagnetic" region (that is, where the magnetic moments are completely disordered) is a problem that undoubtedly evokes strong interest in its own right. Indeed, most theoretical works on Mott insulators deal precisely with this case, which we now proceed to discuss. We will place main emphasis on the metal–insulator transition in the wake of a change in the relative magnitude of the energy V and the band width W.

In his pioneer work [54], Hubbard used the two-time Green's functions. Other investigators, who likewise used his model in their research on the metal–insulator transition, have drawn upon a wide range of various theoretical tools, such as the functional integral method [55], a diagram technique for X operators [56], the Schwinger functional derivative formalism [57], variational methods [58 - 60], and the renormalization group in real space [61], to name only a few. Still, the physical picture of the metal–insulator transition remains fuzzy.

Now let us consider the results of Hubbard's approach to the metal–insulator transition and the description of the insulating state in the paramagnetic

phase. In our presentation we will proceed along the lines of Anokhin *et al.* [62]. (In his original papers [54, 63], Hubbard used a different derivation method.) Our task is to calculate the anticommutative retarded Green's function of electron operators [64]

$$G(\mathbf{k}, E) = \left\langle\langle c_{\mathbf{k}\sigma} | c^+_{\mathbf{k}\sigma}\rangle\right\rangle_E = -i\int_0^\infty dt e^{iEt}\left\langle \{c_{\mathbf{k}\sigma}, c^+_{\mathbf{k}\sigma}(t)\}\right\rangle, \quad \mathrm{Im}\, E > 0, \tag{5.41}$$

where $A(t) = \exp(i\hat{H}t)A\exp(-i\hat{H}t)$ is the Heisenberg representation of operators, the French quotes ⟨...⟩ stand for averaging over Gibbs' ensemble, and the braces, for an anticommutator (here and elsewhere, $\hbar = 1$). To take care of Coulomb interaction at a site, we change over to the X-operator representation even in the lowest approximation [see (5.7)]

$$c^+_{\mathbf{k}\sigma} = \sum_i \exp(i\mathbf{k}\mathbf{R}_i)c^+_{i\sigma} = f^+_{\mathbf{k}\sigma} + g^+_{\mathbf{k}\sigma}; \tag{5.42}$$

$$f^+_{\mathbf{k}\sigma} = \sum_i \exp(i\mathbf{k}\mathbf{R}_i)X_i^{\sigma 0}, \quad g^+_{\mathbf{k}\sigma} = \sum_i \exp(i\mathbf{k}\mathbf{R}_i)X_i^{2\sigma}.$$

The operators $f^+_{\mathbf{k}\sigma}$ and $g^+_{\mathbf{k}\sigma}$ describe the motion of a hole and a couple in the crystal, respectively. According to the definition of the X-operators (5.5), the multiplication rules at the ith site take the form

$$X_i^{\alpha\beta}X_i^{\lambda\mu} = \delta_{\beta\lambda}X_i^{\alpha\mu}, \tag{5.43}$$

where X operators of the Fermi type (that is, those changing the number of electrons at the site to 1) at different sites anticommutate and those of the Bose type (that is, changing the number of electrons at a site to 0 or 2) commutate, similarly to Fermi- and Bose-type operators [20]. Using this property, one can calculate the commutators of X operators with the Hamiltonian $\hat{H}$ (4.36) as well as their commutators and anticommutators with one another. This is necessary in order to set up a string of equations of motion for the two-time Green's function

$$E\langle\langle A|B\rangle\rangle_E = \langle\{A, B\}\rangle + \langle\langle [A, H]|B\rangle\rangle_E. \tag{5.44}$$

The Hubbard Hamiltonian $\hat{H}$ for the canonical ensemble of X operators takes the form [see (5.8) and (5.9)]

$$\hat{H} = \hat{H}_t + \hat{H}_c - \mu\sum_i n_i, \tag{5.45}$$

where

$$\hat{H}_t = \sum_{ij} t_{ij}\Big[\sum_\sigma (X_i^{2\sigma}X_j^{\sigma 2} - X_i^{0\sigma}X_j^{\sigma 0}) + X_i^{+0}X_j^{-2} - X_i^{-0}X_j^{+2} + X_i^{2-}X_j^{0+} - X_i^{2+}X_j^{0-}\Big]; \tag{5.46}$$

$$\hat{H}_c = U\sum_i X_i^{22}, \tag{5.47}$$

μ is the chemical potential, and $n_i = X_i^{22} - X_i^{00} + 1$ is the number of species on a site. If one considers an energy band that is half-filled (the number of electrons is equal to the number of sites) and symmetric (the density of states

$$N_0(E) = \sum_{\mathbf{k}} \delta(E - t(\mathbf{k})) \tag{5.48}$$

is an even function of E), then from the symmetry with respect to the replacement of electrons by holes it follows that $\mu = U/2$, irrespective of the model used. Then, in view of (5.47) and (5.7), we obtain

$$\tilde{H}_c = H_c - \mu\sum_i n_i = \frac{U}{2}\sum_i (X_i^{22} + X_i^{00}) + \text{const}, \tag{5.49}$$

that is, the Hamiltonian is written in a symmetric form. It is an easy matter to show from (5.42) and (5.43) that

$$[f_{k\sigma}, \tilde{H}_c] = -\frac{U}{2}f_{k\sigma}; \quad [g_{k\sigma}, \tilde{H}_c] = \frac{U}{2}g_{k\sigma}. \tag{5.50}$$

Thus, the change-over to the X-operators drastically simplifies commutation with the interaction Hamiltonian in (5.44). Unfortunately, the commutators with H_t are rather cumbersome.

In the paramagnetic state, for the anticommutators in (5.44) we have

$$\left\langle\{f_{\mathbf{k}\sigma}, f^+_{\mathbf{k}\sigma}\}\right\rangle = \left\langle X_i^{00}\right\rangle + \left\langle X_i^{\sigma\sigma}\right\rangle = \left\langle X_i^{00}\right\rangle + \frac{1}{2}\sum_\sigma \left\langle X_i^{\sigma\sigma}\right\rangle$$

$$= \frac{1}{2}\left[\left\langle X_i^{22}\right\rangle + \left\langle X_i^{00}\right\rangle + \sum_\sigma \left\langle X_i^{\sigma\sigma}\right\rangle\right] = \frac{1}{2}; \tag{5.51}$$

$$\left\langle\{g_{\mathbf{k}\sigma}, g^+_{\mathbf{k}\sigma}\}\right\rangle = \frac{1}{2},$$

$$\left\langle\{f_{\mathbf{k}\sigma}, g^+_{\mathbf{k}\sigma}\}\right\rangle = \left\langle\{g_{\mathbf{k}\sigma}, f^+_{\mathbf{k}\sigma}\}\right\rangle = 0,$$

where it is taken into account that for $\langle n_i\rangle = 1$, the number of couples is equal to the number of holes: $\left\langle X_i^{22}\right\rangle = \left\langle X_i^{00}\right\rangle$. Then, by splitting the Green's functions (5.41) according to (5.42) and noting (5.50) and (5.51), we can obtain the exact relations

$$G(\mathbf{k}, E) = \left\langle\langle f_{\mathbf{k}\sigma}|c^+_{\mathbf{k}\sigma}\rangle\right\rangle_E + \left\langle\langle g_{\mathbf{k}\sigma}|c^+_{\mathbf{k}\sigma}\rangle\right\rangle_E; \tag{5.52}$$

$$\left\langle\langle f_{\mathbf{k}\sigma}|c^+_{\mathbf{k}\sigma}\rangle\right\rangle_E = \frac{1/2}{E + U/2}[1 + t(\mathbf{k})G(\mathbf{k}, E)] + \frac{1}{E + U/2}\sum_{\mathbf{q}\sigma'} t(\mathbf{q})\left\langle\langle\delta\{f_{\mathbf{k}\sigma}, f^+_{\mathbf{k}\sigma'}\}c_{\mathbf{q}\sigma'}|c^+_{\mathbf{k}\sigma}\rangle\right\rangle_E; \tag{5.53}$$

$$\left\langle\langle g_{\mathbf{k}\sigma}|c^+_{\mathbf{k}\sigma}\rangle\right\rangle_E = \frac{1/2}{E - U/2}[1 + t(\mathbf{k})G(\mathbf{k}, E)] + \frac{1}{E - U/2}\sum_{\mathbf{q}\sigma'} t(\mathbf{q})\left\langle\langle\delta\{g_{\mathbf{k}\sigma}, g^+_{\mathbf{k}\sigma'}\}c_{\mathbf{q}\sigma'}|c^+_{\mathbf{k}\sigma}\rangle\right\rangle_E, \tag{5.54}$$

where $\delta A \equiv A - \langle A \rangle$. Substituting (5.53) and (5.54) in (5.52) and solving the equation formally for $G(\mathbf{k}, E)$ yields

$$G(\mathbf{k}, E) = \frac{E - UL(\mathbf{k}, E)}{E^2 - Et(\mathbf{k}) - U^2/4}, \quad (5.55)$$

where

$$L(\mathbf{k}, E) = \frac{1}{2}\sum_{\mathbf{q}\sigma'} t(\mathbf{q}) \left\langle \left\langle [\delta\{f_{\mathbf{k}\sigma}, f^+_{\mathbf{k}\sigma'}\} - \delta\{g_{\mathbf{k}\sigma}, g^+_{\mathbf{k}\sigma'}\}]\, c_{\mathbf{q}\sigma'} | c^+_{\mathbf{k}\sigma} \right\rangle \right\rangle_E. \quad (5.56)$$

Equation (5.55) is an exact one, but the function $L(\mathbf{k}, E)$ (5.56) entering into (5.55) can be evaluated only approximately. The simplest approximation, in which the string of equations (5.44) is truncated at the first step, that is, for $L(\mathbf{k}, E) = 0$, was attempted by Hubbard in [63]; since then it has come to be known as the Hubbard approximation I. Now, equation (5.55) suggests the following expression for the Green's function:

$$G(\mathbf{k}, E) = \frac{1}{y(E) - t(\mathbf{k})}, \quad y(E) \equiv E - \frac{U^2}{4E}. \quad (5.57)$$

The poles of this function form two bands

$$E_{1,2} = \frac{1}{2}\left[t(\mathbf{k}) \pm \sqrt{t^2(\mathbf{k}) + U^2}\right],$$

which in the limit of large U are split into $\pm U/2$ and are half as wide as in the case $U = 0$. These bands are called the Hubbard subbands, and the gap between them, the Hubbard gap. By virtue of this gap, the system is an insulator, which is correct for $U \gg W$, but in no way correct for small U. Thus, the Hubbard approximation I is unable to describe the transition to the metallic phase. In the limit of large U, however, it is rather easy to grasp the significance of the Hubbard gap.

In the atomic limit, there are configurations with 0, 1, and 2 electrons and with two excitation energies: $E_1 = 0$ (a $|0\rangle \to |1\rangle$ transition) and $E_2 = U$ (a $|1\rangle \to |2\rangle$ transition). Each transition produces an independent energy band of its own. As a matter of record, this picture of the spectrum was given as early as 1934 - 1936 by Schubin and Vonsovskii in [6 - 9] (see also [10] and the Editor's note to the Russian translation of Mott's monograph [3]). It can also be generalized to the degenerate case where an isolated atom has a discrete energy spectrum $E(nLSJ)$ determined by the electron configuration d^n or f^n and by the term LSJ (the orbital, spin, and total angular momentum quantum numbers). Considering the transfer of energy between atoms, every intraatomic transition produces an energy band of its own; that is the Hubbard subband [20].

If one attempts to describe the case of a not too large U and, notably, the transition to the metallic phase, one will have to step outside the approximation defined by (5.57). By setting up an equation of motion for $L(\mathbf{k}, E)$ and decoupling the accompanying more complex Green's functions at the first step, one obtains [62]

$$G^{(2)}(\mathbf{k}, E) = \left[\frac{y(E)}{\Phi(E)} - t(\mathbf{k})\right]^{-1}, \quad (5.58)$$

where

$$\Phi(E) = 1 + \left(\frac{U}{E}\right)^2 \Psi \sum_{\mathbf{q}} \frac{t(\mathbf{q})}{y(E) - t(\mathbf{q})} \equiv 1 + \left(\frac{U}{E}\right)^2 \Psi \sum_{\mathbf{q}} t(\mathbf{q}) G^{(1)}(\mathbf{q}, E), \quad (5.59)$$

and $\Psi = \langle S_i^2 \rangle$ is the mean square of the electron spin at a site (for a nondegenerate model, $\Psi = 3/4$). However, even this approximation does not lead to a metal–insulator transition, because it preserves an energy gap down to small U. The point is that (5.59) contains the "Hubbard I" Green's function (5.57) that needs to be replaced by the sought Green's function $G(\mathbf{q}, E)$ as part of the self-consistency procedure. To achieve self-consistency, we recast (5.58) and (5.59) in an equivalent form

$$G(\mathbf{k}, E) = [F(E) - t(\mathbf{k})]^{-1}; \quad (5.60)$$

$$F(E) = y(E)/\Phi(E) = \frac{y(E) - \lambda(E)}{1 - \lambda(E)/E}, \quad (5.61)$$

where

$$\lambda(E) = y(E) - \left[\Psi \sum_{q} G^{(1)}(\mathbf{q}, E)\right]^{-1} \quad (5.62)$$

and replace $G^{(1)}(\mathbf{q}, E)$ in (5.62) by $G(\mathbf{q}, E)$ from (5.60). This yields an equation for the Green's function $G(\mathbf{q}, E)$, corresponding to what is known as the Hubbard approximation III [54], which is ordinarily written in terms of the self-energy $\Sigma(E)$

$$G(\mathbf{k}, E) = [E - t(\mathbf{k}) - \Sigma(E)]^{-1}; \quad (5.63)$$

$$\Sigma(E) = \frac{U}{16\Psi} \frac{R(E)}{1 + \Sigma(E)R(E) + \left[\frac{1}{4\Psi} - 1\right] ER(E)}; \quad (5.64)$$

$$R(E) = \sum_{\mathbf{k}} G(\mathbf{k}, E) \equiv \int d\varepsilon \frac{N_0(\varepsilon)}{E - \Sigma(E) - \varepsilon}, \quad (5.65)$$

where $N_0(\varepsilon)$ is the trial density of states (5.48). The Hubbard approximation III can be described in terms of the alloy analogy we used in Ch. 4; it is equivalent to considering electron scattering on spin disorder in the coherent potential approximation [65]. According to Anokhin *et al.* [62], the Hubbard approximation III is equivalent to a selective summation of several series of perturbations in terms of the reciprocal number of nearest neighbors, z^{-1}. It can therefore be validated more rigorously for the classical *s–d* exchange model than for the Hubbard model, where such a parameter is nonexistent. This calls for the use of an additional smallness parameter $1/2S$, where S is the localized spin, and $\Psi = 1/4$.

The density of states $N(E) = -(1/\pi)\mathrm{Im}R(E)$ at the Fermi level $E = 0$ will be nonzero only if

$$\alpha(U) = \lim_{E \to 0} F(E) \quad (5.66)$$

is finite. In the Hubbard approximation I, $F(E) = y(E) \approx U^2/4E$ for E tending to zero, so this condition is not satisfied. From (5.63) - (5.65) it is possible to derive a closed equation for $\alpha(U)$ of the form

$$\frac{U^2}{4} = 4\Psi\alpha\left[\alpha - \frac{1}{R_0(\alpha)}\right], \quad (5.67)$$

where

$$R_0(\alpha) = \int d\varepsilon \frac{N_0(\varepsilon)}{\alpha - \varepsilon} \equiv \sum_{\mathbf{k}} \frac{1}{\alpha - t(\mathbf{k})}. \quad (5.68)$$

Consider equation (5.67) for large $|\alpha|$ (as will be shown later, this corresponds to the vicinity of the metal–insulator transition). Then, one may take advantage of the series expansion

$$R_0(\alpha) = \frac{1}{\alpha} + \frac{\mu_2}{\alpha^3} + \frac{\mu_4}{\alpha^5} + \ldots, \quad (5.69)$$

where μ_n is the nth moment of the bare density of states $N_0(\varepsilon)$ ($N_0(\varepsilon) = N_0(-\varepsilon)$). By substituting (5.69) in (5.67), we find that, with the critical $U = U_c$, where

$$U_c = 4(\Psi\mu_2)^{1/2}, \quad (5.70)$$

the quantity $|\alpha|$ also goes to infinity, such that

$$\alpha(U \to U_c) \approx \left[\frac{2(\mu_4 - \mu_2^2)}{U_c(U - U_c)}\right]^{1/2}. \quad (5.71)$$

We will now show that $U = U_c$ is the point of the metal–insulator transition. Indeed, for $U > U_c$, $\alpha(U)$ is real and large. Then, $N(0) = N_0(\alpha) \equiv 0$ because α lies outside the bare energy band. For $U < U_c$, $\alpha(U)$ is purely imaginary, and

$$N(0) \approx \frac{1}{\pi|\alpha|} \sim (U - U_c)^{1/2}, \quad (5.72)$$

which corresponds to a metallic phase. However, this "metallic" phase is very unusual because its electronic states are strongly damped and it has no well-defined Fermi surface. A more detailed analysis of the electronic spectrum in this approximation shows that the energy gap for U tending to $U_c + 0$ varies as $(U_c - U)^{3/2}$ [54], and the thermodynamic potential has a singularity of the form $|\alpha|^{7/2}$ [56, 62] at the transition point. This implies that in the Hubbard approximation III the metal–insulator transition is a $3^1/_2$ and not a $2^1/_2$ transition, as would be natural to expect in the conventional two-band model. Apart from the unanswered question about the transition to the Fermi liquid state with zero damping at the Fermi surface as U decreases, the Hubbard approximation III poses problems associated with the calculation of thermodynamic properties. This has given ground for criticizing it more than once [57, 62, 66]. However, a more satisfactory approximation that would be free from all of these drawbacks has not yet been proposed. True, Edwards and Hertz [66] have made an attempt to account for the effects of spin dynamics through some simple approximations. In their model, there is a well-defined Fermi surface up to $U = U_{c1}$. Then, as U increases in the range $U_{c1} < U < U_{c2}$, a metallic phase is formed with finite damping at the Fermi level, and finally an energy gap appears at $U > U_{c2}$. However, it is difficult to say at present how realistic this sophisticated picture of the transition is.

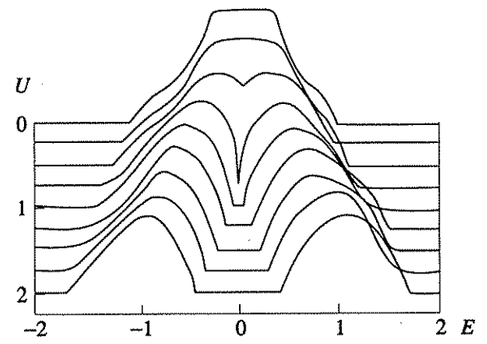

Fig. 5.2. Densities of electronic states in the Hubbard approximation III for a simple cubic lattice with different values of U. The half-width of the conduction band for $U = 0$ is unity [62].

To illustrate the evolution of the energy spectrum in the Hubbard approximation III with changes in U, Fig. 5.2 gives values of $N(\varepsilon)$ calculated for a simple cubic lattice [62].

Among the other approaches used to describe the paramagnetic phase in the Hubbard model, the one worthy of special mention is the variational approach of Gutzwiller [58], which still evokes strong interest (see [59]). Gutzwiller proposed a trial function of the form

$$|\Psi\rangle = \prod_i [1 - (1 - \eta) n_{i\uparrow} n_{i\downarrow}] |\Psi_0\rangle, \quad (5.73)$$

where $|\Psi_0\rangle$ is the Slater determinant describing the state of noninteracting electrons. The parameter η describes the tendency of electrons to form couples under a strong Coulomb repulsion U on one site. For η tending to unity, $|\Psi\rangle = |\Psi_0\rangle$. For $\eta = 0$, no couples exist in the state (5.73), and this is another way of saying that a homopolar state sets in. In the simplest approximation [58], minimization of the average energy in the state (5.73) with respect to η leads to the same result (5.23) for the number of charge carriers as the quasiclassical approximation. (Gutzwiller's variational method was applied to the metal–insulator transition by Brinkman and Rice [67].) The method received further development in studies by Chao and Berggren [68], Ogawa and Kanda [69], and Takano and Okiji [70].

In contrast to the quasiclassical approximation, Gutzwiller's theory takes into account the Pauli exclusion principle explicitly and can be brought in accor-

dance with the Fermi liquid theory (see [59]). Generally, it probably gives a fairly accurate description of the metallic phase. Interestingly, the single-particle distribution function $n_{\mathbf{k}}$ is, according to Gutzwiller [58], a function of the form

$$n_{\mathbf{k}} = \begin{cases} a_1, & \varepsilon_{\mathbf{k}} < \mu, \\ a_2, & \varepsilon_{\mathbf{k}} > \mu, \end{cases} \tag{5.74}$$

where $\varepsilon_{\mathbf{k}}$ is the energy of a quasiparticle with a quasimomentum $\mathbf{k}$, and μ is the chemical potential. The jump $Z = a_1 - a_2$ decreases linearly to zero as U tends to U_c. Because the effective mass m^* of a quasiparticle is inversely proportional to Z [71], one should expect, in keeping with the Gutzwiller theory, that m^* and, consequently, electronic heat capacity and paramagnetic susceptibility will diverge at the metal–insulator transition point [67].

Note further that the result (5.23) for the number of charge carriers can be derived phenomenologically, if one regards Z as an "order parameter" in the spirit of Landau's theory and recalls that $s \sim Z$ [72].

The major shortcomings of the formalisms just discussed are that they are unable to describe the insulator phase (notably, its antiferromagnetism) and contradict the exact solution derived by Lieb and Wu [30]. According to the latter, in the one-dimensional Hubbard model in the nearest-neighbor approximation, the ground state is always an insulating one.

Still, Gutzwiller's variational method gives an estimate of the ground-state energy for small U that is closer to the exact one [59] than the Hartree–Fock state (5.25) or, equivalently, (5.34). It must be stressed, however, that the results in question were obtained subject to some additional approximations in comparison with the trial function (5.73). Generally, its use involves rather sophisticated computational schemes, which are now becoming more popular (as are the exact solution of the Hubbard model for small clusters and some other numerical techniques).

The very multitude of ideas and techniques involved in the problem of Mott insulators and the metal–insulator transition is evidence of its complexity. As usual, one runs into special difficulties with the intermediate values of U and W. A significantly greater headway can be made in the case of the strongest correlation $U \gg W$ for $N_e \neq N$ (for $N_e = N$, it reduces to the problem of the Heisenberg antiferromagnet, which will not be discussed here).

We now proceed to discuss the strong correlation case.

5.6. Electronic States and Magnetism in Strongly Correlated Systems

5.6.1. A Saturated Ferromagnet at Low Temperatures. Consider the case of narrow bands $W \lesssim U$ where, as noted in Section 5.5, the structure of the energy spectrum is determined by the formation of Hubbard subbands and differs qualitatively from that of the spectrum of the normal Fermi liquid. Thus, to one value of a quasimomentum there correspond *one* value of the energy of bare particles and *two* quasiparticle energies differing by the Hubbard gap [see, for example, (5.58)]. This obviously violates the principal postulate of Landau's theory that there must be a mutual one-to-one correspondence between the states of particles and quasiparticles. This implies the violation of other important points of the Fermi liquid theory, such as the Landau–Luttinger theorem on the invariance of the volume of the Fermi surface. Indeed, when the number of electrons is the same as the number of lattice sites, $N_e = N$, the Fermi surface volume for the bare particles is half the volume of the Brillouin zone, Ω_{BZ}, owing to the twofold degeneracy in terms of spin. On the contrary, with large U all states in the lower Hubbard band with any $\mathbf{k}$ are filled, and the volume of the "Fermi surface" separating the filled and empty states is thus Ω_{BZ}. One may therefore expect that, in the case of $N_e \neq N$ as well, the properties of a many-electron system at sufficiently large U will qualitatively differ from those of the normal Fermi liquid. Those are what we will call strongly correlated systems. If $N_e \neq N$, that is, if there are partially filled Hubbard subbands, the substance will be a metal but possibly with properties different from those of ordinary metals. One may class among such systems the heavily doped Mott insulators, including high-temperature superconductors $La_{2-x}Sr_xCuO_4$ and $YBa_2Cu_3O_{6+x}$ [23], some transition-metal oxides such as the metallic ferromagnet CrO_2 [3], the solid solutions $Fe_{1-x}Co_xS_2$ with a pyrite structure [74], etc. Many properties of these systems can be qualitatively interpreted in a model with infinitely large Coulomb repulsion, $U = \infty$. For definiteness, we will consider the case of charge carriers in the upper Hubbard subband ($N_e > N$). Then the condition $U \to \infty$ will signify the exclusion of couple and hole creation. In such a case, the Hamiltonian $\hat{H}_c$ (5.47) need not be taken into account explicitly, and the transfer Hamiltonian $\hat{H}_t$ (5.46) will take the form

$$\hat{H}_t = \sum_{\mathbf{k},\sigma} t(\mathbf{k}) X^{2\sigma}_{-\mathbf{k}} X^{\sigma 2}_{\mathbf{k}} = \sum_{ij,\sigma} t_{ij} X^{2\sigma}_i X^{\sigma 2}_j, \tag{5.75}$$

where $X^{2\sigma}_{\mathbf{k}}$ are the Fourier transforms of the operators $X^{2\sigma}_i$ (5.5). The remaining contributions to the kinetic energy are eliminated by the exclusion of couple–hole pair creation.

Despite its apparent simplicity, the Hamiltonian (5.75) is rather difficult to analyze because of the complicated commutation relations between the X operators.

We begin by reference to the case of a low concentration of couples

$$c = \frac{N_e - N}{N} \ll 1. \tag{5.76}$$

In his fundamental work, Nagaoka [75] has rigorously proved that, for some structures, notably bcc and sc lattices in the nearest-neighbor approximation, the ground state for $N_e = N \pm 1$ is ferromagnetic and saturated (that

is, with a maximally total spin). Rigorous as it is, Nagaoka's proof does not allow one to make any definitive assertion about the state of the system in the thermodynamic limit of N tending to infinity. For one thing, the difference in energy between the ferromagnetic and nonmagnetic states may generally be small in terms of $1/N$. For another, and more importantly, Nagaoka's approach tells very little about the spectrum of electron and spin excitations. Therefore, it would be a good plan to supplement it with research on the stability of the saturated ferromagnetic state, from the outset oriented toward the thermodynamic limit but using the parameter (5.76). This task has been achieved by Irkhin and Katsnel'son [76] through the use of two-time Green's functions (see Section 5.5). At the same time, they have received nontrivial results on the structure of the energy spectrum of the "Nagaoka ferromagnet."

We will now set forth a corresponding approach. It would enable one to investigate the electron and phonon spectra in this state and it seems rather instructive in that it gives insight into the unusual character of X operators compared to Fermi and Bose operators.

We begin by calculating the Green's function

$$G_-(\mathbf{k}, E) = \left\langle\left\langle X^{+2}_{\mathbf{k}} \middle| X^{2+}_{-\mathbf{k}}\right\rangle\right\rangle_E, \tag{5.77}$$

which characterizes the spectrum and state of charge carriers with spin down (that is, against the magnetization).

Using the lattice-site representation, we calculate the commutator required to set up the string of equations of motion (5.44) with the Hamiltonian (5.75)

$$\left[X^{+2}_l, \sum_\sigma X^{2\sigma}_i X^{\sigma 2}_j\right] = \delta_{il} \sum_\sigma \left(X^{+\sigma}_i - \delta_{\sigma+} X^{22}_i\right) X^{\sigma 2}_j \tag{5.78}$$
$$\approx \delta_{il}\left[X^{+-}_i X^{-2}_j + \left(1 - X^{--}_i\right) X^{+2}_j\right].$$

Here, we used the rules of multiplication (5.43) (according to which the terms with $j = l$ do not contribute, as can readily be seen, to the commutator) and the condition of completeness

$$X^{++}_i + X^{--}_i + X^{22}_i = 1 \tag{5.79}$$

(the exclusion of lattice sites from the $|0\rangle$ state stems from the fact that the creation of holes must be accompanied by the appearance of additional couples, but this cannot happen with U tending to infinity). Moreover, we neglected, by virtue of (5.76), the terms containing X^{22}_i (the gas approximation). Now we will set up the first equations of the set (5.44) for the Green's function (5.77). For this purpose, we take the Fourier transform of (5.78) and transpose the term with unity from the right-hand side of (5.78) to its left-hand side. As a result, we obtain the first equation

$$[E - t(\mathbf{k})]\, G_-(\mathbf{k}, E)$$
$$= \alpha + \sum_{\mathbf{q}} t(\mathbf{k} - \mathbf{q}) \left\langle\left\langle X^{+-}_{\mathbf{q}} X^{-2}_{\mathbf{k}-\mathbf{q}} - X^{--}_{\mathbf{k}-\mathbf{q}} X^{+2}_{\mathbf{k}-\mathbf{q}} \middle| X^{+2}_{\mathbf{k}}\right\rangle\right\rangle_E, \tag{5.80}$$

where

$$\alpha = \left\langle X^{++} + X^{22}\right\rangle = 1 - \left\langle X^{--}\right\rangle. \tag{5.81}$$

At $T = 0$ K, the parameter α in the saturated ferromagnetic state will be equal to unity. Next, we use the identities

$$X^{-2}_{\mathbf{k}-\mathbf{q}} = \sum_{\mathbf{p}} X^{-+}_{-\mathbf{p}} X^{+2}_{\mathbf{k}+\mathbf{p}-\mathbf{q}}, \quad X^{--}_{\mathbf{q}} = \sum_{\mathbf{p}} X^{-+}_{\mathbf{p}} X^{+-}_{\mathbf{q}+\mathbf{p}}, \tag{5.82}$$

that are obtained according to the multiplication rules (5.43) by applying the Fourier transformation (which converts a product to a convolution), and insert them in (5.80). Now we reduce all the resultant Green's functions to the "normal" form, in which all X^{--} stand to the left of all X^{+-}. For example,

$$X^{+-}_{\mathbf{p}} X^{-+}_{\mathbf{q}} = X^{-+}_{\mathbf{q}} X^{+-}_{\mathbf{p}} + X^{++}_{\mathbf{p}+\mathbf{q}} - X^{--}_{\mathbf{p}+\mathbf{q}}$$
$$= X^{-+}_{\mathbf{q}} X^{+-}_{\mathbf{p}} + \delta_{\mathbf{pq}} - X^{22}_{\mathbf{p}+\mathbf{q}} - 2X^{--}_{\mathbf{p}+\mathbf{q}}, \tag{5.83}$$

where we used the condition of completeness (5.79). Next, we consider only the terms of order zero with respect to the number of couples (that is, we discard all Green's functions containing the X^{22} operators) and the terms of the first order with respect to the number of spin departures (magnons)

$$N_{\mathbf{p}} = \left\langle X^{-+}_{-\mathbf{p}} X^{+-}_{\mathbf{p}}\right\rangle. \tag{5.84}$$

Note that

$$\sum_{\mathbf{p}} N_{\mathbf{p}} = \left\langle X^{-+}_i X^{+-}_i\right\rangle = \left\langle X^{--}_i\right\rangle = 1 - \alpha, \tag{5.85}$$

which does prove the smallness of $N_{\mathbf{p}}$ near the saturated ferromagnetic state. Then, subject to the approximations involved, equation (5.80) takes the form

$$[E - t(\mathbf{k})]\, G_-(\mathbf{k}, E)$$
$$= \alpha + \sum_{\mathbf{qp}} [t(\mathbf{k} - \mathbf{q}) - t(\mathbf{k} - \mathbf{q} + \mathbf{p})]\, L(\mathbf{q}|\, \mathbf{kp}E), \tag{5.86}$$

where

$$L(\mathbf{q}|\, \mathbf{kp}E) = \left\langle\left\langle X^{-+}_{-\mathbf{p}} X^{+-}_{\mathbf{q}} X^{+2}_{\mathbf{k}-\mathbf{q}+\mathbf{p}} \middle| X^{2+}_{-\mathbf{k}}\right\rangle\right\rangle_E. \tag{5.87}$$

Owing to the general form of equation (5.44) and the Hamiltonian (5.75), the equation of motion for the function L can be written as

$$[E - t(\mathbf{k} - \mathbf{q} + \mathbf{p})]\, L(\mathbf{q}|\, \mathbf{kp}E)$$
$$= \left\langle X^{-+}_{-\mathbf{p}} X^{+-}_{\mathbf{q}} X^{++}_{\mathbf{p}-\mathbf{q}}\right\rangle + \sum_{\mathbf{r}} t(\mathbf{k} + \mathbf{p} - \mathbf{q} - \mathbf{r})$$
$$\times \left\langle\left\langle X^{-+}_{-\mathbf{p}} X^{+-}_{\mathbf{q}} \left(X^{+-}_{\mathbf{r}} X^{-2}_{\mathbf{k}+\mathbf{p}-\mathbf{q}-\mathbf{r}}\right) \middle| X^{2+}_{-\mathbf{k}}\right\rangle\right\rangle_E. \tag{5.88}$$

The Green's function in (5.88) can be simplified owing to the smallness of $N_{\mathbf{p}}$. For example, in view of (5.18), we have

$$X^{+-}_{\mathbf{q}} X^{--}_{\mathbf{r}} = \left[X^{+-}_{\mathbf{q}}, X^{--}_{\mathbf{r}}\right] + X^{--}_{\mathbf{r}} X^{+-}_{\mathbf{q}}$$
$$= X^{+-}_{\mathbf{q}+\mathbf{r}} + X^{--}_{\mathbf{r}} X^{+-}_{\mathbf{q}} \approx X^{+-}_{\mathbf{q}+\mathbf{r}}, \tag{5.89}$$

because, even alone, the operator $X^{-+}_{\mathbf{p}}$ in (5.88) leads to the first-order smallness in $N_{\mathbf{p}}$, and we may neglect the

X_r^{--} immediately following the X_p^{++}. (Note that such estimates can be made solely for operators in normal form!) We can write out the X^{-2} operator in (5.88) according to (5.82), then reduce the corresponding product to the normal form, and use a simplification of the type (5.89). A similar procedure can be applied to the average in (5.88). As a final result, we obtain a closed integral equation for the function L

$$[E - t(\mathbf{k}-\mathbf{q}+\mathbf{p})]\, L(\mathbf{q}|\,\mathbf{kp}E) = N_\mathbf{p}(\delta_{\mathbf{pq}} - 1) + \sum_\mathbf{r} [t(\mathbf{k}+\mathbf{p}-\mathbf{q}-\mathbf{r}) - t(\mathbf{k}+\mathbf{p}-\mathbf{r})]\, L(\mathbf{r}|\,\mathbf{kp}E). \tag{5.90}$$

It is convenient to introduce the function

$$\varphi(\mathbf{q}|\,\mathbf{kp}E) = \frac{1}{[E - t(\mathbf{k})]}\frac{1}{N_\mathbf{p}} L(\mathbf{k}+\mathbf{p}-\mathbf{q}|\,\mathbf{kp}E), \tag{5.91}$$

satisfying, by virtue of (5.90), the integral equation

$$\varphi(\mathbf{q}|\,\mathbf{kp}E) = \delta_{\mathbf{kq}} - \frac{E - t(\mathbf{k})}{E - t(\mathbf{q})} + \frac{1}{E - t(\mathbf{q})}\sum_\mathbf{r} [t(\mathbf{k}+\mathbf{p}-\mathbf{q}-\mathbf{r}) - t(\mathbf{r})]\, \varphi(\mathbf{q}|\,\mathbf{kp}E). \tag{5.92}$$

In view of (5.86) and (5.91), the first two terms of the series expansion of $G_-(\mathbf{k}, E)$ in terms of $N_\mathbf{p}$ take the form

$$G_-(\mathbf{k}, E) = \frac{\alpha}{E - t(\mathbf{k})}\left[1 + \frac{1}{E - t(\mathbf{k})}\Sigma(\mathbf{k}, E)\right], \tag{5.93}$$

where

$$\Sigma(\mathbf{k}, E) = \sum_\mathbf{pq} N_\mathbf{p}\, [t(\mathbf{q}-\mathbf{p}) - t(\mathbf{q})]\, \varphi(\mathbf{q}|\,\mathbf{kp}E). \tag{5.94}$$

Using Dyson's equation for the function $G_-(\mathbf{k}, E)$

$$G_-(\mathbf{k}, E) = \frac{\alpha}{E - t(\mathbf{k}) - \Sigma(\mathbf{k}, E)} \tag{5.95}$$

and comparing (5.95) with (5.93), we see that $\Sigma(\mathbf{k}, E)$ must be the same in these equations. Thus, (5.94) yields an expression for the self-energy of an electron with spin down. This expression is exact in the linear approximation with respect to $N_\mathbf{p}$ and in the zero approximation with respect to the concentration c of couples (or holes).

For $T = 0$ K (and also $\langle X^{--}\rangle = 0$ and $\alpha = 1$), equation (5.95) implies

$$G_-(\mathbf{k}, E) = [E - t(\mathbf{k})]^{-1}, \tag{5.96}$$

that is, charge carriers with spin down move as free particles. Therefore, their distribution function $f_k = \langle X_{-\mathbf{k}}^{2+} X_\mathbf{k}^{+2}\rangle$ at $T = 0$ K is the same as the Fermi function $f(t(\mathbf{k}))$. To find corrections to the electronic spectrum at finite temperatures, one needs to solve the integral equation (5.94). For an sc lattice in the nearest-neighbor approximation, this can be done exactly, because its kernel is degenerate [76]. Furthermore, one needs an expression for $N_\mathbf{p}$, at least for small $\mathbf{p}$, which alone are important at low temperatures. Such an expression will be derived later in this same section by calculating the spin (magnon) Green's function. If one wishes to evaluate the latter, one needs to know the electronic spectrum. The general form of $N_\mathbf{p}$ for small $\mathbf{p}$ may be determined without making any of the calculations to be done later. From phenomenological considerations and on neglecting relativistic interactions with any model of the ferromagnet, we have for the energy of a magnon

$$\omega_\mathbf{p} = Dp^2, \quad p \ll a^{-1}, \tag{5.97}$$

(a is the lattice parameter) and

$$N_\mathbf{p} = (\exp\frac{\omega_\mathbf{p}}{T} - 1)^{-1}, \tag{5.98}$$

where D is the spin stiffness constant [77]. An explicit expression for D in the model in question will be derived later. Then, for the temperature dependence of the conduction band bottom ($\mathbf{k} = 0$), we obtain [76]

$$\Delta t = t_{\mathbf{k}=0}(T) - t_{\mathbf{k}=0}(T=0) = \kappa\frac{3\zeta(5/2)\Omega_0}{32\pi^{3/2}m^*}\left(\frac{T}{D}\right)^{5/2}, \tag{5.99}$$

where ζ is the zeta function, Ω_0 is the volume of the unit cell, m^* is the effective mass of conduction electrons at the bottom of the conduction band, and κ is a numerical factor approximately equal to 0.656 for the sc lattice. For $k \ll (T/D)^{1/2}$ [76], the damping of electronic states near the band bottom is

$$\gamma_k = \kappa^2\frac{15\zeta(7/2)\Omega_0}{256\pi^{3/2}m^*}k\,(\frac{T}{D})^{7/2}. \tag{5.100}$$

For thermal electrons [$k \sim (m^*T)^{1/2}$], it is proportional to T^4 and is small at low temperatures.

An entirely different picture of the spectrum emerges for the electronic states with spin up. In the language of the polar model, they are associated with the transition of a couple to a "simple" site with spin down and are described by the Green's function

$$G_+(\mathbf{k}, E) = \langle\langle X_\mathbf{k}^{-2} | X_{-\mathbf{k}}^{2-}\rangle\rangle_E. \tag{5.101}$$

In the ground state, no sites exist in the $|-\rangle$ state, and, it would seem that such states should not exist at all. But the identity

$$X_i^{2\sigma}X_i^{\sigma 2} = X_i^{22} \tag{5.102}$$

[see (5.43)] implies the sum rule

$$\sum_\mathbf{k}\langle X_{-\mathbf{k}}^{2-}X_\mathbf{k}^{-2}\rangle = \sum_\mathbf{k}\langle X_{-\mathbf{k}}^{2+}X_\mathbf{k}^{+2}\rangle = c, \tag{5.103}$$

whereby the complete filling must be the same for electronic states with spins up and down. This alone indicates that the Green's function $G_+(\mathbf{k}, E)$ must show a rather unusual behavior. In evaluating it, it is convenient to use the relation (5.82) and to write the function as

$$G_+(\mathbf{k}, E) = \sum_\mathbf{q}\langle\langle X_{-\mathbf{q}}^{++}X_{\mathbf{k}+\mathbf{q}}^{+2} | X_{-\mathbf{k}}^{2-}\rangle\rangle_E. \tag{5.104}$$

Using the equation of motion (5.44), evaluating and transforming the commutator similar to the method used in evaluating $G_-(\mathbf{k}, E)$, we have

$$[E - t(\mathbf{k}+\mathbf{q})]\langle\langle X_{-\mathbf{q}}^{++}X_{\mathbf{k}+\mathbf{q}}^{+2} | X_{-\mathbf{k}}^{2-}\rangle\rangle_E = N_\mathbf{q} + f_{\mathbf{k}+\mathbf{q}}. \tag{5.105}$$

Here, we retained the small Fermi distribution function $f_{\mathbf{k}+\mathbf{q}} = \langle X_{\mathbf{k}+\mathbf{q}}^{2+}X_{\mathbf{k}+\mathbf{q}}^{+2}\rangle$ because it is comparable with the likewise small quantity $N_\mathbf{q}$. Substituting (5.105) in (5.104) yields

$$G_+(\mathbf{k}, E) = \sum_\mathbf{q}\frac{N_\mathbf{q} + f_{\mathbf{k}+\mathbf{q}}}{E - t(\mathbf{k}+\mathbf{q})}. \tag{5.106}$$

As a function of the complex variable E, the Green's function (5.106) has not poles but only branch cuts. At $T = 0$ K, it is independent of $\mathbf{k}$, and the distribution function of electrons with spin up

$$\langle X_\mathbf{k}^{2-}X_\mathbf{k}^{-2}\rangle = -(1/\pi)\,\mathrm{Im}\int_{-\infty}^{\infty} dE f(E) G_+(\mathbf{k}, E) = c \tag{5.107}$$

is constant over the entire Brillouin zone [of course, the relation (5.103) is then satisfied]. By the general theorem of the accelerating action of an electric field on the many-electron system of the crystal [78], those are zero-current states. It is only at finite temperatures that they contribute to the conductivity σ owing to the term proportional to $N_\mathbf{p}$ in (5.106). Calculation of this contribution by Kubo's equation in [76] has yielded

$$\sigma_+ = \frac{ce^2}{m^*\Omega_0}\frac{\zeta(3/2) - \zeta(5/2)}{8\sqrt{2}\pi^3}\frac{m^{*1/2}\Omega_0^3}{D^{5/2}}T^2. \tag{5.108}$$

At the same time, for the contribution of electrons with spin down, we have

$$\sigma_- = \frac{ce^2}{m^*\Omega_0}\frac{1}{\gamma_{k\sim k_T}} \sim \frac{1}{T^4}, \tag{5.109}$$

[see (5.100)], and $\sigma_- \gg \sigma_+$ at low temperatures.

A very unusual contribution to the total density of states $N(E)$ comes from electrons with spin up. From (5.106) and (5.96), we have for $T = 0$ K

$$N_+(E) = -\frac{1}{\pi}\sum_\mathbf{k}\mathrm{Im}\, G_+(\mathbf{k}, E) = \begin{cases} N_0(E), & E < E_\mathrm{F}, \\ 0, & E > E_\mathrm{F}, \end{cases} \tag{5.110}$$

$$N_-(E) = N_0(E), \tag{5.111}$$

where $N_0(E)$ is the initial density of states (5.48) and E_F is the Fermi energy for electrons with spin down. The physical significance of (5.110) and (5.111) is fairly simple. To determine $N(E)$ for $E < E_\mathrm{F}$, one needs to remove the particles from the system. In doing so, one breaks up a couple and may choose an electron with spin up or spin down with equal probability. Therefore, for occupied states, $N_+(E) = N_-(E)$. To determine the densities of states for $E > E_\mathrm{F}$, one needs to place the particles in the corresponding states, which cannot be done for electrons with spin up because of the Pauli exclusion principle. Therefore, $N_+(E > E_\mathrm{F}) = 0$.

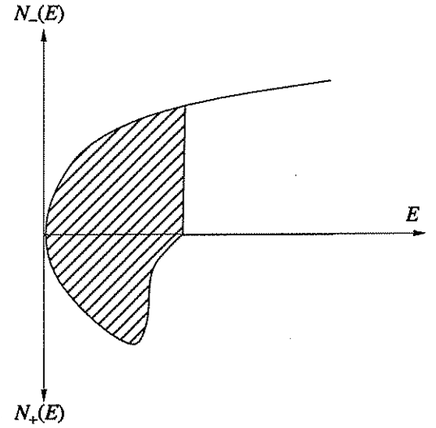

Fig. 5.3. Schematic representation of the density of electronic states in the upper Hubbard subband (the band of couples) for U equal to infinity. The filled states are shown as shaded.

The jump $N(E)$ at $E = E_\mathrm{F}$, resulting from (5.110), spreads out when one takes into account the magnon frequency. Instead of (5.106), a more careful calculation [76] yields

$$G_+(\mathbf{k}, E) = \sum_\mathbf{q}\frac{N_\mathbf{q} + f_{\mathbf{k}+\mathbf{q}}}{E - \varepsilon_{\mathbf{k}+\mathbf{q}} + \omega_\mathbf{q}}. \tag{5.112}$$

Then, in view of (5.97), it can be shown that (5.110) will hold as before for $E_\mathrm{F} - E \gg \bar{\omega}$, where $\bar{\omega}$ is the maximum frequency of magnons, and

$$N_+(E) \sim (E_\mathrm{F} - E)^{3/2} \text{ for } 0 < E_\mathrm{F} - E \ll \bar{\omega}. \tag{5.113}$$

A diagram of $N(E)$ for the case at hand is shown in Fig. 5.3. For the first time, a result similar to (5.113) was obtained by Edwards and Hertz [79] for the broad-band Hubbard model.

Thus, it has been proved for narrow-band Hubbard ferromagnetism with $c \ll 1$ that nonquasiparticle states associated with the branch cuts (but not poles) of the Green's function exist. Those are nearly zero-current states (that is, making a small contribution to the conductivity) and yield a contribution to the density of states suddenly changing near E_F. This is forceful evidence that the systems in question are different from the Fermi liquid. Interestingly, as is shown in [80], the nonquasiparticle states in the case at hand contribute a linear term to heat capacity. For $c \ll 1$, this term is many times greater than the usual band contribution from electrons with spin down. The existence of nonquasiparticle states is a characteristic and important property of strongly correlated ferromagnets [76, 79, 80].

We now proceed to calculate the magnon spectrum. As a matter of fact, this will provide enough ground for

substantiating the adopted hypothesis about the ground state. Acting similar to Irkhin and Katsnel'son [76], we calculate the commutator two-time Green's function

$$\Gamma(\mathbf{q}, \omega) = \left\langle\langle X_{\mathbf{q}}^{+-} | X_{-\mathbf{q}}^{-+}\rangle\right\rangle_{\omega} \tag{5.114}$$

in zero approximation with respect to N_p (that is, for $T = 0$) and in a linear approximation with respect to the electronic distribution function. By writing the equation of motion (5.44) for the Green's function (5.114) and applying transformations similar to those used in deriving $G_{-}(\mathbf{k}, E)$ [see (5.90)], we obtain

$$\omega\Gamma(\mathbf{q}, \omega)$$

$$= M + \sum_{\mathbf{k}} [t(\mathbf{k} - \mathbf{q}) - t(\mathbf{k})] \left\langle\langle X_{\mathbf{q}-\mathbf{k}}^{2-} X_{\mathbf{k}}^{-+} | X_{-\mathbf{q}}^{-+}\rangle\right\rangle_{\omega}$$

$$= M + \sum_{\mathbf{k}, \mathbf{r}} [t(\mathbf{k} - \mathbf{q}) - t(\mathbf{k})] \Phi(\mathbf{k}|\, \mathbf{q}\mathbf{r}\omega), \tag{5.115}$$

where

$$\Phi(\mathbf{k}|\, \mathbf{q}\mathbf{r}\omega) = \left\langle\langle X_{-\mathbf{r}}^{2+} X_{\mathbf{q}-\mathbf{k}+\mathbf{r}}^{+-} X_{-\mathbf{q}}^{++} | X_{\mathbf{q}}^{-+}\rangle\right\rangle_{\omega} \tag{5.116}$$

and $M = \langle X^{++} - X^{--}\rangle$ is the relative magnetization. For the saturated state at $T = 0$ K, $M = 1 - c$. Subsequently, when setting up and solving the set of equations, we may set

$$\left\langle\langle X_{\mathbf{k}}^{2\alpha} X_{\mathbf{r}}^{2\beta} A | X_{\mathbf{q}}^{-+}\rangle\right\rangle_{\omega} = 0;$$
$$\left\langle\langle X_{\mathbf{k}}^{2+} X_{\mathbf{p}}^{-\sigma} A | X_{-\mathbf{q}}^{++}\rangle\right\rangle_{\omega} = 0, \tag{5.117}$$

for any operator A. This is because the first function is proportional to the product of the small occupation numbers of couples, and the second, to the occupation numbers of couples and N_p. This leads to the equation of motion for the function Φ from (5.116)

$$[\omega - t(\mathbf{k}) + t(\mathbf{r})] \Phi(\mathbf{k}|\, \mathbf{q}\mathbf{r}\omega)$$
$$= \delta_{\mathbf{k}\mathbf{r}} f_{\mathbf{r}} - \left\langle X_{-\mathbf{r}}^{2+} X_{\mathbf{q}-\mathbf{k}+\mathbf{r}}^{+-} X_{\mathbf{k}-\mathbf{q}}^{-2}\right\rangle$$
$$+ \sum_{\mathbf{f}} t(\mathbf{f}) \langle\langle X_{-\mathbf{r}}^{2+} X_{\mathbf{q}-\mathbf{k}+\mathbf{r}}^{+-} (X_{\mathbf{k}-\mathbf{f}}^{+-} X_{\mathbf{f}}^{-2} + X_{\mathbf{k}-\mathbf{f}}^{--} X_{\mathbf{f}}^{+2})$$
$$- X_{-\mathbf{f}}^{2-} X_{\mathbf{f}-\mathbf{r}}^{--} X_{\mathbf{q}-\mathbf{k}+\mathbf{r}}^{+-} X_{\mathbf{k}}^{+2} | X_{\mathbf{q}}^{-+}\rangle\rangle_{\omega}. \tag{5.118}$$

By using (5.43), reducing the products of X-operators of the "Bose" type to the normal form, and discarding, in accordance with (5.117), the small terms, we obtain

$$\left\langle\langle X_{-\mathbf{r}}^{2+} X_{\mathbf{q}-\mathbf{k}+\mathbf{r}}^{+-} X_{\mathbf{k}-\mathbf{f}}^{+-} | X_{-\mathbf{q}}^{-+}\rangle\right\rangle_{\omega}$$
$$= \sum_{\mathbf{p}} \left\langle\langle X_{-\mathbf{r}}^{2+} X_{\mathbf{q}-\mathbf{k}+\mathbf{r}}^{+-} X_{\mathbf{k}-\mathbf{f}}^{+-} X_{\mathbf{f}-\mathbf{p}}^{+-} X_{\mathbf{p}}^{+2} | X_{-\mathbf{q}}^{-+}\rangle\right\rangle_{\omega} \tag{5.119}$$
$$\approx \Phi(\mathbf{k}|\, \mathbf{q}\mathbf{r}\omega) + \Phi(\mathbf{q} - \mathbf{k} + \mathbf{p} + \mathbf{f}|\, \mathbf{q}\mathbf{r}\omega),$$

and, similarly, for the remaining Green's functions entering into (5.118). For the second term on the right-hand side of (5.118), we have

$$\left\langle X_{-\mathbf{r}}^{2+} X_{\mathbf{q}-\mathbf{k}+\mathbf{r}}^{+-} X_{\mathbf{k}-\mathbf{q}}^{-2}\right\rangle$$
$$= \sum_{\mathbf{f}} \left\langle X_{-\mathbf{r}}^{2+} X_{\mathbf{q}-\mathbf{k}+\mathbf{r}}^{+-} X_{\mathbf{k}-\mathbf{q}-\mathbf{f}}^{-2} X_{\mathbf{f}}^{+2}\right\rangle \approx f_{\mathbf{r}}. \tag{5.120}$$

Inserting all of the above expressions in (5.118) and introducing the function

$$\chi(\mathbf{k}|\, \mathbf{q}\mathbf{r}\omega) = \frac{\omega}{f_{\mathbf{r}}} \Phi(\mathbf{k}|\, \mathbf{q}\mathbf{r}\omega), \tag{5.121}$$

we obtain for it a closed integral equation of the form

$$\chi(\mathbf{k}|\, \mathbf{q}\mathbf{r}\omega) = \delta_{\mathbf{k}\mathbf{r}} - \frac{\omega}{\omega - t(\mathbf{k}) + t(\mathbf{r})}$$
$$+ \frac{1}{\omega - t(\mathbf{k}) + t(\mathbf{r})} \sum_{\mathbf{f}} [t(\mathbf{k} + \mathbf{f} - \mathbf{q} - \mathbf{r}) - t(\mathbf{f})] \chi(\mathbf{f}|\, \mathbf{q}\mathbf{r}\omega). \tag{5.122}$$

Similar to (5.95), using the Dyson equation for the function $\Gamma(\mathbf{q}\omega)$ from (5.114)

$$\Gamma(\mathbf{q}\omega) = \frac{M}{\omega - \Pi(\mathbf{q}\omega)}, \tag{5.123}$$

recovering $\Pi(\mathbf{q}\omega)$ from the first two terms of the series expansion $\Gamma(\mathbf{q}\omega)$ in terms of $f_{\mathbf{r}}$, and noting (5.115) and (5.121), we obtain [compare with the similar derivation of (5.94)]

$$\Pi(\mathbf{q}\omega) = \sum_{\mathbf{k}\mathbf{r}} [t(\mathbf{k} - \mathbf{q}) - t(\mathbf{k})] f_{\mathbf{r}} \chi(\mathbf{k}|\, \mathbf{q}\mathbf{r}\omega). \tag{5.124}$$

For $\mathbf{q}$ tending to zero, we have $\omega_{\mathbf{q}} \equiv \Pi(\mathbf{q}, 0) = D\mathbf{q}^2$ in full agreement with (5.97). The integral equation (5.122) has the same kernel as (5.92) and can be solved similarly. For the spin stiffness constant D in an sc lattice with $a = 1$, we have

$$D = \kappa c|t|, \tag{5.125}$$

where $\kappa = 0.656$ is the same constant as in (5.99) and (5.100). The result (5.125) follows from the one obtained by Nagaoka [75] for $N_e = N + 1$ upon the natural change $1/N \to c$. It can be shown that the magnon spectrum for a simple cubic lattice is positive definite for all $\mathbf{q}$, and the magnetization M, defined self-consistently from $\Gamma(\mathbf{q}, 0)$ in (5.123) according to spectral relations, is

$$M = 1 - c - 2\langle X^{--}\rangle$$
$$= 1 - c + \frac{2}{\pi} \sum_{\mathbf{q}} \int_{-\infty}^{\infty} d\omega N_B(\omega) \operatorname{Im} \Gamma(\mathbf{q}\omega), \tag{5.126}$$

where $N_B(\omega) = [\exp(\omega/T) - 1]^{-1}$ is the Bose function. Thus equals $1 - c$ at $T = 0$. In this sense, our hypothesis regarding the saturated ferromagnetic state proves self-consistent. ($\langle X^{--}\rangle = 0$ for $T = 0$; that is, the magnetization is maximally possible.) By contrast, the spectrum of spin waves for fcc and hcp lattices at $t < 0$ in the nearest-neighbor approximation is not positively definite [75]. The cause for this is that the density of electronic states $N_0(E)$ at the lower edge of the energy band diverges, which is untypical of three-dimensional lattices; the divergence is removed when considering the next-nearest neighbors. One may therefore think that, in reality, the ferromagnetic state is stable at small c [76].

Considering the succeeding terms of the series expansion of $\Gamma(\mathbf{q}, \omega)$ with respect to N_p, one can calculate the temperature dependence for the frequency $\omega_{\mathbf{q}}$ and damping $\tilde{\gamma}_{\mathbf{q}}$ of magnons and for the magnetization M [76, 80]. We will give, without derivation, only the results of these rather tedious but basically simple calculations.

The damping of magnons takes the form

$$\tilde{\gamma}_{\mathbf{q}} = \begin{cases} q^4 \omega_{\mathbf{q}} \dfrac{\Omega_0^2}{\pi^3} k_F^3 \left[1 + \dfrac{35\pi^2}{16} \left(\dfrac{T}{\omega_{\mathbf{q}}}\right)^2\right], & T \ll \omega_{\mathbf{q}}, \\ q^4 T \dfrac{\Omega_0^2}{48\pi^3} k_F^2 \left[\ln \dfrac{T}{\omega_{\mathbf{q}}} + \dfrac{5}{3}\right], & T \gg \omega_{\mathbf{q}}, \end{cases} \tag{5.127}$$

where

$$k_F = \left(\frac{6\pi^2 c}{\Omega_0}\right)^{1/3} \tag{5.128}$$

is the Fermi momentum for the saturated ferromagnetic case.

The spin stiffness constant varies with temperature as

$$D(T) - D(0) = \frac{\pi^2}{12} T^2 N(E_F) \frac{d}{dE_F} m^{-1}(E_F)$$
$$- \frac{\Omega_0^2 k_F^4}{36\pi^2 \bar{\omega}} T^2 \ln \frac{\bar{\omega}}{T} - \frac{5\sqrt{\pi}}{12} \zeta(5/2) \left(\frac{\Omega_0}{4\pi^2}\right)^2 \frac{k_F}{m^*} \left(\frac{T}{D(0)}\right)^{5/2}, \tag{5.129}$$

where $m^{-1}(E)$ is the reciprocal effective electronic mass averaged over the constant-energy surface, m^{*-1} is its value at the bottom of the band, and $\bar{\omega} = 4Dk_F^2$ is the characteristic magnon frequency. The first term on the right of (5.129) is due to the Fermi distribution function in (5.124), the second is due to the interaction of magnons with charge carriers, and the third, due to the magnon-magnon interaction. The expressions (5.127) and (5.129) are derived in the leading orders of the reciprocal number of nearest neighbors and can change by numerical factors of about unity. Finally, the magnetization strictly obeys Bloch's $T^{3/2}$ law

$$M = 1 - c - \sum_{\mathbf{p}} N_{\mathbf{p}}. \tag{5.130}$$

The coefficient facing N_p in (5.130) is equal to unity, that is, as in a ferromagnetic dielectric, each magnon reduces the total spin by 1. To obtain this correct answer, one should, when calculating M by equation (5.126), take into account the contribution both from the poles and from the branch cuts of the function $\Gamma(\mathbf{q}, \omega)$.

The case $c \ll 1$ and $T = 0$, which we just considered, allows a rigorous analysis and is basic to an understanding of narrow-band ferromagnets, much as the Heisenberg model is basic to an understanding of ferromagnetic insulators. However, the situation becomes confused and ambiguous away from this range of parameters. In the next section, we will present a relevant view based on a study by Auslender *et al.* [81]. We think it to be most convincing because it is in qualitative agreement with a certain set of experimental data, which we proceed to analyze.

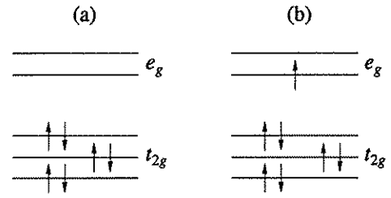

Fig. 5.4. Energy spectrum diagrams for (a) FeS_2 and (b) CoS_2.

5.6.2. Local Magnetic Moments in Narrow-Band Ferromagnets. Application to $Fe_{1-x}Co_xS_2$. In connection with the ferromagnetism of strongly correlated systems considered herein, special interest is evoked by experimental data on $Fe_{1-x}Co_xS_2$ solid solutions with a pyrite structure [74]. They have a fairly simple band structure, and one can therefore regard this system as a model one. In FeS_2, the splitting of the d states of Fe in the crystal field into the t_{2g} and e_g bands is greater than the Hund exchange interaction. Therefore, this substance is a nonmagnetic semiconductor, in which the t_{2g} energy band is completely filled and the twofold-degenerate narrow e_g band is empty (its width is about 1 eV) (Fig. 5.4). The electronic spectrum of substances with a pyrite structure was studied by Folkerts *et al.* [82].

Upon substitution of cobalt for iron, the e_g band, which is only one-fourth filled in the ferromagnetic metal CoS_2, is gradually filled. The isostructural compound NiS_2 with its e_g band half-filled is an antiferromagnetic Mott insulator [3]. This alone is evidence that strong interelectron correlations play a decisive role in the solid-solution system in question. According to Jarrett *et al.* [74], the most unusual feature of the $Fe_{1-x}Co_xS_2$ system is that it is ferromagnetic, even at extremely low concentrations of conduction electrons, $n = x \leq 0.05$. In fact, it is not unlikely that the critical concentration is still lower or is nonexistent because at lower x all or some electrons are localized owing to disorder. Ferromagnetism remains saturated up to $x \approx 0.15$. In contrast to ordinary weak itinerant ferromagnets (such as Ni–Rh alloys), however, there are no signs of any exchange enhancement of Pauli spin susceptibility in the paramagnetic region of compositions; the Curie–Weiss law is satisfied at practically any concentration n of conduction electrons, and the Curie constant C is proportional to n. This behavior seems rather unusual because at low n the gas approximation must hold, and, according to Kanamori [83], this rules out ferromagnetism. Indeed, in Kanamori's theory [83], the

criterion of ferromagnetism takes the form of the Stoner criterion (see Ch. 4), except that Stoner's I is replaced by a quantity on the order of the conduction band width, and $N(E_F)$ tends to zero for n tending to zero. The situation might be different if there were a sharp $N(E)$ peak near the lower edge of the band, but the band calculations performed by Folkerts *et al.* [82] do not confirm that. Moreover, in Kanamori's theory the magnetic susceptibility does not obey the Curie–Weiss law.

The latter impediment is fundamental. The point is that if one interprets the Curie–Weiss law in a most natural way as arising from the existence of localized magnetic moments, then one will not obtain it with any approach that draws upon the perturbation theory and the Fermi liquid picture of the electronic spectrum (for a more detailed discussion of the matter, see Ch. 4). A standard procedure whereby one can deduce the existence of localized magnetic moments in itinerant ferromagnets is to use a static approximation in the functional integration method (see Section 4.4); with it, one replaces a translationally invariant system by a spin-disordered one. Physically, this is a quite reasonable approximation (albeit not controllable in accuracy). On the other hand, it is desirable to be able to deduce the existence of localized magnetic moments by a regular and, possibly, traditional method, such as the Green's function method. Among other things, this would enable one to allow for the dynamic behavior of spin fluctuations from the outset. Following the suit set by Auslender *et al.* [81], we will set forth such a technique, which yields a qualitatively correct description of ferromagnetism in $Fe_{1-x}Co_xS_2$.

To begin with, note that the picture of the electronic spectrum described in subsection 5.6.1 holds solely at low temperatures and for the saturated ferromagnetic state, where the itinerant motion of electrons with spin up is ruled out. In cases where the magnetization M is low (high temperatures or fairly large c), however, charge carriers with both spin projections are sufficiently well-defined quasiparticles and can be described by approximations of the Hubbard I type (see Section 5.5). As demonstrated in [76], the Green's function (5.112) is replaced by an expression of the "band-theoretic" type

$$G_+(\mathbf{k}, E) = \frac{c + \langle X^{--}\rangle}{E - t(\mathbf{k})\,(c + \langle X^{--}\rangle)}, \qquad (5.131)$$

at $c \neq 0$ and $\langle X^{--}\rangle \gtrsim \text{const}/z$, where z is the number of nearest neighbors. In such a case, the structure of the series involved in the perturbation theory is changed.

Keeping in mind the specific $Fe_{1-x}Co_xS_2$ system, we now proceed from couples to holes and consider a model with the Hamiltonian

$$H = \sum_{\mathbf{k}\sigma} \varepsilon(\mathbf{k}) X^{0\sigma}_{-\mathbf{k}} X^{\sigma 0}_{\mathbf{k}} - \frac{1}{2} h \sum_i (X^{++}_i - X^{--}_i), \qquad (5.132)$$

where h is the magnetic field strength in the units of μ_B and $\varepsilon(\mathbf{k}) \equiv -t(\mathbf{k})$ [cf. (5.75)], which corresponds to the case

$$0 < c = 1 - n < 1. \qquad (5.133)$$

We will neglect the twofold degeneracy of the e_g band because it is immaterial for small n. Our objective is to calculate the magnetization (more accurately, the average spin)

$$\langle S^z\rangle = \frac{1}{2}(n_+ - n_-) \equiv M/2, \quad n_\sigma = \langle X^{\sigma\sigma}\rangle \qquad (5.134)$$

and the susceptibility in the paramagnetic phase, $\chi \simeq \langle S^z\rangle/h$. In theory, one can evaluate $\langle S^z\rangle$ either from the Green's function $G_\sigma(\mathbf{k}, E)$, in terms of which one can express n_σ, or from the two-time commutator Green's function (5.114) [see also (5.126)]. The latter method is more fruitful in describing magnetic properties, so we will use it.

To begin with, we set up the first two equations of the set (5.44) for the Green's function $\Gamma(\mathbf{q}, \omega)$ with the Hamiltonian (5.132)

$$(\omega - h)\,\Gamma(\mathbf{q}, \omega)$$

$$= n_+ - n_- + \sum_{\mathbf{k}} (\varepsilon_{\mathbf{k}-\mathbf{q}} - \varepsilon_{\mathbf{k}}) \langle\langle X^{0-}_{\mathbf{q}-\mathbf{k}} X^{+0}_{\mathbf{k}} | X^{-+}_{\mathbf{q}}\rangle\rangle_\omega; \qquad (5.135)$$

$$[\omega - \varepsilon_{\mathbf{k}}(n_+ + c) + \varepsilon_{\mathbf{k}-\mathbf{q}}(n_- + c) - h]\,\langle\langle X^{0-}_{\mathbf{q}-\mathbf{k}} X^{+0}_{\mathbf{k}} | X^{-+}_{\mathbf{q}}\rangle\rangle_\omega$$

$$= n^+_{\mathbf{k}} - n^-_{\mathbf{k}-\mathbf{q}} + (\varepsilon_{\mathbf{k}-\mathbf{q}} n^-_{\mathbf{k}-\mathbf{q}} - \varepsilon_{\mathbf{k}} n^+_{\mathbf{k}})\,\Gamma(\mathbf{q}, \omega)$$

$$+ \sum_{\mathbf{p}} \varepsilon_{\mathbf{p}} \langle\langle X^{0-}_{\mathbf{q}-\mathbf{k}} \delta\,(X^{00}_{\mathbf{k}-\mathbf{p}} + X^{++}_{\mathbf{k}-\mathbf{p}})\, X^{+0}_{\mathbf{p}}$$

$$- X^{0-}_{-\mathbf{p}} \delta\,(X^{00}_{\mathbf{q}-\mathbf{k}+\mathbf{p}} + X^{--}_{\mathbf{q}-\mathbf{k}+\mathbf{p}})\, X^{+0}_{\mathbf{k}}$$

$$+ X^{+-}_{\mathbf{k}-\mathbf{p}} \delta\,(X^{0-}_{\mathbf{q}-\mathbf{k}} X^{-0}_{\mathbf{p}}) - \delta\,(X^{0+}_{-\mathbf{p}} X^{+0}_{\mathbf{k}})\, X^{+-}_{\mathbf{q}-\mathbf{k}+\mathbf{p}} | X^{-+}_{-\mathbf{q}}\rangle\rangle_\omega, \qquad (5.136)$$

where $\delta A = A - \langle A\rangle$ and $n^\sigma_{\mathbf{k}} = \langle X^{0\sigma}_{-\mathbf{k}} X^{\sigma 0}_{\mathbf{k}}\rangle$. By neglecting the fluctuation term in (5.136) (which contains a sum over $\mathbf{p}$), we obtain a closed system of equations and can explicitly define $\Gamma(\mathbf{q}, \omega)$

$$\Gamma(\mathbf{q}, \omega) = \left[2\langle S^z\rangle + \sum_{\mathbf{k}} \frac{(n^+_{\mathbf{k}} - n^-_{\mathbf{k}-\mathbf{q}})\,(\varepsilon_{\mathbf{k}-\mathbf{q}} - \varepsilon_{\mathbf{k}})}{\omega - h - \tau^+_{\mathbf{k}} + \tau^-_{\mathbf{k}-\mathbf{q}}}\right]$$

$$\times \left[\omega - h + \sum_{\mathbf{k}} \frac{(\varepsilon_{\mathbf{k}} n^+_{\mathbf{k}} - \varepsilon_{\mathbf{k}-\mathbf{q}} n^-_{\mathbf{k}-\mathbf{q}})\,(\varepsilon_{\mathbf{k}-\mathbf{q}} - \varepsilon_{\mathbf{k}})}{\omega - h - \tau^+_{\mathbf{k}} + \tau^-_{\mathbf{k}-\mathbf{q}}}\right]^{-1}, \qquad (5.137)$$

where

$$\tau^\sigma_{\mathbf{k}} = \left[\frac{1+c}{2} + \sigma\langle S^z\rangle\right]\varepsilon_{\mathbf{k}}; \qquad (5.138)$$

$$n^\sigma_{\mathbf{k}} = \left[\frac{1+c}{2} + \sigma\langle S^z\rangle\right] f(\tau^\sigma_{\mathbf{k}} + \frac{\sigma h}{2}). \qquad (5.139)$$

The expression (5.139) was derived from the Fermi Green's functions $G_\sigma(\mathbf{k}, E)$ taken in the Hubbard approximation I. Therefore, as noted earlier, it does not hold for low c and T (for n^+_k).

We are interested in either the paramagnetic phase ($h \to 0$, $\langle S^z\rangle = \chi h \to 0$) or the ferromagnetic phase away from saturation ($\langle S^z\rangle \ll 1$). In such cases, the numerator and the denominator in (5.137) can be expanded in a series in terms of $\langle S^z\rangle$ and h, thus yielding an expression of the form

$$\Gamma(\mathbf{q}, \omega) = \frac{\omega A(\mathbf{q}, \omega) + \langle S^z\rangle B(\mathbf{q}, \omega) + hC(\mathbf{q}, \omega)}{\omega - \langle S^z\rangle D(\mathbf{q}, \omega) - hE(\mathbf{q}, \omega)}, \qquad (5.140)$$

where

$$A(\mathbf{q}, \omega) = L(\mathbf{q}, \omega) \sum_{\mathbf{k}} \frac{F_{\mathbf{k}-\mathbf{q}} - F_{\mathbf{k}}}{\omega - \tau_{\mathbf{k}-\mathbf{q}} - \tau_{\mathbf{k}}}; \qquad (5.141)$$

$$L(\mathbf{q}, \omega) = \left[1 + \frac{2}{1+c} \sum_{\mathbf{k}} \frac{F_{\mathbf{k}-\mathbf{q}}\tau_{\mathbf{k}-\mathbf{q}} - F_{\mathbf{k}}\tau_{\mathbf{k}}}{\omega + \tau_{\mathbf{k}-\mathbf{q}} - \tau_{\mathbf{k}}}\right]^{-1} \qquad (5.142)$$

and $\tau_{\mathbf{k}} = \varepsilon_{\mathbf{k}}(1+c)/2$, $F_{\mathbf{k}} \equiv f(\tau_{\mathbf{k}})$. The other functions in (5.140) are rather complex in structure. The expressions that follow will include only their values for $\omega = 0$:

$$B(\mathbf{q}, 0) \equiv b_{\mathbf{q}} = L(\mathbf{q}, 0)$$

$$\times \left[1 + \frac{2}{1+c} \sum_{\mathbf{k}} \left(\frac{\partial}{\partial \tau_{\mathbf{k}}}(\tau_{\mathbf{k}} F_{\mathbf{k}}) - \tau_{\mathbf{k}} \frac{F_{\mathbf{k}-\mathbf{q}} - F_{\mathbf{k}}}{\tau_{\mathbf{k}-\mathbf{q}} - \tau_{\mathbf{k}}}\right)\right]; \qquad (5.143)$$

$$C(\mathbf{q}, 0) \equiv c_{\mathbf{q}} = L(\mathbf{q}, 0) \sum_{\mathbf{k}} \left(\frac{\partial F_{\mathbf{k}}}{\partial \tau_{\mathbf{k}}} - \frac{F_{\mathbf{k}-\mathbf{q}} - F_{\mathbf{k}}}{\tau_{\mathbf{k}-\mathbf{q}} - \tau_{\mathbf{k}}}\right); \qquad (5.144)$$

$$D(\mathbf{q}, 0) \equiv d_{\mathbf{q}}$$

$$= \frac{8L(\mathbf{q}, 0)}{(1+c)^2} \sum_{\mathbf{k}} \left(\tau_{\mathbf{k}-\mathbf{q}} \frac{F_{\mathbf{k}-\mathbf{q}} - F_{\mathbf{k}}}{\tau_{\mathbf{k}-\mathbf{q}} - \tau_{\mathbf{k}}} - \tau_{\mathbf{k}} \frac{\partial F_{\mathbf{k}}}{\partial \tau_{\mathbf{k}}}\right); \qquad (5.145)$$

$$E(\mathbf{q}, 0) \equiv e_{\mathbf{q}} = L(\mathbf{q}, 0)$$

$$\times \left[1 + \frac{2}{1+c} \sum_{\mathbf{k}} \left(\frac{\tau_{\mathbf{k}-\mathbf{q}} F_{\mathbf{k}-\mathbf{q}} - \tau_{\mathbf{k}} F_{\mathbf{k}}}{\tau_{\mathbf{k}-\mathbf{q}} - \tau_{\mathbf{k}}} - \tau_{\mathbf{k}} \frac{\partial F_{\mathbf{k}}}{\partial \tau_{\mathbf{k}}}\right)\right]. \qquad (5.146)$$

If one sets $h = 0$ and $\langle S^z\rangle = 0$ in (5.140) from the outset, then $\Gamma(\mathbf{q}, \omega) = A(\mathbf{q}, \omega)$. The expression for this function in (5.141) takes the usual form of the random-phase approximation with the Stoner enhancement $L(\mathbf{q}, \omega)$. In these circumstances, the Curie–Weiss law cannot, of course, be obtained. If, however, one inserts (5.140) in equation (5.126) for $M = 2\langle S^z\rangle$, while retaining h and $\langle S^z\rangle$ in the numerator and denominator, and writes the integral with the Bose distribution function in a complex plane for small h and $\langle S^z\rangle$, one will obtain the additional contribution from the pole of (5.140) at the point

$$\omega_{\mathbf{q}} = \langle S^z\rangle d_{\mathbf{q}} + h e_{\mathbf{q}} \qquad (5.147)$$

corresponding to the itinerant mode. After calculations, one may let h tend to zero (assuming that $h \ll T$). As a result, one will obtain the equation for χ in the paramagnetic phase

$$\frac{1-c}{2} + \frac{1}{\pi}\int_0^\infty d\omega \,\mathrm{Im} \sum_{\mathbf{q}} A(\mathbf{q}, \omega + i0) \coth \frac{\omega}{T}$$

$$= T \sum_{\mathbf{q}} \left[A(\mathbf{q}, 0) + \frac{\chi b_{\mathbf{q}} + c_{\mathbf{q}}}{\chi d_{\mathbf{q}} + e_{\mathbf{q}}}\right]. \qquad (5.148)$$

In the left-hand side of (5.148) for $T \ll E_F$ one may set $T = 0$ [in accordance with (5.143), the expression for $A(\mathbf{q}, \omega)$ implies that it depends on T only via the parameter T/E_F]. At the same time, the right-hand side of (5.148) contains the temperature T arising from $\coth(\omega_{\mathbf{q}}/2T) \approx 2T/\omega_{\mathbf{q}}$ for $h \ll T$. Then, one can see that χ obeys the Curie–Weiss law

$$\chi = \frac{C}{T - T_C}, \qquad (5.149)$$

where T_C is the Curie temperature definable from (5.148) for χ tending to infinity

$$T_C = \left[\frac{1-c}{2} + \frac{1}{\pi}\int_0^\infty d\omega \,\mathrm{Im} \sum_{\mathbf{q}} A(\mathbf{q}, \omega + i0)\right]$$

$$\times \left[\sum_{\mathbf{q}} \left(A(\mathbf{q}, 0) + \frac{b_{\mathbf{q}}}{d_{\mathbf{q}}}\right)\right]^{-1}. \qquad (5.150)$$

Thus, the transition to the limit $h \to 0$ is nontrivial. It then follows that, if one calculates the susceptibility in the paramagnetic phase by the Green's function method at once in a field $h = 0$, as is usually done, one will not deduce localized magnetic moments (the Curie–Weiss law). The above procedure for calculating χ and $\langle S^z\rangle$ is a complicated version of the Tyablikov approximation for the Heisenberg model [84], where one faces the same problem involving the limiting transition $h \to 0$ for $T > T_C$. Apparently, it is specific precisely for a system with localized magnetic moments. For purely itinerant paramagnets, one can calculate the susceptibility in a direct way for $h = 0$ immediately.

A significant feature of the above approximation is that it describes the ferromagnetic state down to the charge-carrier concentration n tending to zero. It is not clear whether this is a merit or a demerit of the approximation. The point is as follows. On the one hand, it would be natural to expect that with very small n one should pass to the gas limit where, according to Kanamori [83], ferromagnetism cannot exist. On the other hand, judging from experimental data on $Fe_{1-x}Co_xS_2$, this critical concentration may prove to tend toward zero. We will give, without derivation, the characteristics of the ferromagnetic state in the proposed approach for $n \ll 1$. For $T = 0$ and $n \ll 1$, we have an unsaturated ferromagnetic state

$$S_0 = \frac{\alpha n}{2},$$

$$\alpha = 2\sum_{k,q} \frac{(\varepsilon_{k-q} - \varepsilon_k)\,\theta(\varepsilon_{k-q} - \varepsilon_k)}{\varepsilon_{k-q} - \varepsilon_k + \varepsilon_{max} - \varepsilon_q} < 1. \quad (5.151)$$

For the Curie temperature, we have

$$T_C = \frac{S_0}{2}\frac{\varepsilon_{max}^2 m^* k_F}{2\pi^2}\Omega_0 \quad (5.152)$$

and for χ at $T_C \ll T \ll E_F$, we obtain the Curie–Weiss law (5.149), where

$$C = \frac{S_0}{2}. \quad (5.153)$$

Thus, for $n \ll 1$, the main characteristics of the ferromagnetic state are

$$S_0 = 2C = \frac{\alpha n}{2}, \quad D \sim \alpha n^{2/3}, \quad T_c \sim \alpha n^{4/3}, \quad (5.154)$$

where D is the spin stiffness constant. The above results are in qualitative agreement with the general picture of the magnetic properties of $Fe_{1-x}Co_xS_2$. Thus, it is true that the existence of localized magnetic moments, revealed by the Curie–Weiss law, is closely related to the structure of the electronic spectrum typical of strongly correlated systems (Hubbard subbands), as discussed in Section 5.4 from entirely different considerations.

5.7. Spin Polarons and Phase Separation

A very interesting property of strongly correlated systems is that there is a possibility for couples and holes to experience self-localization so that they "lock" themselves in a kind of a magnetic drop known as a spin polaron [85, 86]. This phenomenon is akin to the formation of self-localized states in magnetic semiconductors [87 - 90], also known as ferrons [88, 89] and fluctuons [87].

As previously discussed in detail (see Section 5.3), the Hubbard model in the limit of narrow bands $W \ll U$ for $c = 0$ reduces to the Heisenberg antiferromagnetic model with the exchange integrals $J_{ij} = 2|t_{ij}|^2/U$. At the same time, for $U = \infty$ and $c \neq 0$, the ground state is ferromagnetic (see Section 5.6).

This prompts one to wonder about the nature of the ground state for small but finite values of c and $|t|/U$, when one observes a competition between the tendencies to ferromagnetic and antiferromagnetic order. It has been hypothesized that this might lead to the formation of "skewed structures" with the mutually perpendicular vectors of ferro- and antiferromagnetism [91]. An energetically more favorable development is, however, the formation of spin polarons (ferromagnetic drops in an antiferromagnetic matrix) examined in [85]. Note that these spin polarons are an analog (in the narrow-band limit) of ferrons considered by Nagaev in the *s–d* exchange model (see [88, 89] and the references given there). That phase separation is more favorable energetically in the narrow-band, almost half-filled Hubbard model was demonstrated by Visscher [85] by numerical calculations and from simple qualitative considerations (see also [3]). According to these considerations, if an electron is situated in a ferromagnetic region, it gains, in comparison with the case of an antiferromagnetic environment, an energy $|t|$ (because the band experiences an antiferromagnetic narrowing, see above). At the same time, some energy is lost in the exchange interaction between localized spins (5.15). Because of this, an electron can establish ferromagnetic order only in a region of a finite size L. In addition to the exchange-interaction energy, there is also a loss of the "zero-point" energy related to the indeterminacy of the electronic momentum $\sim\hbar/L$ (a similar issue was raised for the first time in [92]). Then, the energy of an electron locked in a ferromagnetic region is estimated as

$$E(L) \sim \frac{\hbar^2}{m^* L^2} + \frac{z|t|^2}{U}\left(\frac{L}{a}\right)^3 - |t|, \quad (5.155)$$

where a is the lattice parameter, $m^* \sim \hbar^2/|t|a^2$ is the effective mass, and numerical factors on the order of unity are dropped. By minimizing (5.155) with respect to L, we find for the optimal size L_0 an estimate of the form

$$L_0 \sim a(U/z|t|)^{1/5}. \quad (5.156)$$

Moreover, for $U \gg z|t|$, equations (5.155) and (5.156) imply that $E(L_0) < 0$, and self-localization proves to be energetically favorable. Simple estimates do not give enough ground for one to determine if spin polarons can coalesce into macroscopic drops, as Visscher [85] believes they can. Probably, an important factor here is the long-range part of Coulomb interaction, not taken into account in the Hubbard model (see [89]). We will not discuss the structure of the two-phase region. From (5.156) it is possible to form an estimate for its boundary, which is subject to the condition that the total volume of drops is smaller than the volume of the crystal

$$c\left(\frac{L_0}{a}\right)^3 \lesssim 1. \quad (5.157)$$

Equations (5.156) and (5.157) imply that

$$c \lesssim \left(\frac{z|t|}{U}\right)^{3/5}. \quad (5.158)$$

When the inverse inequality is satisfied, ferromagnetic order establishes itself throughout the system. Apparently, there is direct experimental evidence for the existence of a two-phase region in $LaMnO_3$-based solid solutions (a situation of the Hubbard model type: the charge carriers are Mn^{4+} ions with Mn^{3+} in the background) and also in alloyed EuSe and EuTe (a situation of the *s–d* exchange model type) [89].

Auslender and Katsnel'son [86] derived an effective spin Hamiltonian for $0 < c \ll 1$ and $0 < |t|/U \ll 1$, which describes phase separation. To this end, they used the functional integral method in the static approximation [see (4.41) and (4.42)]. The usual procedure, as described in detail in Section 5.4, involves calculating the mean Green's function in some approximation. This is not enough for obtaining the effective spin Hamiltonian because one should be able to calculate the energy of the system and, consequently, the Green's function for each random realization of the unit vectors magnetization $\mathbf{e}_i = \hat{\varepsilon}_i/|\hat{\varepsilon}_i|$ [see (4.42)]. A similar problem arises in the case of Anderson localization in disordered systems (see [93]). As Abou-Chacra *et al.* [94] showed, it can be solved on the so-called Bethe lattice (the Cayley tree), in which there are no closed paths, without self-intersections, of three or more sites [93] (Fig. 5.5).

Instead of a rigorous derivation of the applicable equation, we will limit ourselves to a "physical" reasoning, which will nevertheless yield a rigorous result. The Green's function $G_{ii}(t)$ [the Fourier transform (5.161)] has the significance of the amplitude of the probability of finding an electron on the ith lattice point at time t subject to finding it on the same lattice point at time 0. This amplitude involves two outcomes: either the electron stays on that lattice point at any time (the probability amplitude $G_{ii}^{(0)}(\tau)$ is the Green's function for $t = 0$) or it hops to a neighboring lattice point at some instant $\tau' < \tau$ (the transition amplitude is the transfer integral t) and back (or else it will never come back to the original site on the Bethe lattice). Therefore, one may write a Dyson-like equation (in the site representation) as

$$G_{ii}(\tau) = G_{ii}^{(0)}(\tau) + \sum_{\rho=1}^{z} t^2 \int_0^\tau d\tau' G_{ii}^{(0)}(\tau') G_{i+\rho,\,i+\rho}(\tau - \tau'), \quad (5.159)$$

where ρ labels the nearest neighbors. By applying the Fourier transformation $G_{ii}(\tau) \to G_{ii}(E)$ and taking advantage of the explicit form

$$\hat{G}_{ii}^{(0)}(E) = \frac{1}{E - \hat{\varepsilon}_i\hat{\sigma}}, \quad (5.160)$$

we derive from (5.159) the closed equation

$$\hat{G}_{ii}^{-1}(E) = E - \varepsilon_i\hat{\sigma} - t^2\sum_{\rho=1}^{z}\hat{G}_{i+\rho,\,i+\rho}(E), \quad (5.161)$$

for each realization of the vectors $\hat{\varepsilon}_i$. We seek the solution of equation (5.161) in the form

$$\hat{G}_{ii}^{-1}(E) = a_i + \mathbf{b}_i\hat{\vec{\sigma}}. \quad (5.162)$$

Then,

$$\hat{G}_{ii}(E) = X_i(a_i + \mathbf{b}_i\hat{\vec{\sigma}}). \quad (5.163)$$

Substituting (5.162) and (5.163) in (5.161) yields a system of equations for a_i and $\mathbf{b}_i$. Solving it by iterations with respect to t subject to the condition $|t| \ll \varepsilon_0$, we find that X_i satisfies the equation

$$2t^2\sum_\rho X_i X_{i+\rho}(E^2 + \varepsilon_0^2\mathbf{e}_i\mathbf{e}_{i+\rho}) + X_i(\varepsilon_0^2 - E^2) + 1 = 0. \quad (5.164)$$

We introduce a quantity

$$\cos\theta_i = \frac{1}{z}\sum_\rho \mathbf{e}_i\mathbf{e}_{i+\rho}, \quad (5.165)$$

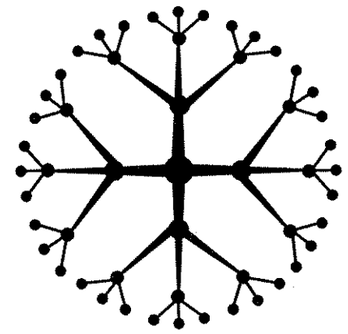

Fig. 5.5. Bethe lattice (Cayley tree).

which characterizes short-range ferromagnetic order ($\theta_i = 0$) or short-range antiferromagnetic order ($\theta_i = \pi$). If $\cos\theta_i$ is taken to be a smooth function, then $X_{i+\rho} \approx X_i$, and equation (5.164) can be solved explicitly. Next, we find the total energy E, which can be expressed in terms of $G_{ii}(E)$ and, in the final analysis, in terms of $X_i(E)$. The simplest way to do this is by using the Hellman–Feynman theorem

$$\frac{\partial E}{\partial t} = \left\langle\frac{\partial H}{\partial t}\right\rangle = \sum_{i,\,i+\rho,\,\sigma}\left\langle c_{i\sigma}^+ c_{i+\rho,\,\sigma}\right\rangle, \quad (5.166)$$

and by expressing the average on the right-hand side of (5.166) in terms of the Green's function in the spectral representation

$$\left\langle c_{i\sigma}^+ c_{i+\rho,\,\sigma}\right\rangle = -\frac{1}{\pi}\mathrm{Im}\int_{-\infty}^{\infty} dE f(E)\,[G_{i,\,i+\rho}(E)]_{\sigma\sigma}. \quad (5.167)$$

Finally, we can minimize the resultant energy $E(\cos\theta_i)$ with respect to the distribution of θ_i. The results can be summed up as follows. Above all, we confirmed the qualitative finding stated earlier that it is advantageous to separate the system into ferromagnetic regions (containing all charge carriers) and antiferromagnetic insulating regions (containing no charge carriers).

The total energy E of the system in the two-phase region, such that $\cos\theta_i/2 = 1$ in the volume fraction x (the ferromagnetic phase) and $\cos\theta_i/2 = 0$ in the volume fraction $1 - x$ (the antiferromagnetic phase), is

$$E(x) = -2z^{1/2}|t|cN + \frac{zt^2}{2\varepsilon_0}xN + \frac{3}{5}\left(\frac{3\pi}{2}\right)^{2/3} z^{1/2}|t|c^{5/3}x^{-2/3}N, \quad (5.168)$$

where $\varepsilon_0 \simeq U/2$ is the length of the vectors $\hat{\varepsilon}_i$. Minimizing (5.168) with respect to x, we find the expression for its optimal value

$$x_0 = c\left[\frac{4}{5}\left(\frac{3\pi}{2}\right)^{2/3}\frac{\varepsilon_0}{z^{1/2}|t|}\right]^{3/5}. \quad (5.169)$$

Then,

$$\frac{E(x_0)}{N} = -2z^{1/2}|t|c + \frac{5}{4}\frac{zt^2}{\varepsilon_0}x_0. \quad (5.170)$$

If we calculate, for purposes of comparison, the energy of a skewed structure in a homogeneous phase ($\cos\theta_i/2 = \text{const}$), then we will find that, for

$$c < c_0 = \left[\frac{5}{4}\left(\frac{2}{3\pi}\right)^{2/3}\frac{z^{1/2}|t|}{\varepsilon_0}\right]^{3/5} \quad (5.171)$$

[cf. (5.158)], it lies above the energy of the two-phase region given by (5.170). We will further find that the ferromagnetic and antiferromagnetic regions are separated by sharp boundaries (on the order of the lattice parameter in thickness). For $c > c_0$, the system is ferromagnetic. In fact, these results follow (except for the numerical coefficients) even from the simple estimates given at the beginning of this section.

Because the ferromagnetic phase contains all the charge carriers, the system owes its conductivity at $0 < c < c_0$ to percolation through the ferromagnetic regions, and this significantly varies with the specific structure.

5.8. Comments on Low-Dimensional Systems and High-Temperature Superconductivity

As already noted in Section 5.1, the upsurge of interest in strongly correlated systems and Mott insulators in the late 1980s was stimulated by the discovery of high-temperature superconductors containing CuO_2 layers, such as $La_{2-x}(Sr, Ba)_xCuO_4$, $YBa_2Cu_3O_{6+x}$, and many others. Anderson [17, 23] stated most definitely that all high-temperature superconductors are alloyed Mott insulators. However, they strongly differ from traditional systems. Compare, for example, $LaMnO_3$ (see Section 5.7) and La_2CuO_4, which are similar even in chemical composition. Both are antiferromagnetic Mott insulators falling in the perovskite family, except that La_2CuO_4 is a layered perovskite and $LaMnO_3$ is a cubic perovskite. Both change to the conducting state as the antiferromagnetic order is destroyed when doped with alkaline-earth metals ($La_{2-x}Sr_xCuO_4$ and $La_{1-x}Ca_xMnO_3$), but with a difference. The former becomes a superconductor and the latter, a ferromagnet. In our view, an explanation of this difference constitutes a serious problem. Possibly, the cause lies in the magnitude of spin ($S = 1/2$ for Cu^{2+} and $S = 3/2$ for Mn^{3+}); possibly, this is due to the specific structural state and dynamics of the La_2CuO_4 lattice. However, the most striking difference is the isotropic, three-dimensional electronic and magnetic excitation spectrum of $LaMnO_3$ and the strongly anisotropic quasi-two-dimensional spectrum of La_2CuO_4. Two-dimensional strongly correlated systems have been the subject of a huge number of publications, but they lie outside the scope of this review. We are forced to limit ourselves to passing comments only on the aspects that have a direct bearing on the problem of electron localization and delocalization.

Doped Mott insulators are usually described in terms of the narrow-band version of the Hubbard model or of the polar model, known as the t–J model, with a Hamiltonian

$$\hat{H} = -\sum_{ij\sigma}' t_{ij}X_i^{0\sigma}X_j^{\sigma 0} + \sum_{ij}' J_{ij}\left(\mathbf{S}_i\mathbf{S}_j - \frac{1}{4}\mathbf{n}_i\mathbf{n}_j\right), \quad (5.172)$$

where $\mathbf{S}_i$ is the spin operator, $\mathbf{n}_i$ is the operator of the number of particles on a site, and $J_{ij} = 2|t_{ij}|^2/U$ is the exchange integral [see (5.15)]. The second term retains the operator n_i, which goes to unity for $N_e = N$, and the first term [cf. (5.132)] describes hole transport. This version of the polar model (but applied to the ferromagnetic case of $J_{ij} < 0$) was apparently investigated for the first time by Katsnel'son [95]. It was found that in the one-dimensional case a hole couples with a spin wave to form a quasiparticle with a band of width $|J|$ (for $|t| \gg |J|$). An unexpected result, extremely vital for the theory of high-temperature superconductors, is that something similar was observed by Kane *et al.* [96] and by von Szczepanski *et al.* [97] in the two-dimensional antiferromagnetic case as well. The scheme leading to this finding is as follows. One chooses the case of a single hole on a plane square lattice with antiferromagnetic exchange and considers t_{ij} and J_j in the nearest-neighbor approximation. To describe the magnetic subsystem, one passes to the magnon representation (a transformation due to either Holstein–Primakoff [96] or Dyson–Maleev [51] and writes the self-energy of conduction electrons $\Sigma(\mathbf{k}, E)$ in terms of the "bold-faced" second-order perturbation theory, where the unperturbed Green's function $G_0(\mathbf{k}, E)$ is replaced by its exact counterpart $G(\mathbf{k}, E)$. As shown in [97], this procedure yields results close to those obtained numerically under the strict diagonalization of the Hamiltonian (5.172) on a finite cluster. For $T = 0$, the structure of the self-energy term related to the interaction of the hole with zero-point vibrations of antiferromagnons takes the form [96]

$$\Sigma(\mathbf{k}, E) = \sum_{\mathbf{q}} M^2(\mathbf{k}, \mathbf{q})G(\mathbf{k}-\mathbf{q}, E-\omega_{\mathbf{q}}), \quad (5.173)$$

where $M^2(\mathbf{k}, \mathbf{q})$ is the electron–antiferromagnon interaction matrix element. At the bottom of the band ($\mathbf{k} = 0$)

$$M^2(0, \mathbf{q}) \sim |t|^2|\mathbf{q}| \text{ for } \mathbf{q} \to 0, \quad (5.174)$$

where $\mathbf{q}$ is the momentum of an antiferromagnon and $\omega_{\mathbf{q}} \sim J|\mathbf{q}|$ for $\mathbf{q}$ tending to zero is the energy of an antiferromagnon. One uses the dominating-pole approximation [96], which consists in using the pole expression in (5.173)

$$G(\mathbf{k}, E) = \frac{a}{E - \xi(\mathbf{k})}, \quad (5.175)$$

where $\xi(\mathbf{k}) \approx a[t(\mathbf{k}) - t_{\min}]$, on neglecting the contribution of nonquasiparticle states. Then, for a one has the condition of self-consistency

$$\frac{1}{a} = 1 - \left.\frac{\partial\Sigma(0, E)}{\partial E}\right|_{E=0}$$

$$= 1 + \sum_{\mathbf{q}} M^2(0, \mathbf{q})\frac{a}{[\xi(\mathbf{k}-\mathbf{q}) - \omega_{\mathbf{q}}]^2} \quad (5.176)$$

$$\approx 1 + a|t|^2\sum_{\mathbf{q}}\frac{|q|}{(a|t|q^2 + Jq)^2} \approx 1 + \text{const}\frac{|t|}{J},$$

where the integral is evaluated for the two-dimensional case, in which for $|J| \ll |t|$ it is defined on the domain of small $\mathbf{q}$. Hence, $a \sim |J/t|$ and $|\xi(\mathbf{k})| \sim J$.

All of this should of course be taken as an elucidation. The actual spectrum $\xi(\mathbf{k})$ can, it appears, be determined solely by numerical calculations for clusters [97]. In general, such techniques appear to be in especial vogue in the theory of strongly correlated systems at present. Moreover, as is shown in [51], the electronic spectrum in the two-dimensional t–J model does not change its structure on passing to finite temperatures $T \ll J$, despite the destruction of antiferromagetic long-range order, owing to the preservation of short-range order (see Section 5.4).

Thus, heavy (to the extent of the smallness of $|J/t|$) quasiparticles can be formed in two-dimensional doped Mott insulators. Anderson [99] proposed an even more radical assertion that the quasiparticle description is inapplicable completely to two-dimensional systems and that the so-called Luttinger liquid is formed in them. We will make a few notes on this matter without claiming, of course, either completeness or rigor.

The term "Luttinger liquid" has its origin in the exactly solvable one-dimensional Tomonaga–Luttinger model [100]. Let the electronic spectrum be linear in the qausimomentum

$$\varepsilon_{\mathbf{k}} = \pm v_F\mathbf{k}, \quad (\mathbf{k} > 0), \quad (5.177)$$

where the "+" sign applies to the electrons moving to the right and the "–" sign to the electrons moving to the left, with a velocity v_F. Then, we may write the kinetic energy Hamiltonian (for simplicity, we omit the spin indices) as

$$H_0 = \sum_{k>0} v_k k\left(c_{1k}^+c_{1k} - c_{2k}^+c_{2k}\right), \quad (5.178)$$

where the subscripts "1" and "2" apply to the electrons moving to the right and left, respectively. We introduce the density operator ($p > 0$, $i = 1, 2$)

$$\rho_i(p) = \sum_{\text{all } k} c_{i,k+p}^+c_{ik},$$

$$\rho_i(-p) = \sum_{\text{all } k} c_{ik}^+c_{i,k+p}, \quad (5.179)$$

and write the interaction Hamiltonian as

$$V = \frac{1}{2L}\sum_{p>0} U_p\left[\rho_1(p)\rho_1(-p) + \rho_2(-p)\rho_2(p) + \rho_1(p)\rho_2(-p)\right], \quad (5.180)$$

where L is the length of the system and U_p is the interaction constant (for simplicity, a contact type of interaction is assumed). We then prove that $\rho_i(p)$ and $\rho_i^+(p)$ are the Bose creation and annihilation operators [accurate to the factor proportional to $(pL/2\pi)^{1/2}$], that the Hamiltonian

$$\hat{H} = \hat{H}_0 + \hat{V}, \quad (5.181)$$

turns out to be quadratic on passing to bosons and can be diagonalized, and that the single-electron Green's functions are proportional to some averages of the exponents of the Bose operators and can be evaluated by analogy with the Debye–Waller factor for phonons [1]. As a result, for the single-electron Green's functions, we have [100]

$$G_i(k, E) \sim \frac{(E^2 - v_F^2k^2)^g}{E \pm v_Fk}, \quad (5.182)$$

where

$$g = \frac{1}{2}\left[\frac{1 - U/2\pi v_F}{(1 - U/\pi v_F)^{1/2}} - 1\right] \approx \frac{1}{8}\left(\frac{U}{\pi v_F}\right)^2, \quad (5.183)$$

and the last equality in (5.183) holds for small U. The Green's function (5.182) generally has no poles but it has branch points for $E = \pm v_Fk$. By the same token and in contrast to, e.g., Fermi liquid, the distribution function $n_{ik} = \langle c_{ik}^+c_{ik}\rangle$ likewise has no discontinuity for $k = \pm k_F$, but it has a singularity of the form $(k_F \pm k)^g$ [100]. This behavior is typical of one-dimensional systems and has, for example, been observed in the one-dimensional Hubbard model for $N_e \neq N$ [98]. The situation is less clear with two-dimensional systems. In this connection, mention should be made of Wen [101] who, using the renormalization group method, demonstrated the stability of the Luttinger liquid in the case of weak overlap between chains (that is, in two-dimensional, but quasi-one-dimensional systems), and Fukuyama *et al.* [102] who argue that in two-dimensional systems with weak interaction the partial derivative $\partial\Sigma(k, E)/\partial E$ displays a divergence of the form $U^3\ln|E|$ (which further implies a breakdown of the Fermi liquid theory).

In conclusion, we will touch on the superconductivity of strongly correlated systems (including low-dimensional ones). With limited space available, we cannot afford a detailed discussion of many and often conflicting views on the nature of superconductivity in real metal–oxide systems and any specific "correlational" mechanisms of superconductivity. We will only dwell in brief on a secondary yet still important issue admitting a rigorous analysis. This is the electron–phonon pairing mechanism, but with allowance for strong electron–electron correlations in the normal phase.

This issue was investigated by Anokhin *et al.* [103]. From among their results, we will only give a fairly compact equation for the superconducting transition temperature T_c in the case of a weak initial electron–phonon coupling (the dimensionless constant $\lambda \gg 1$), taking into account the energy, but not momentum dependence of the self-energy $\Sigma(E)$ in the normal phase

$$1 = \frac{\lambda T_c}{N_0(0)} \sum_{|p_n| < \omega_D} \frac{ip_n}{iP(ip_n)} \int_{-\infty}^{\infty} dE \frac{N(E)}{E^2 + p_n^2}, \qquad (5.184)$$

where $N(E)$ is the exact density of states in the normal phase with allowance for electron–electron interaction (E is reckoned from the chemical potential level), $N_0(E)$ is its value without allowance for interaction, ω_D is the Debye frequency, and $p_n = \pi(2n + 1)T_c$ are the Matsubaru frequencies ($n = 0, \pm 1, \ldots$)

$$iP(ip_n) = ip - \frac{1}{2}[\Sigma(ip_n) - \Sigma(-ip_n)]. \qquad (5.185)$$

If the Fermi-liquid theory is applicable and the pole approximation (5.170) is valid, such that $a > \omega_D/|t|$, then $iP(ip_n) \approx ip_n/a$, $N(E) \approx N_0(E)/a$, and the many-electron renormalizations cancel out in (5.184). Then T_c takes the form

$$T_c \approx 1.13\omega_D e^{-1/\lambda}. \qquad (5.186)$$

As Anderson [104] argues, no such cancelation takes place in the Luttinger-liquid model; instead, the coupling constant $\lambda \to \text{const}\lambda^{1/3}$ in (5.186) is effectively increased. In contrast, the "phonon" superconductivity is completely suppressed in strongly correlated systems when one applies the Hubbard approximation III (for both $N_e < N$, $U < U_c$, and for $N_e \neq N$, $U \gg U_c$) [103]. This implies that the problem of the nature of high-temperature superconductivity cannot in theory be divorced from that of the nature of the normal phase in corresponding systems.

This concludes our roundup of strong-correlation effects in *d* systems in connection with the problem of electron localization and delocalization. In summary, the following statements may be made and tasks stated.

Strong electron–electron interaction can cause electrons to change from itinerant to localized states so that a metal becomes an insulator. The electronic states in the metallic phase near the transition or in the insulating phase upon doping can be quite unusual. They may be strongly damped, the effective mass may experience a large renormalization, the charge carriers may undergo self-localization, a nonquasiparticle state may set in, etc. Moreover, there is a strong cross-influence between the electronic spectrum and magnon (ferro- or antiferromagnetic) order.

The task of describing this broad range of issues can in no way be taken as fully achieved at present. The possibilities of quantitative band-theoretic approaches still remain unclear. The same is true of the applicability of simple Hubbard-type models for describing the properties of specific systems (say, $Fe_{1-x}Co_xS_2$ ferromagnets or high-temperature superconductors). Nor is one certain about the adequacy of specific approximations within the models themselves. Research on these matters constitutes a vigorously developing division in the physics of condensed matter, and the situation here is rapidly changing all the time. We would like to hope, however, that the view set forth in this chapter can at least help the reader to keep track of the key trends in these changes.

In the next chapter, we will consider the *f* systems, which significantly differ from the *d* systems in the degree of electron localization – a fact that, as we will see, leads to qualitatively new traits in electron behavior.

5.9. Conclusion

This chapter dealt with problems that still defy unambiguous treatment. Despite the huge number of studies dealing with the theory of strongly correlated systems (which has increased since the discovery of high-temperature superconductivity), no generally accepted universal formalism has been developed yet. In this chapter, we dwelt mainly on approaches that proceed from the localized limit and use the atomic representation and *X* operators as their working tools, and from the picture of magnetism with localized magnetic moments. We left out many studies based on the Fermi-liquid picture and the band-theoretic approach to the magnetism of strongly correlated systems. We did so because, as we believe, they are not convincing enough even for pure iron (see Ch. 4), to say nothing of narrow-band magnets.

What follows is a summary of the most essential findings and methods set forth in this chapter.

1. We gave a general formulation of the polar model for solids and of the Hubbard model as its special case. We also discussed at length how to use the *X* operators, which seem to give a most natural mathematical description of strongly correlated systems (Section 5.2).

2. We discussed "naïve" approaches to the description of Mott insulators, based on various modifications of the Hartree–Fock approximation and band-theoretic calculations (Sections 5.3 and 5.4). In some cases, they give a befitting description of antiferromagnetic order and the energy gap in the ground state of a Mott insulator. However, they are all but useless in cases where long-range order is nonexistent.

3. We described the metal–insulator transition in the paramagnetic phase within the "alloy" analogy for spin disorder (Section 5.5). This approach, which goes back to Hubbard's classical works, yields a rather strange picture of the metallic phase (with it, the damping of the electronic states is finite at the Fermi level and is even great in comparison with the Fermi energy near the transition). Even now, heated debates are going on as to whether this is a limitation of the approximation or such is physical reality. Whichever is the case, no other sufficiently consistent and formally developed approaches to the problems are available.

4. In Section 5.6, we used the Hubbard model to examine in detail the properties of narrow-band magnets exemplified by $Fe_{1-x}Co_xS_2$ solid solutions. Sufficiently rigorous results can be obtained only for an almost half-filled band. The most interesting of these findings is the existence of nonquasiparticle (spin-polaron) states. It has proved possible to construct an approximate description of the ferromagnetic state over a wide range of charge-carrier concentrations. Among other things, it explains the occurrence of ferromagnetism at small *n* and the Curie–Weiss behavior of magnetic susceptibility for all "ferromagnetic" compositions.

5. The conflict between the tendency of charge carriers in strongly correlated systems to establish ferromagnetic order via the "double exchange" mechanism and the "desire" of the Mott insulator to be an antiferromagnet is resolved through phase separation, in which all charge carriers are locked in ferromagnetic domains within an antiferromagnetic matrix. A theory of this striking development is set forth in Section 5.7.

> The Jury had each formed a different view
> (Long before the indictment was read),
> And they all spoke at once, so that none of them knew
> One word the others had said.
>
> Lewis Carroll, "The Hunting of the Snark"

6. LOCALIZED AND ITINERANT ELECTRONS IN "ANOMALOUS" *f* SYSTEMS

This chapter considers matters related to the formation of the small energy scale in the *f* systems, that is, intermediate-valence and heavy-fermion systems. This includes hybridization, exciton condensation, and the Kondo effect. Main emphasis is placed on narrow-bandgap mixed-valence semiconductors, and the so-called Kondo magnets, which display the transition from localized to itinerant magnetism in the narrow range of variations in external parameters.

6.1. Specific Traits of f Systems

This chapter deals with the degree of electron localization in some classes of the *f* systems. Before we proceed any further, however, it is worth while dwelling on what distinguishes all *f* systems from the *d* systems on the whole.

Calculations of the wave functions for the electrons of free atoms and ions reveal a general pattern: the degree of localization of electronic states abruptly increases with increasing orbital quantum number *l*, whereas within a series with a given *l* it decreases with increasing principal quantum number *n* (see Fig. 6.1 [170]). Therefore, the *d* wave functions are more localized than the *f* functions, and the 3*d* states are more localized than the 4*d* and 5*d* states. The most localized of all states in the partially filled shells are the 4*f* states in the atoms and ions of the rare-earth metals, their alloys, and their compounds. The 5*f* electrons in the actinides are as localized as, or somewhat more localized than, the 3*d* electrons. More accurate information can be obtained by band-theoretic calculations. As seen from Fig. 6.2 [106], which demonstrates variations in the width of the 5*f* band across the actinide series, the 5*f* states are somewhat delocalized in the "light" actinides (up to plutonium), where the *f* band is relatively broad, and are highly localized in the "heavy" actinides, beginning from americium. Two elements stand out; they are cerium in the 4*f* series and plutonium in the 5*f* series. As was discussed in detail in Section 2.6, in cerium the electrons change from the itinerant behavior in the α phase to the localized behavior in the γ phase because of a phenomenon of "collapse." A similar situation exists in plutonium with the transition from the α to the δ phase [107].

With regard to a solid, what counts most is not the localization radius of the *f* function, but its ratio to the interatomic distance. The latter is, in the final analysis, determined by the localization radius of outer-shell electrons that are responsible for chemical bonding. There is, therefore, ample reason to think that the *f* electrons are completely localized in all compounds of all 4*f* elements, except cerium and all "heavy" 5*f* elements. Moreover, they are bound to be localized in the compounds of cerium or "light" 5*f* elements (for example, uranium) if the interatomic distances in them are significantly greater than in the pure elements.

On the whole, such a picture is borne out by a wealth of experimental data. When one speaks of a strong localization of electronic states, one means that even in the crystal they remain "atomlike." In other words, they do not form Bloch states but are described by the orbital, spin, and angular momentum quantum numbers LSJ. The effects of the crystal structure then reduce to a weak splitting of the terms with $J \neq 0$ [removal of the $(2J + 1)$-fold degeneracy in accordance with the symmetry of the crystal environment]. In a most direct way, this picture of the *f* states is confirmed by the equality of magnetic moments in rare-earth metal crystals and in the states of free ions [108], and by the neutron spectroscopy of local excitations [109].

Among the compounds of the 5*f* elements, those best investigated are the uranium compounds. For them, an empirical rule (the Hill rule) has been established, relating the formation of magnetic moments on uranium ions to the distance between the ions [110]. In general, the formation of magnetic moments by itself is a weaker criterion for the localization of the *f* states than the fact that their magnitudes are equal to the "atomic" values. On the whole, the localization of the 5*f* electrons in the actinides presents a more complex problem than that of the 4*f* electrons in the rare-earth metals.

Everything stated above about the complete localization of the *f* electrons holds for the overwhelming majority of rare-earth compounds. There is, however, quite a number of systems that are anomalous in this respect. For one thing, their magnetic properties strongly differ from what one might expect on the basis of the atomic picture. For another, the local excitations associated with the term structure and the crystal field are either nonexistent or strongly diffused. Finally,

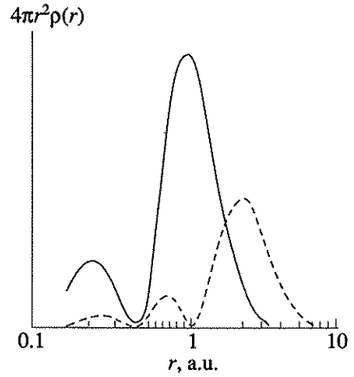

Fig. 6.1. Radial density of 5*f* electrons (the solid curve) and 6*d* electrons (the dashed curve) in an U atom; *r* is the radius (a.u.) on a logarithmic scale [170].

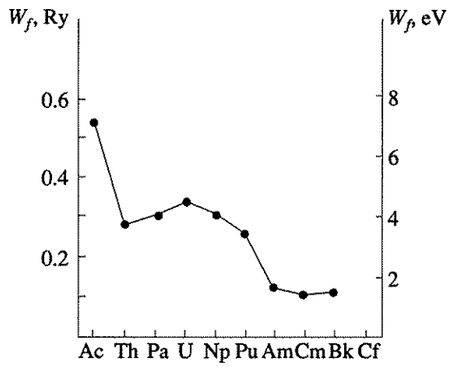

Fig. 6.2. Canonical width W_f of the *f* band across the actinide series [106].

there are indications that the *f* electrons take part in the formation of states near the Fermi energy (for more detail, see Section 6.5 below). In such "anomalous" compounds, the *f* electrons may be regarded as partly itinerant. Moreover, according to the degree and character of delocalization, these compounds may be classified into intermediate-valence (or mixed-valence) systems (with the *f* electrons rather strongly itinerant) and the Kondo lattices or heavy-fermion systems (with a weak localization of an essentially many-electron nature).

We will now discuss these two classes of compounds in turn. The intermediate-valence compounds will be taken up in Sections 6.2 - 6.4 and the heavy-fermion systems, in Sections 6.5 - 6.10.

6.2. Intermediate Valence: A General Outline

The matter of intermediate (or mixed) valence came up in Section 2 in connection with the properties of free atoms. Here, we will consider the properties of real systems in the intermediate-valence state. It is not a simple task to define intermediate valence in formal terms. For one thing, it is not always clear how one should determine valence. The simplest and historically first method of estimating the valence of the rare-earth elements was based on an analysis of variations in, for example, the lattice parameter in a sequence of isostructural compounds of different rare earths [111]. If for any compound of, for example, Sm, the lattice parameter occurred between the values typical of the rare earths known to be di- or trivalent, the Sm ion was taken to be in the intermediate-valence state, which meant that its valence was $2 < n < 3$; it was even possible to estimate *n* by linear interpolation. However, the "valence" estimated in such a way needs an elaboration. For example, according to the jump in the lattice parameter due to a pressure-induced $\alpha \rightarrow \gamma$ transition in Ce (see Section 2), the valence of Ce in the α phase may be recognized as lying between 3 and 4 (in contrast to trivalent γ-Ce). At the same time (as again noted in Section 2), more delicate spectroscopic studies provide unquestionable evidence that the number of electrons having *f* symmetry practically does not change upon the transition. In other cases, when we speak of a transition to the intermediate-valence state with a jump in the lattice parameter (for example, in SmS in the isostructural phase transition under a pressure of 6 kbar from the so-called "black" to "golden" phase), there is convincing evidence that the number of *f* and *d* electrons actually does change [112]. Furthermore, by invoking the concept of average valence estimated from some statistical properties, we run the risk of mechanically combining entirely different systems in one class. These may be golden SmS and transition metals like Ni or Fe (which, according to band-theoretic calculations [113, 114], have a fractional number of *d* electrons), on the one hand, and systems like magnetite Fe_3O_4 (in which di- and trivalent Fe ions are ordered in the lattice at a low temperature [3]), on the other. All in all, there obviously is not much sense in average valence. Actually, magnetite and metallic nickel represent two extreme cases. For Fe_3O_4, we may say that di- and trivalent ions do coexist in the lattice (except the very slow processes of hopping conduction [3]). For Ni, this is completely ruled out because any experiment would demonstrate that all Ni atoms have the same electronic structure corresponding to the average number of *d* electrons.

What makes intermediate-valence systems so specific is as follows. When one is to describe some experimentally observed properties, one has to assume ions of a different valence carrying integer-valued charges, but equivalent ions carrying an average charge when one is to describe other properties [111, 112]. For example, X-ray spectra of golden SmS, SmB_6, and other intermediate-valence systems (in reality, one usually deals with the L_{III} spectra determined by the position of the core 2*p* level) display two separated spectral lines corresponding to Sm^{2+} and Sm^{3+} ions; from the ratio of their intensities, one can readily determine the average valence. On the contrary, the Mössbauer spectra of the Sm nucleus in such systems displays *only one* line with an isomeric shift corresponding to the *intermediate* valence [111]. The point is that for intermediate-valence systems the characteristic valence fluctuation time τ_{fl} is significantly longer than the atomic times τ_{at} (about 10^{-15} s). Therefore, "fast" methods (such as X-ray spectroscopy) take, as it were, an instantaneous picture of "frozen" ions, whereas "slow" methods with a characteristic time $\tau \gg \tau_{fl}$ (including static measurements) yield results determined by the average valence.

Estimation by various techniques, such as heat-capacity measurements, optical spectroscopy, etc. [111, 112], yields a characteristic time τ_{fl} around 10^{-13} s. On the energy scale of the electronic spectrum this corresponds to $E \sim \hbar/\tau_{fl} \gtrsim 10$ meV. Precisely this type of scale identifies intermediate valence as a special state of solids. Among other things, the small energy scale implies that the physical state involved is highly labile, that is, readily changeable in a substantial way in response to relatively weak extraneous factors (pressure, temperature, electric and magnetic fields, etc.).

The specific microscopic mechanisms responsible for the formation of such an energy and time scale have yet to be completely elucidated (for a brief discussion, see Section 2.6). Also, they are apparently different for Ce, its intermetallic compounds, and compounds of 5*f* elements, on the one hand, and for the compounds of Sm and other 4*f* elements (except Ce, see Section 2.6) on the other. In the former case, as follows from the Johanson model discussed in Section 2.6 [115], one has to deal with a strongly correlated electron liquid in the *f* subsystem, which is in principle analogous to the strongly correlated liquid in the *d* subsystems. This situation is discussed in Ch. 5. In the sections that follow, when speaking of intermediate valence, we will have in mind the second case. In it, the microscopic basis is the promotion of the *f* level to the Fermi level and the transition of some *f* electrons to the 5*d* state (the promotion model).

6.3. A Simple Single-Electron Model of Intermediate Valence

In this section, we will demonstrate that many important features of intermediate-valence systems can be properly understood without considering many-electron effects.

If one takes as the starting point the "promotion" picture, the simplest model should, as a minimum, include itinerant electrons with an energy $t_{\mathbf{k}}$ (and creation and annihilation operators $c_{\mathbf{k}}^+$ and $c_{\mathbf{k}}$), localized electrons with an energy level E_0 (and creation and annihilation operators d_i^+ and d_i in the site representation), and the coupling between the subsystems, which in the single-electron approximation can be effected only via the terms c^+d and d^+c. Hence, the Hamiltonian of the model takes the form

$$\hat{H} = \sum_{\mathbf{k}} t_{\mathbf{k}} c_{\mathbf{k}}^+ c_{\mathbf{k}} + E_0 \sum_i d_i^+ d_i + V \sum_i (d_i^+ c_i + c_i^+ d_i), \tag{6.1}$$

where $c_i^+ = \sum_{\mathbf{k}} c_{\mathbf{k}}^+ e^{i\mathbf{k}\mathbf{R}_i}$; *V* is the hybridization parameter assumed constant for simplicity, $V_i = \text{const}$, that is, the hybridization of *c* and *d* electrons takes place only on a given site; and $t_{\mathbf{k}}$ and E_0 are reckoned from the chemical potential.

The model with the Hamiltonian (6.1) is called the hybridization model. As will be shown later (see Sections 6.4, 6.5, and 6.8), it is the basis model for a study into anomalous *f* systems in the sense that in the simplest approximations the problem of intermediate valence and the problem of Kondo lattices both reduce to an effective hybridization model.

To begin with, we turn to the electronic spectrum in the model (6.1) for an isolated impurity (present at site $i = 0$) and for the lattice, when in the $\mathbf{k}$ representation equation (6.1) takes the form

$$\hat{H} = \sum_{\mathbf{k}} [t_{\mathbf{k}} c_{\mathbf{k}}^+ c_{\mathbf{k}} + E_0 d_{\mathbf{k}}^+ d_{\mathbf{k}} + V (d_{\mathbf{k}}^+ c_{\mathbf{k}} + c_{\mathbf{k}}^+ d_{\mathbf{k}})]. \tag{6.2}$$

The simplest way to solve the single-impurity problem is to use two-time retarded Green's functions (see Section 5.5). For the Hamiltonian (6.1) without interaction, they can be evaluated exactly because the string of equations of motion is now closed. Considering the explicit form of the Hamiltonian (6.2), equation (5.44) immediately leads to a closed system of linear equations for the single-particle Green's function

$$(E - E_0)\langle\langle d_0 | d_0^+ \rangle\rangle = 1 + V \sum_{\mathbf{k}} \langle\langle d_0 | c_{\mathbf{k}}^+ \rangle\rangle,$$

$$(E - E_0)\langle\langle d_0 | c_{\mathbf{k}}^+ \rangle\rangle = V \sum_{\mathbf{k}'} \langle\langle c_{\mathbf{k}'} | c_{\mathbf{k}}^+ \rangle\rangle,$$

$$(E - t_{\mathbf{k}})\langle\langle c_{\mathbf{k}'} | c_{\mathbf{k}}^+ \rangle\rangle = \delta_{\mathbf{k}\mathbf{k}'} + V \langle\langle d_0 | c_{\mathbf{k}}^+ \rangle\rangle$$

from which they are all easy to evaluate. The result for localized electrons takes the form

$$\langle\langle d_0 | d_0^+ \rangle\rangle_E = [E - E_0 - V^2 R(E)]^{-1}, \tag{6.3a}$$

$$\begin{aligned} R(E) &= \sum_{\mathbf{k}} (E - t_{\mathbf{k}} + i0) \\ &= \mathcal{P} \sum_{\mathbf{k}} (E - t_{\mathbf{k}})^{-1} - i\pi\rho(E), \end{aligned} \tag{6.3b}$$

where $\rho(E) = \sum_{\mathbf{k}} \delta(E - t_{\mathbf{k}})$ is the density of states of *c* electrons, and $\mathcal{P}$ is the principal value symbol. The real part $R(E)$ describes the shift of the initial level E_0 and leads to no qualitative changes. For simplicity, it may be

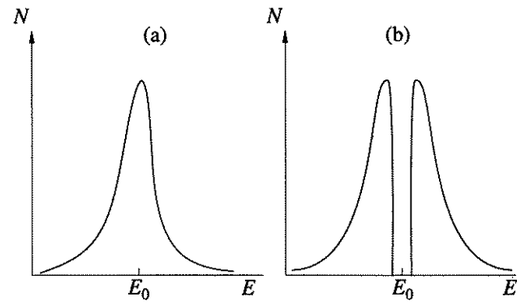

Fig. 6.3. Diagram of the density of electronic states in the hybridization model for (a) an isolated impurity and (b) the lattice.

dropped, presuming that it is lumped with E_0. Then, (6.3) corresponds to a quasilocal level with a density of states

$$N_d(E) = -\frac{1}{\pi}\mathrm{Im}\left\langle\langle d_0|d_0^+\rangle\right\rangle_E = \frac{\Gamma}{\pi[(E-E_0)+\Gamma^2]} \quad (6.4)$$

of width $\Gamma = \pi V^2\rho(E_0)$. Also, $n_d = \langle d_0^+ d_0\rangle$ is the number of d electrons ("valence"). It is equal to

$$n_d = \int_{-\infty}^{0} dE N_d(E) = \frac{1}{2} + \frac{1}{\pi}\tan^{-1}\frac{E_0}{\Gamma} \quad (6.5)$$

and markedly differs from 0 and 1 for $|E_0| \lesssim \Gamma$. If $|V| \ll W$ (where W is the width of the conduction band) and $|E_0| \ll W$ (that is, if the localized level is situated close to the Fermi level), then $\Gamma \ll W$ determines the scale of the characteristic valence fluctuation time $\tau_{fl} \sim \hbar/\Gamma$. Schematically, $N_d(E)$ is shown in Fig. 6.3a.

For the lattice, the corresponding quadratic form in the Hamiltonian (6.2) can be diagonalized for every $\mathbf{k}$ by applying the transformation

$$c_\mathbf{k} = \cos(\theta_\mathbf{k}/2)\,\alpha_\mathbf{k} + \sin(\theta_\mathbf{k}/2)\,\beta_\mathbf{k},$$
$$d_\mathbf{k} = -\sin(\theta_\mathbf{k}/2)\,\alpha_\mathbf{k} + \cos(\theta_\mathbf{k}/2)\,\beta_\mathbf{k}, \quad (6.6)$$

where $\theta_\mathbf{k}$ is defined so as to cancel out the terms $d_\mathbf{k}^+\beta_\mathbf{k}$. We have

$$\sin\theta_\mathbf{k} = 2V/E_\mathbf{k},$$
$$\cos\theta_\mathbf{k} = \frac{t_\mathbf{k}-E_0}{E_\mathbf{k}}, \quad E_\mathbf{k} = [(t_\mathbf{k}-E_0)^2 + 4V^2]^{1/2}, \quad (6.7)$$

$$\hat{H} = \sum_\mathbf{k}[\varepsilon_\alpha(\mathbf{k})\alpha_\mathbf{k}^+\alpha_\mathbf{k} + \varepsilon_\beta(\mathbf{k})\beta_\mathbf{k}^+\beta_\mathbf{k}], \quad (6.8)$$

where $\varepsilon_{\alpha,\beta}(\mathbf{k}) = (1/2)(t_\mathbf{k} + E_0 \pm E_\mathbf{k})$ are two branches of the new energy spectrum. Then the renormalized density of states is

$$N(E) = \sum_\mathbf{k}[\delta(E-\varepsilon_\alpha(\mathbf{k})) + \delta(E-\varepsilon_\beta(\mathbf{k}))]. \quad (6.9)$$

It is characterized by split peaks of width $\sim\Gamma$ and by a bandgap (likewise of width $\sim\Gamma$) near $E = E_0$. For smooth $\rho(E)$, the graph of $N(E)$ is given in Fig. 6.3b. The transformation of a resonance (a quasilocal level) to a bandgap in the energy spectrum when one passes from the single-impurity case to the lattice is a fairly common and important property of resonance-scattering models. Indeed, for the band spectrum of a one-dimensional string of point scatterers, one has the relation [116]

$$\cos ka = \cos(\kappa a + \delta_0(\kappa))/\cos\delta_0(\kappa), \quad (6.10)$$

where k is the quasimomentum, a is the lattice parameter, $\kappa = (2mE/\hbar^2)^{1/2}$, and δ_0 is the symmetric-scattering phase (there is no antisymmetric scattering). Near the resonance, we have $\delta_0(\kappa) \approx \pi/2$ and, by virtue of (6.10), $|\cos ka| > 1$ (a forbidden band). Generally, if V depends on k, as in the hybridization model, or if the model contains nonpoint scatterers [116], then the change-over from a single impurity to a lattice of scatterers might produce a pseudogap rather than a gap; it might be shifted relative to E_0; etc. However, the formation of a fine resonance structure is a common result. As we will see in the next section, it is important for an understanding of the physical properties of intermediate-valence systems.

Thus, the simplest hybridization model (6.1), (6.2) may yield noninteger-valued valences in the range $0 < n_d < 1$ and is able to explain why a small energy scale $\Gamma \ll W$ exists near the Fermi level. Moreover, the energy spectrum for the lattice model (6.2) consists of two bands with well-defined peaks of width Γ at the edges, separated by an energy gap, likewise of width Γ. Two questions remain, however, unanswered: (1) How does this picture agree with reality? and (2) How much will this picture remain unchanged or will change when one takes into account many-particle effects, which *a priori* may be important for the f systems?

6.4. Narrow-Gap Intermediate-Valence Semiconductors. Many-Particle Effects in the Exciton Approach

In this section, we will describe the exciton-hybridization model of intermediate-valence systems [129], which allows for many-particle effects. We will demonstrate that in this model the energy spectrum in the self-consistent field approximation has the same form as in the hybridization model, but with parameters significantly dependent on temperature and magnetic field strength. We will discuss the optical properties of intermediate-valence semiconductors (the frequency dependence of permittivity and the Franz–Keldysh effect); the temperature dependence of energy gap, heat capacity, and magnetic susceptibility; the metal–semiconductor transition in a magnetic field; and the low-temperature heat capacity of doped intermediate-valence semiconductors.

At present, it apparently may be taken as proven that some intermediate-valence compounds, such as SmB_6 [117, 118], golden SmS [119], TmSe [120, 121], and YbB_{12} [122, 123], are narrow-bandgap semiconductors and not metals, as was believed previously [111]. Recently, a family of PuX compounds (X = S, Se, Te) having similar properties was investigated by Wachter *et al.* [124]. The presence of a bandgap several tens or even hundreds of kelvins wide has been confirmed by measurements of electrical resistivity and heat capacity at low temperatures [119, 122, 123], direct optical observations [118, 119], tunneling experiments [125], and NMR [123] and ESR [126] spectroscopy. Very interesting properties of such systems are the semiconductor–metal transition in a magnetic field at $H \gtrsim 200$ kOe detected in YbB_{12} [127], a strong temperature dependence of the energy gap in SmB_6 [126], the nonmonotonic temperature dependences of magnetic susceptibility $\chi(T)$, Schottky-type anomalies in heat capacity $C(T)$ (see the discussion in [118]), and sharp absorption peaks in the IR region. As is pointed out in [118] and [125], the structure of the energy spectra of the systems in question corresponds, on the whole, to the hybridization model, that is, it has sharp $N(E)$ peaks at the edges of the energy gap. The spectrum takes the form

$$\varepsilon_{\alpha,\beta}(\mathbf{k}) = \frac{1}{2}\{t_\mathbf{k} + E_0 \pm [(t_\mathbf{k}-E_0)^2 + 4V^2]^{1/2}\} \quad (6.11)$$

[see (6.8) and (6.7)] and is shown schematically in Fig. 6.4. As is seen, the bandgap is not direct (that is, the maximum of the valence band and the minimum of the conduction band are shifted in the k space). Being on the order of $\Gamma \sim V^2/W$ (see the previous section), it is considerably smaller than the direct gap $2|V|$. In this sense, the situation drastically differs from zero-gap or narrow-gap semiconductors of the (Hg, Cd)Te type, where the smallness (or even the disappearance) of the bandgap is associated with the fact that the valence band touches the conduction band at certain, symmetry-related points in the k space [128].

An important distinction one observes in the energy spectra of intermediate-valence semiconductors is the abnormally strong decrease in the bandgap with temperature [126]. This fact can be explained if one takes into account the many-particle effects. They involve the strong "Hubbard-like" f–f repulsion at one site, the Coulomb and exchange interactions of f and d electrons and also f electrons of different sites, electron–phonon interaction, and the like. The need to take into account the Hubbard-like f–f repulsion is beyond any doubt; the relative implications and magnitude of the other interactions listed above are not known in real systems.

In the detailed analysis of the intermediate-valence picture that follows, we use the approach described in [129]; this is among the simplest techniques, is well-developed, and seems to offer an opportunity to describe a large collection of properties of intermediate-valence systems in qualitative terms. In this sense, it may be regarded as a reasonable semiphenomenological scheme, although the detailed microscopic significance of the model parameters may in principle change with further advances in the microscopic theory.

Of all many-electron effects, we will for the time being consider only Coulomb attraction between a conduction electron (the d type) and a hole at the f level. The simplest generalization of the hybridization model

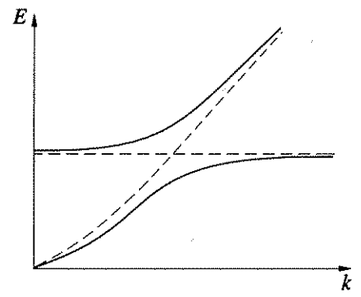

Fig. 6.4. Energy spectrum diagram for the hybridization model.

with due regard to these effects is the generalized spinless model of Falicov–Kimball, investigated by many authors in connection with the intermediate-valence problem (see, for example, [111, 129, 130]). The Hamiltonian of this generalized model takes the form

$$\hat{H} = \sum_\mathbf{k}[t_\mathbf{k}c_\mathbf{k}^+c_\mathbf{k} + (\Delta+G)f_\mathbf{k}^+f_\mathbf{k} + V(c_\mathbf{k}^+f_{-\mathbf{k}}^+ + f_{-\mathbf{k}}c_\mathbf{k})] - \frac{G}{N}\sum_i f_i^+f_ic_i^+c_i, \quad (6.12)$$

where we, in contrast to the hybridization model (6.2), changed to the hole representation ($\Delta = -E_0$, $f_\mathbf{k}^+ = d_{-\mathbf{k}}$) and took into consideration the contact interaction G^- of d and f electrons, which can lead to exciton effects. Owing to the spinless character of the model, one can easily take into account the limitations related to the strong ($U \gg W$) repulsion of f electrons at a site; for consideration of magnetic properties, however, the model must be modified (see below). The choice of such a model can be substantiated as follows. Because a change in the valence of the ion changes its electrostatic potential, the need to take into account the Coulomb interactions is obvious. Then, one may think that the exchange interactions related to the spin degrees of freedom are weaker than their Coulomb counterparts. Moreover, local magnetic moments and magnetic order are nonexistent in any of the systems in question (except the antiferromagnetic TmSe). The Coulomb interaction of f and d electrons is regarded (similarly to hybridization) as being of the contact type solely for simplicity. If one abandoned these approximations, this would not lead, in theory, to any difficulty, provided one is in a position to define how V_{ij} and G_{ij} at different sites vary with the distance between them. However, this is not known for real systems, and one has to be content with a limited set of parameters. Finally, the Coulomb interaction of f electrons at different sites would be essential for processes of the charge ordering type (see, for example, [22]). Convincing experimental findings that might be evidence of such processes in the systems in question apparently have not yet been obtained.

For $G = 0$, the Hamiltonian (6.12) is the same as (6.2) subject to the change $E_0 = -\Delta - G$, $f_k^+ \leftrightarrows d_k$. Its spectrum is found by a strict diagonalization procedure [cf. (6.6)]

$$c_k = \cos(\theta_k/2)\,\alpha_k + \sin(\theta_k/2)\,\beta_k,$$
$$f_{-k}^+ = -\sin(\theta_k/2)\,\alpha_k + \cos(\theta_k/2)\,\beta_k, \quad (6.13)$$

applied so as to cancel out the terms containing $\alpha_k^+\beta_k$. The same result can be obtained in a different way: one writes the trial function of the ground state as a function of the BCS type [131]

$$|\Phi\rangle = \prod_k (\cos\frac{\theta_k}{2} + \sin\frac{\theta_k}{2} c_k^+ f_{-k}^+)\,|\text{vacuum}\rangle, \quad (6.14)$$

takes the average over the ground state $E_0 \equiv \langle\Phi|\hat{H}|\Phi\rangle$, and determines $\cos\theta_k$, $\sin\theta_k$ so as to minimize E_0. As can be proven by direct calculations, this yields the exact value for the energy of the ground state. It is physically reasonable to use the function (6.14) as the trial one, even for $G \neq 0$. Indeed, the attraction of an f hole and a conduction electron can produce a bound state, i.e., an exciton, and the expression (6.14) describes precisely such a process. To state this more accurately, if the number of holes were the same as that of electrons and equal to N, it would be natural, by analogy with the Hubbard model [see equation (5.34)], to seek the trial function describing the "electron condensate" in the form

$$|\Phi_N\rangle = \left(\sum_k \varphi(\mathbf{k}) c_k^+ f_{-k}^+\right)^N |\text{vacuum}\rangle, \quad (6.15)$$

where $\varphi(\mathbf{k})$ is the trial function. In contrast to the Hubbard model, however, the number of f electrons is not preserved at the expense of the terms proportional to V, and a need arises to write the trial function in a more general form

$$|\Phi'\rangle = \sum_{M=0}^{N} \exp\left[\frac{\lambda(M)}{2}\right] \frac{1}{\sqrt{M!}} |\Phi_M\rangle \quad (6.16)$$

with the variable functions $\lambda(M)$ and $\varphi(\mathbf{k})$ [entering into $|\Phi_M\rangle$ in (6.15)]. As shown in [129], the ground-state energies obtained by use of (6.16) and (6.14) are the same. Therefore, one can take the function (6.14) as a successful trial function from the view point of both the exciton approach and the hybridization model.

As noted in passing, the function of the form (6.14) is formally analogous to the one used in the BCS theory of superconductivity [131]. Therefore, the characteristics of the ground state and the spectrum of quasiparticles can be calculated fully by analogy with that theory. We will give, without derivation, the results presented in [129].

In this approach, the energy spectrum is the same as the one in the hybridization model (6.7) and (6.8), except for some renormalization of the parameters E_0 and V

$$\varepsilon_{\alpha,\beta}(\mathbf{k}) = \frac{1}{2}[t_k - \Delta - G \pm E(\mathbf{k})],$$
$$E(\mathbf{k}) = [X^2 + (t_k - Y)^2]^{1/2}, \quad (6.17)$$

where X and Y are defined (for $T = 0$) by the equations

$$X\left[\frac{G}{N}\sum_k \frac{1}{E(\mathbf{k})} - 1\right] = 2V, \quad (6.18a)$$

$$Y + \Delta = \frac{G}{N}\sum_k \frac{Y - t_k}{E(\mathbf{k})}. \quad (6.18b)$$

Moreover, Y is simply related to valence as

$$\langle f_i^+ f_i\rangle = \frac{1}{2}(1 + \frac{Y+\Delta}{G}). \quad (6.19)$$

For $\lambda = G\rho(E_F) \ll 1$ (where E_F is the initial Fermi level in the conduction band), equations (6.18) reduce to the form

$$X(2\lambda \ln\frac{\alpha W}{|X|} - 1) = -2V, \quad (6.20)$$

where α is a coefficient on the order of unity. An analysis of this equation in [129] demonstrated that, with a given valence, either one or three solutions exist for the direct gap X, depending on the value of the initial hybridization parameter V. For V greater than some critical value V_c

$$|V| > V_c = \alpha W\lambda \exp(-\frac{1}{2\lambda} - 1) \quad (6.21)$$

(α is a numerical factor on the order of unity and W is the half-width of the conduction band), equation (6.18a) has only one solution with

$$X_1 \simeq \frac{2V}{2\lambda \ln\frac{\alpha W}{|V|} - 1}, \quad (6.22)$$

which describes a bandgap of "hybridization" nature, renormalized owing to interaction. For $|V| < V_c$, two more solutions of the "exciton" type exist, which for $|V| \ll V_c$ take the form

$$|X_{2,3}| = \alpha W \exp(-\frac{1}{2\lambda}) \pm \frac{|V|}{\lambda}. \quad (6.23)$$

According to [129], in order to describe experimental values of the direct and indirect energy gaps in SmB_6 and other narrow-bandgap semiconductors, one should take $\lambda \approx 0.2$, then $|V| \sim V_c$, thus the energy gap is of a mixed exciton-hybridization nature, which means that G and V determine it to about the same extent.

The approach we are dealing with is a version of the self-consistent field approximation and, as with any variational approach, it needs, strictly speaking, a formal substantiation. As such, we note that the effective hybridization equation $V^* \equiv X/2$, derived in [132] for $\lambda \ll 1$ by the renormalization-group method, is the same as (6.20). Interestingly, according to [132], the effective hybridization parameter for the single-impurity case is renormalized differently than for the lattice case: here, terms of the form $\ln(W/|V|)$ are collected to give a power dependence, $(|V|/W)^\beta$, where $\beta \ll 1$, rather than a geometric progression as in (6.22).

The model parameters can be derived from optical spectra in the IR range [118, 119]. Calculation of the polarizability $\alpha_{ij}(\omega)$ [129] yields [cf. (5.36)]

$$\alpha_{ij}(\omega) = \frac{e^2X^2}{2N\Omega_0} \times \sum_k \frac{\partial t_k}{\partial k_i}\frac{\partial t_k}{\partial k_j}\frac{1}{E^3(\mathbf{k})[E^2(\mathbf{k}) - (\omega + i0)^2]},$$
$$\text{Im}\,\alpha_{ij}(\omega) = \frac{\pi e^2X^2}{4N\Omega_0\omega^4} \times \sum_k \frac{\partial t_k}{\partial k_i}\frac{\partial t_k}{\partial k_j}[\delta(\omega - E(\mathbf{k})) - \delta(\omega + E(\mathbf{k}))], \quad (6.24)$$

where Ω_0 is the unit cell volume and e is the electron charge. The absorption edge, corresponding to direct optical transitions, is $\omega_{min} = |X|$; near it, $\text{Im}\,\alpha_{ij}(\omega)$ has a sharp maximum owing to the factor ω^{-4}. For SmB_6, Travaglini and Wachter [118] give $|X| \approx 0.1$ eV. They also observed a substantial contribution to the absorption from indirect transitions (related to processes involving impurities or phonons) with an indirect bandgap $2\delta \approx 30$ - 60 K, which is in agreement with heat capacity, tunneling, and resistivity measurements. As already noted, the character of IR spectra fit the hybridization model on the whole.

With $\omega \gg |X|$ and neglecting $E^2(\mathbf{k})$ in comparison with ω^2, from (6.24), we have for cubic symmetry

$$\varepsilon(\omega) = 1 + 4\pi\alpha(\omega) = 1 - \omega_p^2/\omega^2,$$
$$\omega_p^2 = \frac{4\pi e^2}{\Omega_0}\rho(E_F)\left\langle\left(\frac{\partial t_k}{\partial k_x}\right)^2\right\rangle_{E_F}. \quad (6.25)$$

Here, the French quotes denote averaging over the Fermi surface in the initial band and ω_p is the plasma frequency. Thus, for $\omega \gg |X|$ (and, notably, for visible light), the bandgap does not affect optical properties. Among other things, this explains why golden SmS has a metallic luster. Calculating the static permittivity $\varepsilon(0)$ from (6.24) subject to $|X| \ll W$ yields

$$\varepsilon(0) = \frac{2}{3}(\frac{\hbar\omega_p}{X})^2. \quad (6.26)$$

Hence, for SmB_6 one has $\varepsilon(0) \approx 200$ (according to [118], $\hbar\omega_p \approx 1.75$ eV), which is of the same order of magnitude as the experimental data.

At finite temperatures, by analogy with the BCS theory, equations (6.18) are modified owing to the Fermi functions $f_{\alpha,\beta}(\mathbf{k}) \equiv f(\varepsilon_{\alpha,\beta}(\mathbf{k}))$ and take the form

$$X\left[\frac{G}{N}\sum_k \frac{1 - f_\alpha(\mathbf{k}) - f_\beta(\mathbf{k})}{E(\mathbf{k})} - 1\right] = 2V, \quad (6.27a)$$

$$Y + \Delta = \frac{G}{N}\sum_k \frac{Y - t(\mathbf{k})}{E(\mathbf{k})}(1 - f_\alpha(\mathbf{k}) - f_\beta(\mathbf{k})). \quad (6.27b)$$

Generally, equation (6.27) calls for a numerical solution. To determine the general form of the function $X(T)$, we will examine the analytically simplest case where the conduction band is symmetric ($\rho(E) = \rho(-E)$) and $\Delta = 0$, so that $Y = 0$ by virtue of (6.18b) and $\langle f_i^+ f_i\rangle = 1/2$ by virtue of (6.19), whereas the chemical potential $\mu = Y - G/2 = -G/2$ is independent of temperature. Then equation (6.27) takes the form

$$X = \frac{2V}{GL - 1}, \quad L = \frac{1}{N}\sum_k \frac{1}{E(\mathbf{k})}\tanh\frac{E(\mathbf{k}) + t(\mathbf{k})}{2T}. \quad (6.28)$$

For $|X| \ll W$, we find

$$L = \int_{-W}^{W} \frac{d\varepsilon\rho(\varepsilon)}{[\varepsilon^2 + X^2]^{1/2}}\tanh\frac{[\varepsilon^2 + X^2]^{1/2} + \varepsilon}{4T} \approx \rho(0)\int_{\delta/2T}^{W/2T}\frac{d\tau}{\tau}\tanh\tau, \quad (6.29)$$

where we denote the indirect bandgap by $2\delta = X^2/2W$.

Solving equations (6.28) and (6.29) yields

$$X(T) \simeq \begin{cases} \dfrac{2V}{\lambda\ln(T^*/T)}, & T \gg \delta, T^* \\ X(0) - \dfrac{8TW}{X(0)}\exp\left[-\dfrac{\delta(0)}{T}\right] & \\ \times \dfrac{1}{1 - 2\lambda(\ln\dfrac{2W}{|X(0)|} - 1)}, & T \ll \delta, T^*, \end{cases} \quad (6.30)$$

where

$$T^* = \frac{\pi W}{8\gamma}\exp(-\frac{1}{\lambda}) \quad (6.31)$$

[for $|V| \sim V_c$, $T^* \sim \delta(0)$], $\gamma = e^c \approx 1.14\pi/2$ (c is the Euler constant).

By analogy with the BCS theory [131], the electronic heat capacity C can be calculated from the entropy of quasiparticles

$$S = -\sum_{k,\,i=\alpha,\beta}[f_i(\mathbf{k})\ln f_i(\mathbf{k}) + (1 - f_i(\mathbf{k}))\ln(1 - f_i(\mathbf{k}))], \quad (6.32)$$

specifically,

$$C = T\frac{\partial S}{\partial T} = \frac{1}{T}\sum_{\mathbf{k},\, i=\alpha,\beta}\left[-\frac{\partial f_i(\mathbf{k})}{\partial \varepsilon_i(\mathbf{k})}\left(1-\frac{T}{2}\frac{\partial}{\partial T}\right)\varepsilon_i^2(\mathbf{k})\right]. \tag{6.33}$$

In the specific case at hand with $\Delta = 0$, $\rho(E) = \rho(-E)$, the expression (6.33) can be reduced to the form

$$C(T) = \frac{\rho(0)}{T}\int_{\delta/2T}^{\infty}\frac{d\tau}{\cosh^2\tau}\left[X^2(T) - T\frac{\partial X^2(T)}{\partial T} + 4T^2\tau^2\right]. \tag{6.34}$$

At low temperatures $T \ll \delta(0)$, the heat capacity (6.34) decreases exponentially

$$C(T) \approx \frac{2\rho(0)}{T}X^2(0)\exp\left[-\frac{\delta(0)}{T}\right], \tag{6.35}$$

and for $T \gg \delta(0) \sim T^*$ (which actually means $T \gtrsim 100$ K for SmB_6), we find from (6.34) and (6.30)

$$C(T) \approx \frac{\rho(0)}{T}X^2(T)\left[1-\frac{2}{\ln(T^*/T)}\right] + \frac{\pi^2}{3}\rho(0)T. \tag{6.36}$$

The first term in (6.36) dominates over the linear contribution in a broad temperature range $\delta \ll T \ll |X|$, so that $C(T)$ decreases with increasing T. At $T \sim \delta$, the heat capacity $C(T)$ has a maximum, which is truly characteristic of intermediate-valence semiconductors (for example, SmB_6; see the overview of experimental findings in [112]).

A theoretical study of magnetic properties is carried out after one includes electron spin in the model by changing over from the spinless operators f^+, f to the many-electron X operators. The associated manipulations are very tedious (see [129]), and we give only the end results.

The spectrum of single-particle excitations in a magnetic field h (defined, as usual, by varying the total energy in terms of occupation numbers) takes the form

$$\varepsilon^{\alpha,\beta}_{\mathbf{k},\sigma}(h) \approx \varepsilon^{\alpha,\beta}_{\mathbf{k},\sigma}(0) - \frac{1}{2}\sigma h\left[\mu_d + \mu_f \pm (\mu_d - \mu_f)\frac{t(\mathbf{k}) - E_F}{E(\mathbf{k})}\right], \tag{6.37}$$

where $\sigma = \pm 1$ are the spin projections, and μ_d and μ_f are the magnetic moments of d and f electrons. The indirect bandgap turns out to vary with the magnetic field in a very simple way

$$\delta(h) \approx \frac{1}{2}[\min\varepsilon^{\alpha}_{\mathbf{k}\uparrow}(h) + \min\varepsilon^{\beta}_{\mathbf{k}\uparrow}(h)] \approx \delta(0) - \mu_f h. \tag{6.38}$$

At $\mu_f h \approx \delta(0)$, a transition to the metallic state occurs, observed by Sugiyama *et al.* [127] in YbB_{12} at $h \approx 200$ kOe. In Sm compounds, a similar transition must, it appears, take place in still unattainable strong fields owing to the smallness of the μ_f of the Sm ion in comparison with Yb. The decrease in the indirect bandgap leads to a strong dependence of heat capacity on field strength. Equations (6.34) and (6.38) imply

$$\frac{C(h,T)}{C(0,T)} \approx \begin{cases} \cosh(\mu_f h/T), & T \ll \delta, \\ 1 + \delta(\mu_f h)^2/T^3, & T \gg \delta,\ \mu_f h. \end{cases} \tag{6.39}$$

An increased heat capacity in a magnetic field has, for example, been observed by Berton *et al.* [133] in TmSe.

The magnetic susceptibility $\chi(T)$ can be found from the occupation numbers for d and f electrons with spin σ in a field h:

$$\chi(T) = \lim_{h\to 0}\sum_{\sigma}\sigma\frac{\mu_f n_{f\sigma} + \mu_d n_{f\sigma}}{h}. \tag{6.40}$$

For $T = 0$, the magnetic susceptibility turns out to be on the same order as the Pauli spin susceptibility

$$\chi(0) = 2(\mu_d - \mu_f)^2\rho(E_F). \tag{6.41}$$

Because the ground state of the system is a condensate of singlet excitons, for $\mu_d = \mu_f$ we have $\chi(0) = 0$. The fact that $\chi(0)$ is on the same order as the usual Pauli spin susceptibility of the transition metals, might appear strongly contradictory to data on intermediate-valence semiconductors, according to which $\chi(0)$ must be significantly greater. One should, however, bear in mind that in samarium-based semiconductors a large Van Vleck contribution is made to the susceptibility $\chi \sim \mu_f^2/\Delta$ [108] from the Sm^{2+} ion (formally nonmagnetic) because the first excited state is just $\Delta = 410$ K distant from the ground state [112]. It is this contribution (two orders of magnitude greater than the Pauli spin susceptibility) that determines the order of magnitude of χ. At the same time, it is important to take into account conduction electrons in order to determine the form of the temperature dependence of $\chi(T)$ (see below). For YbB_{12}, the corresponding van Vleck contribution is small. It is relevant to note that according to Kasaya *et al.* [123] the experimental value of $\chi(0)$ varies from specimen to specimen and is apparently determined by the impurity Yb_2O_3. Equation (6.41) implies that in ultrapure YbB_{12} specimens the value of χ for T tending to zero must fall to about the Pauli spin susceptibility.

We now turn to the case of high temperatures $T \gg \delta$. Here, the main contribution to the temperature dependence of susceptibility comes from intraband transitions. This contribution takes the form

$$\Delta\chi(T) = \frac{1}{2}\sum_{\mathbf{k}}\{\frac{-\partial f_\alpha(\mathbf{k})}{\partial\varepsilon^{\alpha}_{\mathbf{k}}} \times [\mu_f(1-\cos\theta_{\mathbf{k}}) + \mu_d(1+\cos\theta_{\mathbf{k}})]^2 + \frac{-\partial f_\beta(\mathbf{k})}{\partial\varepsilon^{\beta}_{\mathbf{k}}}[\mu_f(1+\cos\theta_{\mathbf{k}}) + \mu_d(1-\cos\theta_{\mathbf{k}})]^2 \simeq \frac{\mu_f^2}{T}\rho(0)W, \quad \cos\theta_{\mathbf{k}} \equiv \frac{t_{\mathbf{k}} - Y}{E_{\mathbf{k}}}. \tag{6.42}$$

The contribution (6.42) obeys the Curie law, and the Curie constant corresponds to the nonintegral atomic magnetic moment $\mu \equiv \mu_f[\rho(0)W]^{1/2}$. As the temperature decreases, $\Delta\chi(T)$ increases until it reaches a maximum on the order of $\rho(0)W\mu_B^2/\delta$ at $T \sim \delta$, and then suddenly falls [$\Delta\chi \sim \exp(-\delta/T)$ for $T \ll \delta$]. The contribution in question must be dominant in ultrapure YbB_{12} specimens, except at very low temperatures. In SmB_6 and SmS it appears to be responsible for the maximum in $\chi(T)$. This behavior of $\Delta\chi(T)$ was examined by Irkhin [134] within the hybridization model with special reference to d metals.

With the approach in question, one takes care of correlation effects only when one calculates a single-particle spectrum, following which one calculates the susceptibility (and the heat capacity) by the usual equations of the single-electron theory. As is known, for metallic Kondo lattices [135] this approach yields results accurate to coefficients of the Wilson number type, which is very nearly unity for the many-fold-degenerate f level and, consequently, for real systems.

The small bandgap renders the energy spectrum sensitive to both a magnetic field [see (6.38)] and a homogeneous dc electric field F. Application of a field gives rise to optical absorption at $\omega < |X|$ (the Franz–Keldysh effect [136]). For the imaginary part of the permittivity at $\omega < |X|$ Irkhin and Katsnel'son [129] derived the expression

$$\mathrm{Im}\,\varepsilon(\omega, F) \propto \exp\left[-\frac{X}{\hbar|e|Fv_F}A\left(\frac{\omega}{X}\right)\right], \tag{6.43}$$

$$A(y) = \sin^{-1}\sqrt{1-y^2} - y\sqrt{1-y^2} \approx \begin{cases} \pi/2, & y = 0 \\ \frac{4\sqrt{2}}{3}(1-y)^{5/2}, & y \to 1, \end{cases}$$

where v_F is the Fermi velocity in the initial conduction band. Hence [using (6.40)], the effective decrease in the indirect bandgap in an electric field is estimated to be

$$\delta X \sim \frac{(|e|F\hbar v_F)^{2/3}}{X^{1/3}}. \tag{6.44}$$

Thus far, we were dealing with the intrinsic semiconductor. However, Bader *et al.* [137] observed a large linear term in the heat capacity of golden SmS at low temperatures. It is therefore of interest to investigate the heavily doped case, where the chemical potential lies near the edge of the upper or lower hybridization subband.

In the symmetric case ($\Delta = 0$, $Y = 0$), the excitation spectrum has two branches $\varepsilon_\alpha \equiv -\varepsilon_\beta = \varepsilon$ [see (6.17)]

$$\varepsilon(\mathbf{k}) = \frac{1}{2}\{[t^2(\mathbf{k}) + X^2]^{1/2} - t(\mathbf{k})\}, \quad \text{and}$$
$$N(\varepsilon) = \left|\frac{dt}{d\varepsilon}\right|\rho(f(\varepsilon)) = \left(1 + \frac{X^2}{4\varepsilon^2}\right)\rho\left(\frac{X^2}{4\varepsilon} - \varepsilon\right). \tag{6.45}$$

Near the upper edge of the band one then obtains

$$\rho(t) \approx A(t_{\max} - t)^{1/2}, \tag{6.46}$$

and near the edge of the hybridization band,

$$N(\varepsilon) \approx A^*(\varepsilon_{\max} - \varepsilon)^{1/2}, \quad A^* \approx A\left(\frac{2t_{\max}}{X}\right)^2 \approx A\frac{W}{\delta}. \tag{6.47}$$

In view of the renormalization of the chemical potential μ (reckoned from the top of the band) for a given charge carrier concentration, one obtains for the renormalization of the linear term in the heat capacity

$$\frac{\gamma^*}{\gamma} = \frac{N(\mu^*)}{\rho(\mu)} = \frac{A^*}{A}\left(\frac{\mu^*}{\mu}\right)^{1/2} = \left(\frac{A^*}{A}\right)^{2/3} = \left(\frac{W}{\delta}\right)^{2/3}. \tag{6.48}$$

According to (6.48), the enhancement in the linear term of the electronic heat capacity is anywhere between 40 and 50 (the experimental figure is several hundred). The insufficient amount of enhancement may be associated, at least in part, with screening anomalies [related to the residue of the Green's function $Z \ll 1$, $\gamma \sim Z^{-1}$ (see Section 3)] because what one faces is a typical "two-peak" situation. According to Section 3.4, in order to estimate Z^{-1}, one must, above all, find the static polarization operator $\overline{\Pi}(0)$ averaged over the Brillouin zone for the spectrum (6.17). For $T = 0$ in the symmetric case ($\Delta = Y = 0$), one has

$$\overline{\Pi}(0) = \sum_{\mathbf{k},\mathbf{k}'}\frac{1}{\varepsilon_\beta(\mathbf{k}) - \varepsilon_\alpha(\mathbf{k}')} \approx \frac{\rho^2(0)X^4}{2}\int_{\delta}^{\infty}\frac{dz}{z^2}\int_{\delta}^{\infty}\frac{dy}{y^2}\frac{1}{z+y} \approx \frac{8}{3}(1+\ln 2)(\rho(0)W)^2\frac{W}{X^2}, \tag{6.49}$$

and

$$Z^{-1} \approx 1 + \frac{2\pi}{3}(1+\ln 2)\frac{e^2}{k_F^2\Omega_0}\frac{(\rho(0)W)^2}{\delta} \simeq \frac{e^2}{k_F^2\Omega_0\delta} \gg 1. \tag{6.50}$$

In summary, the generalized hybridization model adjusted for correlation effects yields a qualitative description of a wide range of properties of intermediate-valence semiconductors. In this model, some of the f electrons are rendered itinerant as they mix with the d

conduction electrons through both hybridization and exciton effects (a mobile d electron is coupled with a heavy f hole and partly entrains it).

6.5. The Localized Behavior of f Electrons in Heavy-Fermion Systems

In Sections 6.5 through 6.8 we will describe the basic properties of Kondo lattices, which are customarily identified with heavy-fermion systems. Later (see Section 6.10), it will be shown that such an identification is not always valid.

In recent years, a wide range of compounds, mainly Ce- and U-based, have been synthesized and investigated, and have come to be known as heavy-fermion systems or heavy-electron systems (see, for example, [135, 138, 139, 140]). These are $CeAl_3$, $CeCu_6$, UPt_3, and UBe_{13}, to name but a few. They owe their last name to the high value of the linear term in the electronic heat capacity $C_e = \gamma T$, $\gamma > (10^2 - 10^3)$ mJ/(mol K^2). In the free-electron approximation, this corresponds to an effective mass m^*, which is several thousand times the mass of a free electron.

For better insight into the role that f electrons play in forming a heavy-fermion system, we will compare experimental values of the linear terms in the heat capacity for heavy-fermion and some d systems with extremely high γ (see Table 6.1 and [138]).

The existence of heavy electrons at the Fermi surface of heavy-fermion systems also shows up in the high values of Pauli spin susceptibility [138] and in IR absorption spectra [141]. Noteworthy is the shape of the Fermi surface determined from the de Haas–Van Alphen effect in, for example, UPt_3 tallies with the results of conventional band-theoretic calculations, although the calculated γ differs from the experimental by a factor of several tens [139]. All of this leads one to suppose that the heavy f electrons contribute significantly to the formation of the Fermi surface and of the states near it and that in this sense they are itinerant (delocalized). Additionally, the neutron spectroscopy of local excitations (see, for example, [112, 140, 143]) reveals that in heavy-fermion systems the f level has a term structure, likewise split in the crystal field as in the case of "normal" f systems, albeit strongly diffuse. This evidence is more in favor of the localized model. Spectroscopy (notably, photoemission spectroscopy) usually demonstrates that the f band has a typical "two-peak" structure with a greater proportion of spectral density concentrated below E_F (usually by about 2 eV) and narrow peaks next to E_F (see [139, 143]); the latter can be clearly seen in IR spectra [141]. Therefore, with reference to heavy-fermion systems, one cannot say that the f states come up to E_F in the same literal sense as in the case of intermediate-valence systems. This, too, is evidence more in support of the localized f electron model. One thus runs into a situation where electronic states display a kind of localized–delocalized duality.

We will try to visualize a theoretical scheme that could describe such a specific behavior, assuming the correlation effects in the f systems to be important. A great enhancement in the effective mass, m^*/m_0, might be due to the smallness of the residue of the Green's function at a pole

$$Z = \left[1 - \frac{\partial \Sigma(E, k_F)}{\partial E}\bigg|_{E=0}\right]^{-1} \ll 1, \qquad (6.51)$$

because

$$\frac{m^*}{m_0} = \frac{1}{Z}\left[1 + \frac{m_0}{k_F}\frac{\partial \Sigma(0, k_F)}{\partial k_F}\right]. \qquad (6.52)$$

(For simplicity, we assume that the Fermi surface is a sphere of radius k_F; the energy E is reckoned from the Fermi level.) We will now state arguments proving that the term in the square brackets in (6.52) is on the order of unity. Indeed, we have, by the Landau–Luttinger theorem of the conservation of volume under the Fermi surface [71],

$$k_F = \left(\frac{n}{3\pi^2}\right)^{1/3}, \qquad (6.53)$$

where n is the number density of electrons. The chemical potential μ is then given (see, for example, [71]) by

$$\mu = \frac{k_F^2}{2m_0} + \Sigma(0, k_F). \qquad (6.54)$$

Therefore,

$$1 + \frac{m_0}{k_F}\frac{\partial \Sigma(0, k_F)}{\partial k_F} = \frac{m_0}{k_F}\frac{\partial \mu}{\partial k_F} = \left(\frac{\partial \mu}{\partial n}\right)^* \Big/ \left(\frac{\partial \mu}{\partial n}\right)_0 = \kappa_0/\kappa^*, \qquad (6.55)$$

where the asterisk denotes the quantity renormalized by many-particle effects, the subscript 0 stands for the initial value, and $\kappa = (1/n^2)(\partial n/\partial \mu)$ is the compressibility. There is no experimental evidence that would suggest any significant anomalies in the bulk modulus

Table 6.1. Linear term in electronic heat capacity [mJ/(mol K^2)] in heavy-fermion systems, some record-breaking values (given for comparison) of γ for d-systems [138]; results of conventional band-theoretic calculations for three systems (the second line for γ_T)

Compound	γ, mJ/(mol K^2)	γ_T
$CeCu_6$	1450	–
$CeAl_3$	1600	–
$CeCu_2Si_2$	1100	11.4
UBe_{13}	1100	33.3
UCd_{11}	840	–
U_2Zn_{17}	500	–
UPt_3	450	14.9
V_3Ga	33	–
$V_{1.97}O_3$	54	–
$TiBe_2$	56	–

of heavy-fermion systems (except the nonmonotonic behavior of its temperature dependence within a few percent as, for example, in CeB_{13} [144]).

One may thus associate the large effective mass with the first factor in (6.52) rather than with the second. The small Z implies a small "pole" (quasiparticle) contribution to the spectral density of the f electrons

$$A(\mathbf{k}, E) = -\frac{1}{\pi}\mathrm{Im}\, G(\mathbf{k}, E) = Z\delta\left(E - \frac{k_F}{m^*}(k - k_F)\right) + \tilde{A}(\mathbf{k}, E), \qquad (6.56)$$

where for the Green's function of the f electrons, $G(\mathbf{k}, E)$, we adopted the formally exact presentation

$$G(\mathbf{k}, E) = \frac{Z}{E - \frac{k_F}{m^*}(k - k_F)} + \tilde{G}(\mathbf{k}, E) \qquad (6.57)$$

in which the nonpole part $\tilde{G}(\mathbf{k}, E)$ and the contribution to the spectral density $\tilde{A}(\mathbf{k}, E)$ are written as separate terms. To obtain the experimentally observed two-peak picture of this density, it will suffice to assume that $\tilde{G}(\mathbf{k}, E)$ and, consequently, $\tilde{A}(\mathbf{k}, E)$ depend only slightly on k and, similarly to the function E, have a maximum at $E \equiv -E_0 < 0$. Then, in the close vicinity of E_F,

$$|E| \lesssim E^* \equiv E_F\frac{m}{m^*} = E_F Z, \qquad (6.58a)$$

the dominant term is the pole contribution to A [the first term in (6.56)], and one has a picture of heavy, but itinerant quasiparticles that take part in forming the Fermi surface. However, the complete contribution of this term to the spectral density is small ($\sim Z$), and it is therefore immaterial in quantities such as total energy, elastic modulus, etc. The behavior of the f system as a whole, that is, on an energy scale greater than E^*, is determined by the second contribution to (6.57), which describes the localized f level "buried" rather deeply below E_F (by an amount $|E_0| \gg E^*$), which has a term structure, split in the crystal field, etc. An applicable diagram of the spectral density is shown in Fig. 6.5.

It is of interest to compare this picture with the conditions that define the applicability of the adiabatic approximation in metals [145, 146]. For them, the energy scale is on the order of the average phonon frequency ω_{ph}. Therefore, for $|E| \leq \omega_{ph}$, the renormalization of Z does not produce a small ω_{ph}/E_F (that is, on the order of unity). At the same time, the effect of phonons on the integral characteristics in terms of this parameter is small. In heavy-fermion systems, the role of ω_{ph} is to some extent played by E^* with the important difference that $Z \sim 1/E^* \gg 1$ for $|E| < E^*$. In both cases, $\Sigma(E)$ abruptly changes in a narrow layer near E_F (Fig. 6.3). In the case of electron–phonon interaction, however, the total change Σ itself is on the order of ω_{ph} (and, therefore, $Z \sim 1$), whereas in heavy-fermion systems, $\Delta\Sigma(E) \sim E_F$.

As is known [1, 100], however, Z does not enter into the magnetic susceptibility χ directly. Therefore, if one

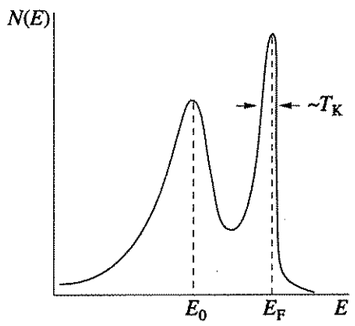

Fig. 6.5. Sketch of the density of electronic states in Kondo lattices.

wishes to explain why not only the linear term in the heat capacity γ, but also the magnetic susceptibility χ take on large values, one is forced to suppose that the interaction leading to small Z is spin-dependent (in contrast to the case of electron–phonon interaction). The most popular and best investigated model of heavy-fermion systems, which involves precisely this interaction, is the Kondo lattice model (see, for example, [135, 139]).

The Kondo effect (see the reviews [147 - 149]) arises when conduction electrons in a metal are scattered on a magnetic impurity, provided "antiferromagnetic" exchange interaction between the electron and impurity spins is $I < 0$. If so, specific many-particle effects cause conduction electrons and the impurity to form a coupled state with an energy on the order given by

$$T_K = W\exp\left[-\frac{1}{\rho(E_F)|I|}\right] \qquad (6.58b)$$

(the Kondo temperature). At $T > T_K$, the Kondo effect shows up as contributions, logarithmic with respect to temperature, to resistivity, heat capacity, magnetic susceptibility, and other properties, as abnormally large thermo-emf, etc. [147].

At $T < T_K$, an extremely unusual situation arises. The localized magnetic moment (which shows up at $T > T_K$ as the Curie law $\chi_i \sim 1/T$ for the impurity contribution to the susceptibility and makes the contribution ln 2 to the entropy) seems to disappear (is balanced out), thus giving way to a quasilocal level at E_F in the fermionic (electronic) energy structure. This situation is known as the local Fermi liquid [150]. The reason is that, in these circumstances, the impurity contributions to the heat capacity $C_i(T)$ and the susceptibility $\chi_i(T)$ behave as they would in Fermi systems: $C_i(T) = \gamma_i T$ and $\chi_i(T) \sim \gamma_i = \mathrm{const}$ for T tending to zero. Then, as for the ordinary Fermi liquid theory [1], one may write

$$\frac{\chi_i}{\chi_0} = \frac{\gamma_i}{\gamma_0}\frac{1}{1 + B_0}, \qquad (6.59)$$

where χ_0 and γ_0 refer to the conduction electrons, and B_0 is the exchange interaction constant. For an impurity with spin 1/2, the enhancement factor $(1 + B_0)^{-1}$ is 2. (This is known as Wilson's relation, derived by him

from numerical calculations and explained within the local Fermi liquid theory by Noziéres [150].) The values of γ_i and χ_i themselves are great, being proportional to $1/T_K$. This behavior has been investigated theoretically by various techniques, including exact solutions of appropriate models [149]. Most revealingly, it can be interpreted as being due to the fact that E_F acquires a quasilocal impurity peak of width T_K and of height $1/T_K$ (the so-called Suhl–Abrikosov resonance) [147 - 150]. In the Kondo center lattice, this resonance must split (as discussed in Section 6.3), but the energy scale, which is on the order of T_K, remains unchanged. With reference to heavy-fermion systems, it is natural to identify T_K with E^*. In effect, heavy-fermion systems are usually regarded as Kondo lattices, with the Ce or U ions acting as Kondo centers.

We will now demonstrate with reference to some formal model that the physical picture of the Kondo lattice does agree with the phenomenological description of heavy-fermion systems set forth above.

This picture has been the subject of a large number of dedicated studies, which have used various models. The most popular among them is the so-called N-fold-degenerate model proposed by Anderson in the limit of infinite repulsion of f electrons and a large degeneracy multiplicity N. (Below, we will call it simply the Anderson model; see, for example, [139, 151] and their references.) The Hamiltonian in this model takes the form

$$\hat{H} = \sum_{\mathbf{k},m} \varepsilon(\mathbf{k}) c^+_{\mathbf{k}m} c_{\mathbf{k}m} + \sum_m \varepsilon_f X_0^{mm} + V \sum_{\mathbf{k},m} (c^+_{\mathbf{k}m} X^{0m}_{-\mathbf{k}} + X^{m0}_{-\mathbf{k}} c_{\mathbf{k}m}), \tag{6.60}$$

where $\varepsilon(\mathbf{k})$ is the conduction electron spectrum; ε_f is the position of the f level as reckoned from the Fermi level ($\varepsilon_f < 0$), $m = 1, 2, ..., N$; and $X^{\alpha\beta}_{\mathbf{k}}$ is the Fourier transform of the X operators describing the f electrons with a wave vector $\mathbf{k}$. Furthermore, $|0\rangle$ is the state without f electrons, $|m\rangle$ is the state with one f electron having an orbital quantum number m, and V is the hybridization parameter. For $\rho(E_F)V^2 \sim |\varepsilon_f|$, this model describes the intermediate-valence state (see Sections 6.3 and 6.4). For

$$\rho(E_F)V^2 \ll |\varepsilon_f|, \tag{6.61}$$

one can use a canonical transformation that eliminates terms linear in V and reduces it [147, 149] to the s–f exchange model with

$$I = V^2/\varepsilon_f < 0 \tag{6.62}$$

and the corresponding value of T_K [see (6.58b)]. Then $T_K \ll W$, with an exponential smallness in terms of V^2. Perhaps the most elegant and simplest way to consider the model (6.60) is to introduce the so-called auxiliary boson (see, for example, [151]). Indeed, the f electrons described by the creation operators $X^{m0}_{-\mathbf{k}}$ (and not by Fermi operators!) are thus not Fermi particles. The point is that, owing to the infinity of repulsion at one site, they are subject, in addition to the Pauli exclusion principle, to an exclusion principle specific for groups of states. It requires that if a state with a given $|m\rangle$ is occupied, the remaining states must be free. As demonstrated (see Sections 5.2 and 5.3), the X operators satisfy certain commutation and anticommutation relations. One can satisfy all of these relations and pass from the X operators to the "true" fermions f^+_{mi} and f_{mi} if one additionally introduces a boson field b^+_i and b_i (where i is the label for sites)

$$X^{00}_i = b^+_i b_i, \quad X^{m'm}_i = f^+_{im'} f_{im}, \quad X^{0m}_i = b_i f_{im}, \quad X^{m0}_i = f^+_{im} b^+_i. \tag{6.63}$$

It is understood that b^+, b, f^+, and f satisfy the usual commutation and anticommutation relations applicable to Fermi and Bose fields, and the space of states in question is limited by the requirement

$$\hat{Q}_i = \sum_m f^+_{im} f_{im} + b^+_i b_i = 1. \tag{6.64}$$

In view of the representation (6.63) and subject to the additional condition (6.64), one can write the statistical sum of the model (6.60) in terms of a functional integral [151]. In the limit of N tending to infinity, the latter can be calculated by the saddle-point method. This basically reduces to the replacement of the operators $\hat{b}^+_i$ and $\hat{b}_i$ by the number $r \equiv \langle \hat{b}_i \rangle$ independent of i. Then the Hamiltonian (6.60) reduces to the effective hybridization model

$$\hat{H} = \sum_{\mathbf{k},m} [\varepsilon(\mathbf{k}) c^+_{\mathbf{k}m} c_{\mathbf{k}m} + (\varepsilon_f + \lambda) f^+_{\mathbf{k}m} f_{\mathbf{k}m} + Vr(f^+_{\mathbf{k}m} c_{\mathbf{k}m} + c^+_{\mathbf{k}m} f_{\mathbf{k}m}) + \lambda r^2], \tag{6.65}$$

where λ is a Lagrangian multiplier (also independent of i in the limit of N tending to infinity) introduced in order to satisfy the conditions (6.64) in the mean $\langle \hat{Q}_i \rangle = 1$. Then, the parameters λ and r can be determined subject to these conditions by minimizing the free energy (see [139, 151]). As a result, both the renormalized position of the f level ($\tilde{\varepsilon}_f = \varepsilon_f + \lambda$) and the effective resonance width $\Gamma = \pi\rho(E_F)V^2 r^2$ turn out to be on the order of T_K. Thus, an energy structure arises near E_F, as it does in the hybridization model, with a characteristic scale proportional to T_K. At the same time, the energy structure of the density of f states is mainly defined by the hybridization model, in which the f level takes up an initial position ε_f and has an initial width $\Gamma = \pi\rho(E_F)V^2$. The electronic Green's function does take the form of (6.57) with $Z \sim T_K/W$. It can also be shown [139] that in the Anderson model the formation of the Kondo structure in the density of states near E_F is related to the partial delocalization of f electrons also in the sense that the occupancy of the f level is other than unity

$$1 - n_f = Z \ll 1. \tag{6.66}$$

If the condition (6.61) is violated, then T_K and, consequently, Z increases and n_f decreases. This is accompanied by a gradual transition to the intermediate valence state where $|\varepsilon_f| \sim T_K$, and the two-peak structure no longer exists; instead, a single energy scale is formed near E_F. In the Anderson model, T_K does the same job as δ in Section 6.4.

With increasing T, the approximation in question entails a phase transition of the second kind at $T \sim T_K$ for r tending to zero. Such a transition is a drawback of the approximation, but it can be corrected by taking into account the higher orders of the parameter $1/N$. Such corrections are, however, responsible for terms of the form $\ln T$ that appear in the observables at $T > T_K$ [151].

With a change-over from the Anderson to the s–f-exchange model [152, 153] (by, for example, letting V^2 and ε_f tend to infinity with their ratio held constant, $V^2/\varepsilon_f = I = \text{const}$), the localization problem would, it might seem, cease to exist because then $n_f = 1$ (the homopolarity condition for the f system). Then it is even more striking that, as shown in [154], this model can be reduced to the effective hybridization model with a spectrum structure analogous to the Anderson model [although the relation (6.66) is not satisfied]. In this sense, the situation still looks like one of a partial delocalization [to the extent of T_K/E_F] of f electrons owing to their interaction with conduction electrons, but such that the homopolarity condition is also satisfied. This illustrates how formidable a task it is to give a clearly evident description of the quantum behavior of many-particle systems.

It is worthwhile comparing how things stand with heavy-fermion systems and the d systems. In the latter case (as with any other many-particle Fermi systems), it is also possible to separate the contributions into "quasiparticle" (itinerant) and "nonquasiparticle" ones. However, because $Z \sim 1$ and $E^* \sim E_F$, both types are generally quite significant over the entire d band (except the vicinity of E_F, where itinerant contributions are always dominant, provided the Fermi surface exists.) These matters were discussed in Ch. 5. In a heavy-fermion system, a clear demarcation line is drawn between the itinerant and localized traits in the behavior of f electrons in terms of energy. One may say that in a heavy-fermion system the f electrons behave as itinerant, albeit very heavy, quasiparticles in the narrow layer of the order of T_K located near E_F, but they behave as localized ones on a larger energy scale.

We now turn to a more systematic scrutiny of the Kondo lattice model for heavy-fermion systems.

6.6. The Problem of Kondo Magnets. A Roundup of Experimental Findings[4]

Until now we did not touch upon the magnetic properties of heavy-fermion systems (except for a few remarks on their high magnetic susceptibility). Meanwhile, they are quite unusual.

It was traditionally believed that the competition between the indirect spin–spin RKKY interaction and the Kondo screening of the magnetic moment by conduction electrons could give rise to either a magnetic state or a nonmagnetic Kondo lattice state [155]. Recently, it has, however, been found that many substances customarily placed in the latter class either do change to a magnetically ordered state at low temperatures or display pronounced spin fluctuations. For example, antiferromagnetic order with a very small saturation magnetic moment M_0 has been detected in the classical "nonmagnetic" heavy-fermion systems, such as UPt_3 ($M_0 \sim 0.02\mu_B$, $T_N \sim 5$ K) [157], $CeAl_3$, $CeCu_2Si_2$, and $CeInCu_2$ [140, 158], and also in UBe_{13} under a pressure of about 25 kbar [159].

Still more recently, Kleiman *et al.* [160] have detected antiferromagnetism in UBe_{13} under normal pressure. The compound UPt_3 changes to an ordinary antiferromagnet with a fairly high M_0 upon the addition of 5% Pd instead of Pt, or of Th instead of U [140], whereas $CeCu_6$ does so upon the addition of a small amount of Ag [161]. Earlier, the discovery [140] of a great number of "Kondo" antiferromagnets (such as $UAgCu_4$, U_2Zn_{17}, UCd_{11}, UCu_5, $CeAl_2$, $CeAg_2Ge_2$, and TmS) and several "Kondo" ferromagnets (such as $CeRh_3B_2$, $CeSi_x$ for $x \lesssim 1.85$, $CeSi_{2-x}Ge_x$, $CeNi_xPt_{1-x}$, $Ce_xLa_{1-x}Ge_2$, and Ce_4Bi_3) was reported. The impression is that in the ground state "Kondo lattices" have, as a rule, magnetic order or exist "at the brink" of order, and that their magnetic properties are extremely sensitive to external factors (pressure, alloying, etc.).

In experiment, the class of Kondo magnets is usually identified on the basis of the following features.

1. The logarithmic dependence of resistivity on temperature (above the Kondo temperature), similar to what is observed in the classical dilute Kondo systems [147]. This dependence is shown in Fig. 6.6 for $Ce_xLa_{1-x}Ge_2$ [162].

2. The low magnetic entropy $S(T_m)$ at the magnetic ordering point T_m, related to the Kondo suppression of low-temperature heat capacity [147, 149]. As an example, for $Ce_xLa_{1-x}Ge_2$, where the ground state of the Ce ion is a doublet, in the absence of the Kondo effect, $S(T_m)$ would be about $R\ln 2$. Experimental evidence [162] indicating that $S(T_m) \ll R\ln 2$ is given in Fig. 6.7.

3. The low saturation moment in comparison with the "high-temperature" moment M_C in the Curie constant, a fact which places Kondo magnets closer to weak itinerant magnets. For example, for $CeRh_3B_2$ one has $M_0 \approx 0.37\mu_B$, $M_C \approx 3\mu_B$ ($M_C \approx 2.54\mu_B$ for the Ce^{3+} ion).

4. The paramagnetic Curie temperature θ is negative even for ferromagnets and significantly greater in absolute value than T_m. For $CeRh_3B_2$, $\theta \approx -370$ K, whereas the Curie temperature is $T_C = 115$ K. This is because a major contribution to the susceptibility comes from the single-impurity Kondo effect ($\chi(0) \sim 1/T_K$) and θ is

[4] This and the subsequent sections are based on a paper by Irkhin and Katsnel'son [156].

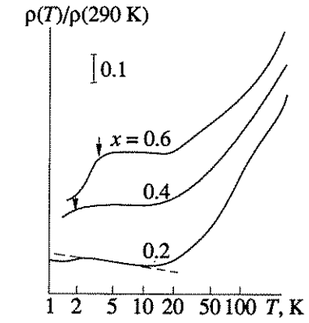

Fig. 6.6. Temperature dependence of the electrical resistivity for $Ce_xLa_{1-x}Ge_2$. The curves are shifted relative to one another along the ordinate axis. The arrows label the positions of T_C. The abscissas axis uses a logarithmic scale. The system is ferromagnetic at $0.4 \le x \le 1.0$.

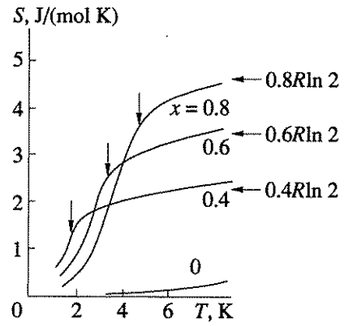

Fig. 6.7. Temperature dependence of entropy for $Ce_xLa_{1-x}Ge_2$. The arrows label the positions of T_C.

thus not a characteristic of short-range magnetic order. Simple theoretical estimation yields $\theta \approx -4T_K$.

In an analysis of the properties of Kondo magnets, a fundamental point is the ratio between T_m and the Kondo temperature. The latter determines the temperature and energy scale on which a crossover takes place from the free local moment condition to the tight binding condition. This ratio can vary from one system composition to another. The experimental concentrational dependences $T_C(x)$, $T_K(x)$, and $M_0(x)$ for $CeNi_xPd_{1-x}$ are given in Fig. 6.8 [163]. As a rule (including heavy-fermion systems, where $T_K \lesssim 12$ K), $T_K \gtrsim T_m$. Cerium and uranium magnets with $T_K \ll T_m$ also were reported, such as $UAgCu_4$ ($T_N = 18$ K, $T_K \sim 3$ K) [164], and $CeAl_2Ga_2$ [165]. The latter represents a transition to ordinary magnets with a completely suppressed Kondo effect.

Finally, a few words are in order about the increase in the "stiffness" of spin excitations with decreasing temperature [165], observed in U_2Zn_{17} and interpreted as a manifestation of the renormalization (enhancement) of the RKKY interaction at low temperatures [140].

Thus, empirically, Kondo magnets are close in many properties (above all, in the low saturation magnetization and T_m) to weak itinerant magnets such as Ni_3Al and $ZrZn_2$. However, in the *d* system, we analyzed (see Ch. 4) the formation of magnetic order and localized magnetic moments from band-theoretic considerations. By contrast, for Kondo magnets, it is more natural to reverse the problem: one should consider the destruction of local magnetic moments and a transition to the "quasiband" behavior owing to the Kondo cancellation of local magnetic moments (see Section 6.5). Moreover, it is important to understand why this cancellation is very strong but not yet complete in most cases. A likely angle of attack on the problem, central to the understanding of the nature of the magnetism of Kondo systems, has been proposed in [184]. In Section 6.7, we will consider the behavior of the systems at $T > T_K$ within the perturbation theory; Section 6.8 will be concerned with the condition for the formation of the magnetic state as visualized in [184]; and Section 6.9 will examine the properties of that state at $T = 0$.

6.7. Cancellation of Magnetic Moments from the High-Temperature Side

As was noted in Section 6.5, at $T \gg T_K$, where T_K is the Kondo temperature, the Kondo effect shows up in the logarithmic temperature dependence of the corrections to various physical quantities, including the magnetic susceptibility χ and, as a consequence, the magnitude of local magnetic moments. In Kondo lattices, however, this logarithmic behavior is "truncated" at the characteristic energy of spin–spin interaction, that is, at the spin dynamic frequency $\bar{\omega}$. In turn, this frequency is renormalized owing to the Kondo effect. These effects can be calculated within the *s–f* exchange model using the theory of perturbations in terms of the *s–f* exchange parameter. In more detail, the applicable calculations were done in [167]. Here, we will only outline the computational scheme used and discuss the results.

We will proceed from the *s–f* exchange model with the Hamiltonian

$$\hat{H} = \hat{H}_0 + \hat{H}_{sf}; \quad \hat{H}_0 = \sum_{\mathbf{k},\sigma} \varepsilon_{\mathbf{k}} c^+_{\mathbf{k}\sigma} c_{\mathbf{k}\sigma} + \hat{H}_f;$$
$$\hat{H}_{sf} = -I \sum_{\mathbf{k},\mathbf{q};\alpha,\beta} \mathbf{S}_{\mathbf{q}} \hat{\boldsymbol{\sigma}}_{\alpha\beta} c^+_{\mathbf{k}+\mathbf{q},\alpha} c_{\mathbf{k}\beta}, \tag{6.67}$$

where I is the *s–f* exchange parameter, $c^+_{\mathbf{k},\sigma}$ are the electron creation operators with spin projection $\sigma = \uparrow\downarrow(\pm)$, σ are the Pauli matrices, $\mathbf{S}_{\mathbf{q}}$ is the Fourier component of the localized spin operators, and

$$\hat{H}_f = -\sum_{\mathbf{q}} J_{\mathbf{q}} \mathbf{S}_{-\mathbf{q}} \mathbf{S}_{\mathbf{q}} \tag{6.67a}$$

is the Heisenberg Hamiltonian of the localized spin subsystem. Actually, the site–site interaction is a result of an indirect RKKY interaction via conduction electrons and is proportional to I^2 [108]. For our purposes, however, it is convenient to define $\hat{H}_f$ explicitly.

We can determine the inhomogeneous magnetic susceptibility $\chi_{\mathbf{Q}}$ with a wave vector $\mathbf{Q}$ by the Kubo equation [64]

$$\chi_{\mathbf{Q}} = (S^z_{\mathbf{Q}}, S^z_{-\mathbf{Q}})$$
$$\equiv \int_0^\beta d\lambda \left\langle \exp(\lambda H) S^z_{\mathbf{Q}} \exp(-\lambda H) S^z_{-\mathbf{Q}} \right\rangle, \quad \beta = T^{-1}. \tag{6.68}$$

For the homogeneous static susceptibility ($\mathbf{Q} = 0$) in the second order with respect to I, we have

$$\chi = \frac{S(S+1)}{3T} + \chi^{(2)},$$

where

$$\chi^{(2)} = \int_0^\beta d\lambda \int_\lambda^\beta du_1 \int_0^\lambda du_2$$
$$\times \left\langle [S^z_0 \exp(u_1 H_0) H_{sf} \exp(-u_1 H_0)] \right.$$
$$\left. \times [S^z_0 \exp(u_2 H_0) H_{sf} \exp(-u_2 H_0)] \right\rangle, \tag{6.69}$$

(compare with the single Kondo impurity case [147]). Calculating the commutator in (6.69) and introducing the spectral density with the Hamiltonian $\hat{H}_f$

$$\tilde{J}_{\mathbf{q}}(\omega) = -\frac{1}{\pi} N_B(\omega) \operatorname{Im} \left\langle S^z_{\mathbf{q}} | S^z_{-\mathbf{q}} \right\rangle_\omega,$$

where $N_B(\omega)$ is the Bose function, we find

$$\chi^{(2)}_{\text{sing}} = -\frac{4I^2}{T} \sum_{\mathbf{pq}} \int_{-\infty}^{\infty} d\omega \tilde{J}_{\mathbf{p}-\mathbf{q}}(\omega) \frac{f_{\mathbf{p}}(1-f_{\mathbf{q}})}{(\varepsilon_{\mathbf{p}} - \varepsilon_{\mathbf{q}} + \omega)^2}, \tag{6.70}$$

where $f_{\mathbf{p}} = f(\varepsilon_{\mathbf{p}})$ and $f_{\mathbf{q}} = f(\varepsilon_{\mathbf{q}})$ are the Fermi distribution functions. Within the diffusion approximation, such that

$$J_{\mathbf{q}}(\omega) = \frac{S(S+1)}{3\pi} \frac{Dq^2}{\omega^2 + (Dq^2)^2},$$

where D is the spin diffusion coefficient, we obtain

$$\chi^{(2)}_{\text{sing}} = \frac{S(S+1)}{3T} 2I^2 \rho^2 \int dE dE' \frac{\partial f(E)}{\partial E} \frac{\partial f(E')}{\partial E'}$$
$$\times \ln \frac{(E+E')^2 + d^2}{W^2} \tag{6.71}$$
$$\approx \frac{S(S+1)}{3T} 2I^2 \rho^2 \ln \frac{T^2 + d^2}{W^2},$$

where $d = 4Dk_F^2 \simeq \bar{\omega}$, ρ is the density of states at the Fermi level, and W is the width of the conduction band, so that the spin dynamics renders the singularity diffuse.

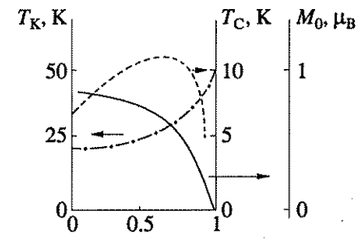

Fig. 6.8. Schematic representation of concentration dependences of saturation magnetization (solid curve), T_C (dashed curve), and T_K (dash-and-dot curve) for $CeNi_xPd_{1-x}$.

For $\mathbf{Q} \neq 0$ and in the absence of dynamics, instead of (6.70), we obtain from (6.69)

$$\chi^{(2)}_{\mathbf{Q}} = -\frac{4I^2}{T} \sum_{\mathbf{p},\mathbf{q}} \frac{f_{\mathbf{p}}(1-f_{\mathbf{q}})}{(\varepsilon_{\mathbf{p}} - \varepsilon_{\mathbf{q}})} \left\langle S^z_{\mathbf{p}-\mathbf{q}-\mathbf{Q}} S^z_{\mathbf{q}-\mathbf{p}+\mathbf{Q}} \right\rangle. \tag{6.72}$$

By changing to real space

$$\chi_{\mathbf{Q}} = \int \mathbf{dr} \exp(i\mathbf{Q}\mathbf{r}) K(\mathbf{r}), \quad K(\mathbf{r}) = \beta \left\langle S^z S^z(\mathbf{r}) \right\rangle, \tag{6.73}$$

(the last equality holds for $T \gg T_m$ and also for any $T > T_m$ in the classical approximation), and by isolating the singular terms, we find

$$K^{(2)}(\mathbf{r}) = -4I^2 \rho^2 K(\mathbf{r}) a_r^2 \ln \frac{W}{T}, \tag{6.74}$$

$$a_r = \langle \exp(i\mathbf{k}\mathbf{r}) \rangle_{E_F} = \frac{\sin(k_F r)}{k_F r}. \tag{6.75}$$

The expression for inhomogeneous susceptibility in the presence of spin–spin exchange interaction takes the form

$$\bar{\chi}_{\mathbf{Q}} = \frac{\chi_{\mathbf{Q}}}{1 - J_{\mathbf{Q}} \chi_{\mathbf{Q}}} \approx \chi_{\mathbf{Q}} (1 + J_{\mathbf{Q}} \chi_{\mathbf{Q}}). \tag{6.76}$$

In view of the correction (6.74), equation (6.76) yields the contribution

$$\frac{\delta K(\mathbf{r})}{K(\mathbf{r})} = \frac{C(T)}{T} J(\mathbf{r}, T), \tag{6.77}$$

which contains the effective value of the Curie constant

$$C(T) = \frac{S(S+1)}{3} (1 - 4I^2 \rho^2 \ln \frac{W}{T}) \tag{6.78}$$

and the spin–spin exchange parameter

$$J(\mathbf{r}, T) = J(\mathbf{r}) \left[1 + 4I^2 \rho^2 (1 - a_r^2) \ln \frac{W}{T} \right]. \tag{6.79}$$

Expression (6.79) is similar to the one derived by Abrahams and Varma [140] for the two-impurity problem. By analogy with (6.71), the spin dynamics leads to the change $T \to \max(\bar{\omega}, T)$ in (6.79). Thus, the Kondo effect enhances spin–spin exchange interactions with decreasing temperature. As follows from our consideration, this renormalization holds not only for the RKKY interaction but also for exchange interactions of any other nature (such as direct exchange, Kramers indirect exchange).

Previously, we investigated how the spin dynamics influences the Kondo effect. To develop a self-consistent picture (within the perturbation theory), it is important to consider the converse, that is, how the Kondo effect influences the characteristic frequency of spin fluctuations. In the paramagnetic phase, the latter can be estimated from the second moment of dynamic susceptibility

$$\left\langle \omega_{\mathbf{Q}}^2 \right\rangle = \frac{L_{\mathbf{Q}}}{\chi_{\mathbf{Q}}} \equiv \frac{\dot{S}_{\mathbf{Q}}^z, \dot{S}_{-\mathbf{Q}}^z}{S_{\mathbf{Q}}^z, S_{-\mathbf{Q}}^z}. \tag{6.80}$$

By expanding (6.80) as a series in terms of I (with $J_{\mathbf{Q}}$ taken as not being small) and neglecting the spin dynamics in the correlators ($T^2 \gg \left\langle \omega_{\mathbf{Q}}^2 \right\rangle$), we obtain

$$\begin{aligned} L_{\mathbf{Q}} &= L_{\mathbf{Q}}^{(0)} + L_{\mathbf{Q}}^{(2)}, \\ L_{\mathbf{Q}}^{(0)} &= \left[\frac{2}{3} S(S+1)\right]^2 \beta \sum_{\mathbf{q}} (J_{\mathbf{Q}-\mathbf{q}} - J_{\mathbf{q}})^2; \end{aligned} \tag{6.81}$$

$$\begin{aligned} L_{\mathbf{Q}}^{(2)} &= 4I^2 \rho^2 \beta \ln \frac{W}{T} \bar{F}_{\mathbf{k}-\mathbf{k}'}, \\ F_{\mathbf{q}} &= \sum_{\alpha} \left\langle [S_{\mathbf{Q}}^z, S_{\mathbf{q}}^{\alpha}] S_{-\mathbf{Q}}^z S_{-\mathbf{q}}^{\alpha} \right\rangle, \end{aligned} \tag{6.82}$$

where the overscribed bar denotes averaging over the Fermi surface with respect to $\mathbf{k}$, $\mathbf{k}'$

$$\bar{\Phi}_{\mathbf{k},\mathbf{k}'} = \rho^{-2} \sum_{\mathbf{k},\mathbf{k}'} \delta(\varepsilon_{\mathbf{k}}) \Phi_{\mathbf{k},\mathbf{k}'},$$

for an arbitrary function Φ. By evaluating $S_{\mathbf{Q}}^z = i[H_f, S_{\mathbf{Q}}^z]$, we find for $T \gg T_m$

$$\bar{F}_{\mathbf{k}-\mathbf{k}'} = -(2-\alpha_{\mathbf{Q}}) \sum_{\mathbf{p}} (J_{\mathbf{Q}-\mathbf{p}} - J_{\mathbf{p}}) \left[\frac{2}{3} S(S+1)\right]^2; \tag{6.83}$$

$$\alpha_{\mathbf{Q}} = \sum_{\mathbf{p}} (J_{\mathbf{p}} - J_{\mathbf{Q}-\mathbf{p}}) \frac{(\bar{J}_{\mathbf{p}-\mathbf{k}+\mathbf{k}'} - \bar{J}_{\mathbf{Q}-\mathbf{p}+\mathbf{k}-\mathbf{k}'})}{\sum_{\mathbf{q}} (J_{\mathbf{Q}-\mathbf{q}} - J_{\mathbf{q}})^2} \tag{6.84}$$

$$= \frac{\sum_{\mathbf{r}} J^2(\mathbf{r}) a_{\mathbf{r}}^2 (1 - \cos(\mathbf{Q}\mathbf{r}))}{\sum_{\mathbf{r}} J^2(\mathbf{r})} (1 - \cos(\mathbf{Q}\mathbf{r})).$$

Equation (6.84) implies that $0 < \alpha_{\mathbf{Q}} < 1$. Substituting (6.81) - (6.83) and (6.72) in (6.80) gives

$$\begin{aligned} \left\langle \omega_{\mathbf{Q}}^2 \right\rangle &\approx \frac{4}{3} S(S+1) \sum_{\mathbf{q}} (J_{\mathbf{Q}-\mathbf{q}} - J_{\mathbf{q}})^2 \\ &\times \left[1 - 4I^2 \rho^2 \ln \frac{W}{T} (1 - \alpha_{\mathbf{Q}})\right]. \end{aligned} \tag{6.85}$$

Thus, the average frequency of spin fluctuations in the paramagnetic phase decreases with decreasing temperature owing to the Kondo effect. The net decrease is related to the fact that the moment is cancelled ($\langle S^2 \rangle$ is decreased) by a far larger amount than the effective exchange interaction (6.79) is enhanced.

As already noted, a crucial question in the theory of Kondo magnets is why the magnetic moment is not cancelled out completely. Generally, two mechanisms may be involved here. One is the incomplete cancellation of individual moments (for $S > n/2$, where n is the number of scattering channels for conduction electrons, we have $S \to S - n/2$ for T tending to zero [149]), and the other is multi-impurity effects. Apparently, the first mechanism is effective in the TmS Kondo lattice and in the TmSe intermediate-valence systems, where both feasible states of the Tm ion are magnetic. However, this mechanism is unable to explain the situation with a small magnetic moment for $T = 0$, which, as has been noted, is typical. Therefore, one may suppose that the Kondo effect and magnetic order owe their existence to spin–spin interactions or, in other words, the spin dynamics. The above results, derived within the perturbation theory, enable one to describe how the state of Kondo magnetism is formed in qualitative terms.

Suppose we have the paramagnetic phase and lower the temperature. As a result, the magnetic moment will be "cancelled." In contrast to the single-impurity situation, however, the degree of cancellation will be determined by $T + a\bar{\omega}$ (where a is on the order of unity) or $(T^2 + \bar{\omega}^2)^{1/2}$, rather than by T. Importantly, $\bar{\omega}$ likewise decreases with decreasing temperature. This process cannot be described analytically within the perturbation theory. If, however, one assumes a single energy scale on the order of T_K (which is what distinguishes the Kondo systems), one must assume that $\bar{\omega}$ is proportional to T_K at $T \lesssim T_K$. Indeed, as one can see from numerous experimental data on the quasielastic scattering of neutrons in the Kondo systems (see Ch. 7 in [140]) for T tending to zero, the characteristic width of the central peak is $\Gamma \sim \bar{\omega} \sim T_K$. Thus, the cancellation of the magnetic moment terminates somewhere at the boundary of the tight-binding region, and a finite (although, perhaps, small) saturation moment is formed.

Outwardly, the above mechanism whereby magnetism with small M_0 is formed radically differs from the conventional one, where weak itinerant magnets are assumed to be located in the close vicinity of the Stoner instability [108]. One should bear in mind, however, that in the Kondo systems both the energy spectrum of new Fermi quasiparticles formed under tight-binding conditions and the effective interaction between them undergo strong renormalizations. It is all but obvious that the Stoner criterion is inapplicable when used with the initial parameters characteristic of the Kondo magnets.

A continuous transition exists between the Kondo systems and the "conventional" systems of itinerant electrons (Pauli paramagnets may be regarded as systems with high T_K proportional to E_F). This prompts one

to wonder about the role of many-particle effects in the case of "classical" weak itinerant magnets such as $ZrZn_2$ and Sc_3In as well. It might seem that the very closeness to the Stoner instability point, that is, the smallness of M_0, is determined not so much by the initial density of electronic states and the initial interaction parameter, as by their renormalization. In view of this, it would be of interest to try to describe weak itinerant magnets by looking at them not from the "band" angle, as is usually done, but from the angle of local magnetic moments, which can be all but cancelled. Because, as is customary to class them at present, the weak itinerant ferromagnets include not only $ZrZn_2$, but also $CeRh_3B_2$ and $CeSi_x$ [140], the second approach looks less natural than the first. Formally, the Hubbard model, which is ordinarily used to describe itinerant magnets, is rendered almost analogous to the *s–d(f)* exchange model, if one postulates the existence of local moments [167, 171].

Of the many interesting problems, the one that deserves special mention is the high sensitivity of the parameters of Kondo magnets (especially M_0) to small additions of impurities and pressure. It might happen, for example, that the renormalization described earlier in this section leads to several fixed points with different M_0 and that small changes in the external factors cause significant changes in the overall behavior. As will be demonstrated in the next section, however, the situation is apparently less complicated – there is only one fixed point with parameters strongly dependent on the initial coupling constant.

6.8. Formation of Magnetic Order in Kondo Lattices

To begin with, we will derive the renormalization-group equations (the scaling equations) for the effective *s–f* exchange interaction, the spin dynamic frequency, and the magnetic moment with reference to the ferromagnetic phase. The results that apply to the antiferromagnetic and paramagnetic phases will be discussed without derivation (in more detail, all calculations are given in [184]). We will next analyze the equations and find criteria for the formation of a nonmagnetic Kondo lattice, a magnetic Kondo lattice, and a "conventional" magnet. We will also dwell on why the parameters of Kondo magnets are highly sensitive to external factors.

As in Section 2.5, we will use the renormalization-group method in a form called "a poor man's scaling" by Anderson [185], who investigated the case of a single Kondo impurity. For this purpose, one partitions the space of the states of s electrons into layers of energy $C < E < C + \delta C$ and calculates the contribution of each layer to the effective *s–f* exchange parameter $I_{ef}(C)$. In the ferromagnetic case, for a system described by the Hamiltonian (6.67), the latter may be written as

$$\mathrm{Re}[\Sigma_{\downarrow}(k_F, E=0) - \Sigma_{\uparrow}(k_F, E=0)] = 2I_{ef}(C)S, \tag{6.86}$$

where $\Sigma_\sigma(k, E)$ is the self-energy for the Green's function of an s electron

$$\left\langle \left\langle c_{\mathbf{k},\sigma} | c_{\mathbf{k},\sigma}^+ \right\rangle \right\rangle_E = \frac{1}{E - \varepsilon_{\mathbf{k}} - \Sigma_\sigma(\mathbf{k}, E)}, \tag{6.87}$$

and k_F is the Fermi momentum subject to the condition $\varepsilon_{k_F} = 0$ (the energy is reckoned from the Fermi level). Thus, I_{ef} is determined by the amount of spin splitting for the states at the Fermi level.

The simplest way to evaluate $\Sigma_\sigma(\mathbf{k}, E)$ for the ferromagnetic phase is to use the Holstein–Primakoff representation for spin operators [108]

$$\begin{aligned} S_i^+ &= \sqrt{2S}\left[1 - \frac{b_i^+ b_i}{2S}\right]^{1/2} b_i, \\ S_i^- &= \sqrt{2S} b_i^+ \left[1 - \frac{b_i^+ b_i}{2S}\right]^{1/2}, \\ S_i^z &= S - b_i^+ b_i, \end{aligned} \tag{6.88}$$

where b_i are the boson operators of magnon annihilation at the ith site, and then to invoke the theory of perturbations in terms of I. By the second-order perturbation theory, we find (see, for example, [167])

$$\Sigma_\uparrow(\mathbf{k}, E) = -IS + 2I^2 S \sum_{\mathbf{q}} \frac{f_{\mathbf{q}\downarrow} + N_{\mathbf{k}-\mathbf{q}}}{E - \varepsilon_{\mathbf{q}\downarrow} + \omega_{\mathbf{k}-\mathbf{q}}}, \tag{6.89a}$$

$$\Sigma_\downarrow(\mathbf{k}, E) = IS + 2I^2 S \sum_{\mathbf{q}} \frac{1 - f_{\mathbf{q}\uparrow} + N_{\mathbf{k}-\mathbf{q}}}{E - \varepsilon_{\mathbf{q}\uparrow} - \omega_{\mathbf{k}-\mathbf{q}}}, \tag{6.89b}$$

where $N_{\mathbf{q}} = N_B(\bar{\omega}_{\mathbf{q}})$, and $\bar{\omega}_{\mathbf{q}}$ is the magnon frequency.

Taking advantage of the definition (6.86), we find the contribution $\delta I_{ef}(C)$ from a layer with an energy in the interval $(C, C + \delta C)$

$$\begin{aligned} \delta I_{ef}(C) &= I^2 \\ &\times \left[\sum_{C < \varepsilon_{\mathbf{q}\uparrow} < C + \delta C} \frac{1}{\varepsilon_{\mathbf{q}\uparrow} + \omega_{\mathbf{k}-\mathbf{q}}} + \sum_{C < \varepsilon_{\mathbf{q}\downarrow} < C + \delta C} \frac{1}{\varepsilon_{\mathbf{q}\downarrow} + \omega_{\mathbf{k}-\mathbf{q}}}\right] \\ &\approx \frac{\rho I^2}{\bar{\omega}} \ln\left(\frac{C - \bar{\omega}}{C + \bar{\omega}}\right) \delta C, \end{aligned} \tag{6.90}$$

where $\bar{\omega} = 4Dk_F^2$, and D is the spin stiffness coefficient. For the magnon spectrum, we adopted $\omega_{\mathbf{q}} = D\mathbf{q}^2$ for $q \le 2k_F$.

By evaluating $\partial I_{ef}/\partial C$ in the limit of δC tending to zero, changing the corresponding expression $I \to I_{ef}$ in agreement with the general idea of the renormalization-group method, and introducing a dimensionless coupling constant

$$\begin{aligned} g_{ef}(C) &= -2I_{ef}(C)\rho, \\ g &= -2I\rho, \end{aligned} \tag{6.91}$$

we obtain a scaling equation of the form

$$\frac{\partial g_{ef}(C)}{\partial C} = \frac{g_{ef}^2(C)}{2\bar{\omega}_{ef}(C)} \ln\left|\frac{C+\bar{\omega}_{ef}(C)}{C-\bar{\omega}_{ef}(C)}\right|. \quad (6.92)$$

As is shown in [184], in order to find the dependence of the effective spin wave frequency $\bar{\omega}_{ef}$ on the "truncation" parameter C, one should proceed as follows:

(1) determine the contributions that come to the spin wave frequency from the magnon–magnon interaction

$$\omega_q = 2S(J_0 - J_q) + 2\sum_p (J_p + J_q - J_{p-q})\langle b_p^+ b_p\rangle; \quad (6.93)$$

(2) take into account the contribution to the average magnon occupation numbers from the *s–f* exchange interaction in the second-order perturbation theory

$$\delta\langle b_p^+ b_p\rangle = 2I^2 S\sum_k \frac{f_{k\downarrow}(1-f_{k+p,\uparrow})}{(\varepsilon_{k\downarrow} - \varepsilon_{k+p,\uparrow} - \omega_p)^2}; \quad (6.94)$$

(3) define the contribution from the layer $C < \varepsilon_{k\downarrow} < C + \delta C$; and

(4) replace I by $I_{ef}(C)$ in the corresponding equation for $\partial\omega_{ef}/\partial C$. Generally, the renormalization of ω_{ef} will be different for different q. If, however, one applies the nearest-neighbor approximation to $J(r)$, then $\partial\omega_q/\partial C$ will be proportional to ω_q with coefficients independent of q, and the scaling equation will take the form

$$\frac{\partial\bar{\omega}_{ef}(C)}{\partial C} = -\frac{1-\alpha}{4} g_{ef}^2(C) \ln\left|\frac{C+\bar{\omega}_{ef}(C)}{C-\bar{\omega}_{ef}(C)}\right|, \quad (6.95)$$

where $\alpha = (\sin k_F r/k_F r)^2$ [cf. (6.84) and (6.75)], and r is the distance between the nearest neighbors.

Finally, the magnetic-moment renormalization $\bar{S}_{ef}(C)$ can be determined in a similar way subject to the equality

$$\bar{S} = S - \sum_p \langle b_p^+ b_p\rangle, \quad (6.96)$$

which follows from (6.88). As a result, all scaling equations will be written as

$$\frac{\partial g_{ef}(C)}{\partial C} = \Lambda; \quad (6.97a)$$

$$\frac{\partial \ln\bar{\omega}_{ef}(C)}{\partial C} = -\frac{1-\alpha}{2}\Lambda; \quad (6.97b)$$

$$\frac{\partial \ln\bar{S}_{ef}(C)}{\partial C} = -\frac{1}{2}\Lambda; \quad (6.97c)$$

$$\Lambda = \Lambda(C, \bar{\omega}_{ef}(C)) = \frac{g_{ef}^2(C)}{C}\varphi\left(\frac{\bar{\omega}_{ef}(C)}{C}\right), \quad (6.97d)$$

where

$$\varphi(x) = \frac{1}{2x}\ln\left|\frac{1+x}{1-x}\right|. \quad (6.98a)$$

It can be shown [184] that the equations for a ferromagnet and a paramagnet will differ only in the form of the function $\varphi(x)$, that is,

$$\varphi(x) = \frac{1}{2x}\tan^{-1}x \quad (6.98b)$$

for a paramagnet, and

$$\varphi(x) = \begin{cases} -\frac{1}{x^2}\ln|1-x^2|, & 3D, \\ \frac{1}{\sqrt{1-x^2}}, & 2D, \end{cases} \quad (6.98c)$$

for an antiferromagnet in the three-dimensional (3D) and the two-dimensional (2D) cases. We included the result for a two-dimensional antiferromagnet because it may be of interest for copper-oxygen antiferromagnets, such as $Pr_{1-x}Y_xBa_2Cu_3O_7$ (see [184]).

In all cases, the function $\varphi(x)$ satisfies the condition $\varphi(0) = 1$, and this ensures a correct limiting transition of equations (6.97a) - (6.97d) to the single-impurity case for $\bar{\omega}_{ef}$ tending to zero.

We will now analyze the system of equations (6.97). We can express $\bar{\omega}_{ef}(C)$ in terms of $g_{ef}(C)$ from (6.97a) and (6.97b)

$$\bar{\omega}_{ef}(C) = \bar{\omega}\exp\{-\frac{1}{2}(1-\alpha)[g_{ef}(C) - g]\}, \quad (6.99)$$

where $\bar{\omega}$ is the initial frequency of Kondo fluctuations (without Kondo renormalizations), and $\bar{S}_{ef}(C)$, from a comparison of (6.97b) and (6.97c)

$$\left[\frac{\bar{S}_{ef}(C)}{S}\right] = \left[\frac{\bar{\omega}_{ef}(C)}{\bar{\omega}}\right]^{\frac{1}{1-\alpha}}. \quad (6.100)$$

In view of (6.99), there remains only one equation for g_{ef}, which we will write as

$$\frac{\partial g_{ef}(\xi)}{\partial\xi} = g_{ef}^2(\xi)\psi\left[\lambda + \frac{1}{2}(1-\alpha)g_{ef}(\xi) - \xi\right], \quad (6.101)$$

where

$$\psi(x) = \varphi(e^{-x}), \quad \psi(x \gg 1) = 1, \quad (6.102)$$

$$\xi = \ln\left|\frac{W}{C}\right|, \quad \lambda = \ln\left|\frac{W}{\bar{\omega}}\right| \gg 1, \quad (6.103)$$

and W is the truncation energy of the order of the initial width of the conduction band.

The initial condition for the differential equation (6.101) is $g_{ef}(\xi = 0) = g$ [see equation (6.91)]. In view of this, equation (6.101) can be written in integral form as

$$\frac{1}{g_{ef}(\xi)} = \frac{1}{g} - X(\xi), \quad (6.104a)$$

$$X(\xi) = \int_0^\xi d\xi'\psi\left[\lambda + \frac{1-\alpha}{2}g_{ef}(\xi') - \xi'\right]. \quad (6.104b)$$

Here, we will limit ourselves to the Kondo case $g > 0$ ($I < 0$). Whereas $\psi(x)$ is a positive monotonically increasing function of x, $g_{ef}(\xi)$ is a monotonic increasing function of ξ. The ground state of a Kondo lattice is determined by the behavior of $g_{ef}(\xi)$ for ξ tending to infinity.

A general analysis of equation (6.104) for ξ tending to infinity can be done without finding the specific form of the function $\varphi(x)$ and, consequently, of the function $\psi(x)$. To demonstrate, let

$$g^* = g_{ef}(\xi = \infty) < \infty. \quad (6.105)$$

Then

$$M(\lambda) < X(\infty) < M(\lambda + \frac{1-\alpha}{2}g^*), \quad (6.106)$$

where

$$M(x) = \int_0^\infty d\xi\psi(x-\xi) = \int_{-\infty}^x d\xi\psi(\xi) \approx x, \quad \text{for } x \gg 1, \quad (6.107)$$

by virtue of (6.102). Substitution of (6.105) - (6.107) in (6.104) yields

$$\lambda < \frac{1}{g} - \frac{1}{g^*} < \lambda + \frac{1-\alpha}{2}g^*. \quad (6.108)$$

Equation (6.108) demonstrates that the finiteness condition (6.105) for g^* leads to a contradiction if $\lambda g > 1$, that is,

$$\bar{\omega} < T_K = W\exp(-\frac{1}{g}). \quad (6.109)$$

Then there inevitably exists a point ξ^* where $g_{ef}(\xi^*) = \infty$. By equations (6.99) and (6.100), at that point both $\bar{\omega}_{ef}$ and $\bar{S}_{eff}$ tend to zero. Thus, given that the condition (6.109) is satisfied, a tight-binding state is formed with a completely suppressed spin dynamics. The energy

$$T_K^* = W\exp(-\xi^*) \quad (6.110)$$

plays the role of the boundary of the tight-binding region, that is, of the effective Kondo temperature for the lattice. As will be shown in Section 6.9, even in this case, the ground state can, in theory, be magnetically ordered if the number of electrons is not equal to the number of f spins because one charge carrier can form a singlet coupled state only with one spin. For $\lambda g < 1$, a fixed point with the effective coupling constant g^* exists. The inequality (6.108) implies that variations of g in the interval

$$\frac{1}{\lambda} < g < \frac{1}{\lambda} + \frac{c}{\lambda^2} \quad (6.111a)$$

or, equivalently,

$$T_K < \bar{\omega} < AT_K, \quad (6.111b)$$

where c and A are numerical factors of zero order in g, cause g^* to vary from a value of the order of g to values substantially greater than unity. Also, by virtue of (6.99) and (6.100), the effective spin $\bar{S}^* = \bar{S}_{ef}(\xi = \infty)$ and the effective frequency $\bar{\omega}^* = \bar{\omega}_{ef}(\xi = \infty)$ vary from the initial values to zero. These sudden changes occur within a small range of the initial coupling constant $|\delta g| \sim g^2$ [see equation (6.111)]. This explains the high lability of magnetic Kondo lattices. Finally, for

$$\bar{\omega} \gg T_K \quad (6.112)$$

$g^* \approx g$, and we have the case of Kondo-corrected ordinary magnets that can be treated within the perturbation theory.

We now turn to a more detailed analysis of the most interesting case of a tight-binding solution.

6.9. The Ground State of Kondo Magnets in the Mean-Field Approximation

As we saw in Section 6.8, it is rather difficult to describe the crossover during a transition from the high-temperature region (where the perturbation theory is applicable) to the tight-binding solution. It is, therefore, of interest to consider the low-temperature region $T \ll T_K$. This can be done within the formalism recently developed by Coleman and Andrew (for details of calculations, see [172, 173]). Following [154], we will use the saddle-point method in evaluating the functional integral that describes the system. Then, in the mean-field approximation, the Hamiltonian of the *s–f* exchange from (6.67) (for spin $S = 1/2$) takes the form

$$-I\sum_{\alpha\beta} c_{i\alpha}^+ c_{i\beta}(\sigma_{\alpha\beta}S_i - \frac{1}{2}\delta_{\alpha\beta}) \to c_i^+\hat{V}_i f_i + f_i^+\hat{V}_i c_i - \frac{1}{2I}\mathrm{Tr}(\hat{V}_i^+\hat{V}_i). \quad (6.113)$$

Here, we use the spinor notation $c_i^+ = (c_{i\uparrow}^+; c_{i\downarrow}^+)$, etc.; $f_{i\sigma}^+$ are the pseudofermion creation operators [154]; and $\hat{V}_i$ is the effective hybridization matrix whose elements are defined so as to minimize the free energy. In contrast to Coleman and Andrew [154], who derived the anomalous averages corresponding to the spin-liquid state from the Heisenberg Hamiltonian $\hat{H}_f$, we consider the simpler case of long-range magnetic order. For a ferromagnet, we have [172]

$$V_i^{\sigma\sigma'} = v_\sigma\delta_{\sigma\sigma'};$$

$$H_f = -J\langle S^z\rangle\sum_{i,\sigma}\sigma f_{i\sigma}^+ f_{i\sigma}; \quad J = J_{q=0}, \quad (6.114)$$

$$\hat{H} - \mu\hat{n} = \sum_{k,\sigma}[(\varepsilon_k - \mu)c_{k\sigma}^+ c_{k\sigma} + w_\sigma f_{k\sigma}^+ f_{k\sigma} + v_\sigma(c_{k\sigma}^+ f_{k\sigma} + f_{k\sigma}^+ c_{k\sigma}) + \text{const}, \quad (6.115)$$

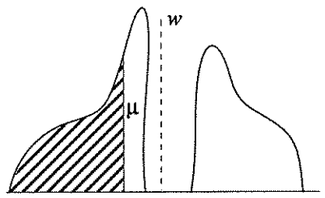

Fig. 6.9. Schematic representation of the complete density of electronic states (including the density of states for pseudofermions) in the effective hybridization model (6.115) for the nonmagnetic case.

where $w_\sigma = w - \sigma J\langle S^z\rangle$, $|w| \sim T_K$, and w plays the role of the chemical potential for pseudofermions. By diagonalizing the quadratic form (6.115)

$$c^+_{k\sigma} = \cos(\theta_{k\sigma}/2)\,\alpha^+_{k\sigma} - \sin(\theta_{k\sigma}/2)\,\beta^+_{k\sigma};$$
$$f^+_{k\sigma} = \sin(\theta_{k\sigma}/2)\,\alpha^+_{k\sigma} + \cos(\theta_{k\sigma}/2)\,\beta^+_{k\sigma};$$
$$\sin\theta_{k\sigma} = 2v_\sigma/E_{k\sigma}; \qquad (6.116)$$
$$\cos\theta_{k\sigma} = (\varepsilon_k - \mu - w_\sigma)/E_{k\sigma};$$
$$E_{k\sigma} = [(\varepsilon_k - \mu - w_\sigma)^2 + 4v_\sigma^2]^{1/2},$$

we obtain for the spectrum of quasiparticles

$$\varepsilon^{\alpha,\beta}_{k\sigma} \equiv \varepsilon^{1,2}_{k,\sigma} = \frac{1}{2}(\varepsilon_k - \mu + w_\sigma \pm E_{k\sigma}). \qquad (6.117)$$

The quantities v_σ and w_σ, the chemical potential μ, and the magnetization $\langle S^z\rangle$ are determined from the equations

$$v_\sigma = 2I\sum_k \langle c^+_{k\sigma} f_{k\sigma}\rangle = -\frac{2I\sum_k (n^\beta_{k\sigma} - n^\alpha_{k\sigma})}{E_{k\sigma}}; \qquad (6.118)$$

$$n = \sum_{k\sigma}\langle c^+_{k\sigma} c_{k\sigma}\rangle = \frac{1}{2}\sum_{k\sigma,\,j=1,2}[1 - (-1)^j\cos\theta_{k\sigma}]\,n^j_{k\sigma}; \qquad (6.119)$$

$$n_{f\sigma} = \sum_{k\sigma}\langle f^+_{k\sigma} f_{k\sigma}\rangle = \frac{1}{2} + \sigma\langle S^z\rangle$$
$$= \frac{1}{2}\sum_{kj}[1 + (-1)^j\cos\theta_{k\sigma}]\,n^j_{k\sigma}, \qquad (6.120)$$

where n is the concentration of conduction electrons, and $n^j_{k\sigma} = [\exp\beta\varepsilon^j_{k\sigma} + 1]^{-1}$.

Thus, with the approximation in question, the energy spectrum is of hybridization character, that is, near E_F there is a "Kondo" bandgap centered at w_σ with sharp density-of-states peaks at the edges (Fig. 6.9). The principal contribution to the density of states near E_F comes from the pseudofermions that arise upon the "disassembly" of localized spins. This picture of a spectrum has been confirmed for heavy-fermion systems by IR and microcontact spectroscopy [141], and the delocalization of "heavy" pseudofermions by observations of the de Haas–Van Alphen effect in heavy-fermion systems with large m^* [142]. In the case of ferromagnetic Kondo systems, the hybridization form of the spectrum is apparently suggested by the nonmonotonic temperature dependences of magnetization in Sm_4Sb_3 and Sm_4As_3 [174][5] (compare with the temperature-induced ferromagnetism discussed in [175]).

If $|v_\sigma| \ll W$, then $\cos\theta_{k\sigma} \approx \mathrm{sgn}(\varepsilon_k - \mu - w_\sigma)$, and this simplifies equations (6.118) - (6.120). We define the function $\mu(c)$ by the equation

$$c = 2\int_0^{\mu(c)} d\varepsilon\rho(\varepsilon), \qquad (6.121)$$

where $\rho(\varepsilon)$ $(0 < \varepsilon < W)$ is the initial density of states. Then, equation (6.119) takes the form $\mu(n) = \mu$.

Consider various types of ferromagnetic solutions. For definiteness, we will limit ourselves to the case $n < 1$. If $\langle S^z\rangle$ is not too great, then, as in the nonmagnetic case, $w_\sigma > v_\sigma^2/(W - \mu)$ for both spin projections, that is, μ lies below the energy gap. Then, from equations (6.118) - (6.120) we obtain

$$1 = -2\int_0^{\mu+\lambda_\sigma} \frac{d\varepsilon\rho(\varepsilon)}{[(\varepsilon - \mu)^2 + 4v_\sigma^2]^{1/2}}, \qquad (6.122)$$

$$\lambda_\sigma \equiv v_\sigma^2/w_\sigma = \mu(n + 2n_{f\sigma}) - \mu(n). \qquad (6.123)$$

By evaluating the integral in (6.122) with due regard to the terms of the leading and subsequent orders with respect to $1/\ln[v_\sigma/W] \simeq 4I\rho$, we find the ratio $w_\uparrow/w_\downarrow$ from (6.123) and derive the self-consistent equation for magnetization

$$\tanh\left[\frac{1}{4\rho}\int_{\mu_1}^{\mu_2} d\varepsilon\frac{\rho(\varepsilon) - \rho}{\varepsilon - \mu}\right] = \frac{J\langle S^z\rangle}{w}, \qquad (6.124)$$
$$\mu_{1,2} = \mu(n + 1 \mp 2\langle S^z\rangle).$$

This equation has only trivial solutions for $\rho(\varepsilon) = \mathrm{const}$. However, solutions with $\langle S^z\rangle \neq 0$ may arise for some $\rho(\varepsilon)$ if the right-hand and left-hand sides of equation (6.124) are on the same order, that is, if $J \sim w \sim T_K$.

If $w_\downarrow > v_\downarrow^2/(W - \mu)$, then $-v_\uparrow^2/\mu < w_\uparrow < v_\uparrow^2/(W - \mu)$, that is, μ lies in the energy band for $\sigma = \uparrow$ (this is called a semimetallic ferromagnet), and we have $n_{f\uparrow} = 1 - n/2$, $n_{f\downarrow} = n/2$, and $\langle S^z\rangle = (1 - n)/2$. Such a solution exists if

$$-\psi/\mu < [\mu(2n) - \mu]^{-1} - J(1 - n)/v_\downarrow^2 < \psi/(W - \mu);$$
$$\psi \equiv \left(\frac{v_\uparrow}{v_\downarrow}\right)^2 = \exp\left[\frac{1}{\rho}\int_{\mu(2n)}^{W}\frac{d\varepsilon\rho(\varepsilon)}{\varepsilon - \mu}\right]. \qquad (6.125)$$

If $\rho = \mathrm{const}$, then (6.125) takes the form $J < T_K/(1 - n)$.

[5] A similar $M(T)$ dependence recently was reported for the mixed-valence ferromagnetic EuNi in [176].

In order to investigate the energy stability of the state in question, we first calculate the corresponding total energy

$$E(n) = \langle\hat{H} - \mu\hat{n}\rangle + \mu n - w, \quad \mu = \mu(n), \quad n_f = 1, \qquad (6.126)$$

$$\langle\hat{H} - \mu\hat{n}\rangle = \sum_{ki\sigma}\varepsilon^j_{k\sigma} n^j_{k\sigma} + J\langle S^z\rangle - \frac{1}{2I}\sum_\sigma v_\sigma^2. \qquad (6.127)$$

Integration in the case of $\rho = \mathrm{const}$ gives

$$E(n) = \frac{n^2}{4\rho} - \frac{n}{2}T_K - J\langle S^z\rangle^2; \quad T_K \equiv W\exp\frac{1}{2I\rho}, \qquad (6.128)$$

which is always lower than the energy of the nonmagnetic Kondo state $E(n) = n^2/4\rho - nT_K/2$. Thus, the saturated Kondo ferromagnet (the semimetallic ferromagnetic state), in which every conduction electron cancels out one localized moment (as in the s–$d(f)$ model with $I \to -\infty$), is stable at small J. We must compare (6.128) with the energy of the ordinary magnetic state ($v_\sigma = 0$, $\langle S^z\rangle = 1/2$), $E(n) = n^2/4\rho - J/4$. As can be easily seen, the energy of the latter decreases at $J(1 - n/2) = T_K$, and, as J increases, a transition of the first order with a complete suppression of the Kondo effect takes place at that point.

Still another possibility is solutions with $w_\downarrow > v_\downarrow^2/(W - \mu)$ and $w_\uparrow < -v_\uparrow^2/\mu$ (μ lies in the lower hybridization subband for $\sigma = \downarrow$ and in the upper one, for $\sigma = \uparrow$). Notably, for $\rho = \mathrm{const}$, the solution takes the form

$$2J\langle S^z\rangle = T_K, \quad \frac{1 - n}{2} < \langle S^z\rangle < \frac{1}{2}, \quad T_K < J < \frac{T_K}{1 - n}. \qquad (6.129)$$

The corresponding total energy is

$$E(n) = n^2/4\rho + \frac{1}{2}(1 - n)\,T_K + J\langle S^z\rangle^2,$$

that is, the state (6.129) is energetically unfavorable.

As is seen, for the criterion of ferromagnetism an important factor is the dependence of the effective hybridization on σ. By contrast, in the case of antiferromagnetic order, when in the mean field approximation, we have

$$H_f = -J_\kappa\langle S^z_\kappa\rangle\sum_k (f^+_{k+\kappa,\uparrow} f_{k,\uparrow} + f^+_{k,\uparrow} f_{k+\kappa,\uparrow}), \qquad (6.130)$$
$$J_\kappa = \max_q J_q,$$

the corrections to v and w are on the order of $J_\kappa\langle S^z_\kappa\rangle^2/W$ and immaterial. Therefore, the criterion of antiferromagnetism takes the usual form $J_\kappa\chi_\kappa > 1$, where χ_Q is the inhomogeneous magnetic susceptibility of pseudofermions in the effective hybridization model (6.115). The principal contribution to it comes from transitions between the hybridization subbands

$$\delta\chi_\kappa = 2\sum_k \cos^2(\theta_k/2)\sin^2(\theta_{k+\kappa}/2)\frac{n^\beta_k - n^\alpha_{k+\kappa}}{\varepsilon^\alpha_{k+\kappa} - \varepsilon^\beta_k}$$
$$\sim \frac{W}{v^2} < \frac{1}{T_K}. \qquad (6.131)$$

Thus, the antiferromagnetizm appears at $J_\kappa \gtrsim T_K$.

Another substantial contribution to the formation of the ground state can come from fluctuations. For example, calculation of the correction for the magnetization due to Heisenberg interaction fluctuations (actually, due to perturbations in J/T_K) gives

$$\delta\langle S^z\rangle \sim -(J/T_K)\ln(T_K/J), \qquad (6.132)$$

so that for $J \sim T_K$ one has $\delta\langle S^z\rangle \sim \langle S^z\rangle$, and a state with a low saturation moment can be formed.

Although the model with a hybridization spectrum of Fermi excitations examined in this section is one of itinerant magnetism, the criterion of magnetism in it differs radically from the Stoner criterion. Roughly speaking, in the latter [with a density of states $N(E_F) \sim 1/T_K$], the interaction within the atom is replaced by the Heisenberg interaction between sites. In this sense, one may say that Kondo lattices are "localized."

6.10. Separation of Spin and Charge Degrees of Freedom and the Problem of Heavy Fermions

In Sections 6.5 through 6.9, we discussed the view, widely accepted at present, according to which heavy-fermion systems are described as Kondo lattices. In our opinion, such a physical picture is well-founded for most heavy-fermion systems. However, a wide range of systems (see below) do not fit such a description. A distinction of such systems (which include not only f but also d systems) is the lack of correlation between the linear term in the heat capacity γT and the electrophysical properties (the number of charge carriers). Some of them, with large γ, are semiconductors and not metals. At the same time, the value of γ closely correlates with the presence or absence of magnetic or charge order. This apparently suggests the non-Kondo origin of large γ. The point is that, as was shown in Section 6.8, the condition for the formation of the Kondo lattice state only slightly depends on magnetic order, being qualitatively the same for the paramagnetic, ferromagnetic, and antiferromagnetic phases. In this section, we will dwell in brief on the likely nature of such "unusual" heavy-fermion systems.

To begin with, we should answer the question: Is the linear term in the heat capacity always of an electronic nature, that is, related to charge carriers? The answer is undoubtedly "no" in the one-dimensional case, where the heat capacity is linear in temperature, for example, in the antiferromagnetic Heisenberg chain with $S = 1/2$ [186], which has no charge carriers at all. The linear contribution to heat capacity in the Kondo problem,

discussed in Section 6.5, is traceable to the *interaction* between spin and conduction electrons. Therefore, it may, in theory, be interpreted as the spin heat capacity (renormalized at the expense of *s* electrons) or as the electronic heat capacity when due regard is given to the Suhl–Abrikosov resonance. The latter approach is more generally accepted and, apparently, more correct in substance. The point is that in Kondo lattices high densities of states at the Fermi level show up, as a rule, in the properties where the charge-related degree of freedom is obviously essential. These are the behavior of resistivity with temperature, IR spectra, the jump in heat capacity in the superconductivity transition [135, 138], and sometimes the de Haas–Van Alphen effect [142]. It must be admitted, though, that in the latter case the situation still needs to be clarified completely. An alternative view is also discussed in the literature [187].

For three-dimensional systems, the possibility of zero-current excitations contributing to γ was first pointed out in [188]. Later [80], it was shown that in a narrow-band Hubbard ferromagnet with a low hole concentration the principal contribution to γ comes from zero-current "nonquasiparticle" states. It was not until Anderson [17] had developed his resonating valence bond (RVB) theory for high-temperature superconductors, however, that the possible nonelectron contribution to γ received proper attention. Although rigorous results are still lacking (especially for the three-dimensional, and not for the two-dimensional, case), the idea appears attractive and can apparently throw light on the properties of "nontraditional" heavy-fermion systems. Anderson's theory assigns the crucial role to spin–spin exchange interactions.

We first turn to the possible "constructive" role of site–site exchange interactions in forming states of the heavy-fermion system type. In this connection, special interest is evoked by systems with competing exchange interactions (when, for example, nearest- and next-nearest-neighbor interactions are comparable in magnitude and each favors the formation of a magnetic structure of its own).

Until now it was assumed that the effects of site–site interactions reduce the effective low-energy scale T_K (see the discussion of the spin dynamics above) and hinder the suppression of magnetism. Recently, attempts to gain insight into the nature of high-temperature superconductivity spurred advances in the resonating valence bond (RVB) or quantum spin-liquid theory [177]. The state dealt with in this theory is an example of the reverse situation: the competitive character of site–site exchange interactions J_{ij} leads to the suppression of magnetic order (see Section 5.8). As the RVB theory tells us, the spin-liquid state with a low-energy scale $|J|$ can be formed in purely spin two-dimensional (and, possibly, three-dimensional) systems with competing interactions. In these circumstances (in the case of the zero-gap version of the RVB state with a spin on Fermi surface), a linear term in the heat capacity with $\gamma \sim 1/|J|$ appears.

We will demonstrate the suppression of magnetic order via a simple spin-wave treatment of a two-dimensional Heisenberg antiferromagnet with $S \gg 1$ (see also [178]). The correction for the magnetization of the sublattice due to zero-point vibrations takes the form

$$\delta\bar{S} = -\sum_{\mathbf{q}} \nu_{\mathbf{q}}^2; \tag{6.133}$$

$$\nu_{\mathbf{q}}^2 = \frac{1}{4} S\,(4J_{\mathbf{K}} - J_{\mathbf{K}+\mathbf{q}} - J_{\mathbf{K}-\mathbf{q}} - 2J_{\mathbf{q}})/\omega_{\mathbf{q}} - \frac{1}{2},$$

$$\omega_{\mathbf{q}}^2 = 2S^2\,(J_{\mathbf{K}} - J_{\mathbf{q}})\,(2J_{\mathbf{k}} - J_{\mathbf{K}+\mathbf{q}} - J_{\mathbf{K}-\mathbf{q}}).$$

For $\mathbf{q}$ tending to zero, let

$$2J_{\mathbf{k}} - J_{\mathbf{K}+\mathbf{q}} - J_{\mathbf{K}-\mathbf{q}} \approx \frac{1}{2}\alpha q^2 + \frac{1}{2}\beta f(\varphi) q^4, \tag{6.134}$$

where $\beta > 0$, $f(\varphi) \sim 1$ is a positive function of the polar angle of the vector $\mathbf{q}$. For α tending to zero (frustration), we find

$$\bar{S} = S - a\ln\frac{\beta}{\alpha}; \quad a = \frac{1}{(4\pi)^2}\,(J_{\mathbf{K}} - J_0)^{1/2} \int_0^{2\pi} \frac{d\varphi}{\sqrt{\beta f(\varphi)}}. \tag{6.135}$$

This implies that $\bar{S} = 0$ in some range of parameters $\alpha < \beta\exp(-S/a)$. The existence of nonmagnetic spin liquid in three-dimensional systems with competing interactions remains an open question. However, as we will soon see, there is some experimental evidence that favors both such a possibility and the formation of a state with a partially suppressed magnetism.

In most cases, the Kondo effect is undoubtedly the principal cause of anomalous properties in the *f* systems. Yet, the *f–f* exchange interaction, too, makes a substantial contribution to the formation of their energy spectrum [173]. Apparently, a state standing midway between Kondo magnets and spin liquid occurs quite often. In Kondo lattices with a small number of charge carriers, competing exchange interactions may be even more influential than the Kondo effect. For instance, the semimetal CsSb is a classical example of a system with competing exchange interactions and an elaborate magnetic phase diagram (a devil's ladder). According to Sera *et al.* [179], $Ce_{0.8}La_{0.2}Sb$ has a very high electronic heat capacity at low temperatures.

The $Y_{1-x}Sc_xMn_2$ system, too, exhibits unusual properties. The compound YMn_2 is an itinerant antiferromagnet with a complex magnetic structure. At $x = 0.03$, magnetic order disappears, and γ goes as high as 140 mJ/(mol K^2), which is a record-breaking figure for the *d* systems [180]. The magnetic insulator NiS_2 has magnetic order, but one may speak of the suppression of magnetism because $T_N \approx 45$ K is small in comparison with the paramagnetic Curie temperature $|\theta| \sim 1500$ K. Moreover, the slope of the line in the phase diagram suggests that the insulating phase has a large entropy [25].

A striking example of the spin-liquid state is, it appears, the intermediate-valence semiconductor Sm_3Se_4, which is a system with charge (and not spin)

degrees of freedom. In contrast to some isostructural compounds, Sm_3Se_4 has no charge order, and γ has a giant value of 4500 mJ/(mol K^2) at low T [181]. The derivation of the effective anisotropic pseudospin Hamiltonian for a model system with charge frustration is given in [182], In the $Yb_4As_{3-x}P_x$ system (which has charge order near 300 K), γ is large and increases from 200 to 400 mJ/(mol K^2) as x changes from 0 to 0.3, whereas the charge-carrier concentration (about 0.001 per atom) remains practically unchanged [183]. Quite likely, doping with phosphorus augments frustrations and partly destroys the ordered state.

The above mechanism of charge frustrations (or the similar mechanism responsible for the melting of the Wigner crystal due to zero-point vibrations) can be realized in some intermediate-valence compounds customarily described as Kondo lattices with high T_K [155]. Examples are Eu-based systems of the EuM_2Si_2 and $EuPd_2P_2$ type, where an increase in pressure or temperature brings about a transition from an inhomogeneous to a homogeneous intermediate valence.

In summary, the problem of Kondo magnets, as can be seen from the foregoing (see Sections 6.6 through 6.10), does evoke exceptional interest from the viewpoint of the general theory of magnetism – it demonstrates a broad variety of properties, offers examples of both purely itinerant and purely localized behavior, and encompasses all intermediate states.

6.11. Conclusion

The *f* systems demonstrate what seem to be the most striking and finest of all phenomena associated with the localized and itinerant behavior of electrons in metals. We refer to the properties of two groups of substances: intermediate (or mixed)-valence compounds and heavy-fermion systems. In both cases, the *f* electrons are rendered, in a sense (see Section 6.5), itinerant in a narrow energy layer ΔE near the Fermi level (or, more accurately, to include semiconductors, near the chemical potential level) and thus behave as band electrons over the time interval $\tau \gtrsim h/\Delta E$ and as localized electrons at smaller times. In intermediate-valence systems, $\Delta E \gtrsim 100$ - 1000 K and, accordingly, τ is about 10^{-13} s. In heavy-fermion systems, ΔE is one or two orders of magnitude smaller, and τ is longer by the same amount. For both intermediate-valence and heavy-fermion systems, the energy spectrum has a characteristic hybridization structure with narrow peaks of densities of electronic states, separated by a bandgap or a pseudogap of the same width as the peaks themselves. However, for intermediate-valence systems it is generally more typical that the chemical potential level falls within the bandgap, and the system is thus a narrow-gap semiconductor. In heavy-fermion systems, the Fermi level ordinarily lies near the peak of the density of electronic states.

Such are, in a general outline, the basic points of the semiphenomenological description of the anomalous *f* systems we presented in this chapter. In such a presentation, it appears quite established. The microscopic models that lead to this behavior can be different. In this review, we gave preference to the view that most heavy-fermion systems are Kondo lattices (which is almost generally accepted, but see Section 6.10). In intermediate-valence systems, however, the key factors are the effects associated with the hybridization of the *f* and *d* states and the exciton effects (other views are likewise discussed in the literature, but the one we hold at present appears to be the most natural).

It appears, however, that a specific description of the properties of intermediate-valence systems depends little on the microscopic model adopted, at least in the mean-field approximation, to which we limited ourselves.

Special consideration (see Sections 6.6 - 6.9) was given to the properties of Kondo magnets, which include heavy-fermion and some other related systems (primarily, Ce- or U-based) with a somewhat greater energy scale ΔE, that demonstrate ferromagnetic or antiferromagnetic order.

> In contradictory phenomena, we find distinct but equally essential aspects of a single, clearly defined complex of knowledge about objects.
>
> Niels Bohr

7. THE SUMMING-UP

Throughout the review, we tried our best to demonstrate the usefulness to metal physics of both a purely band-theoretic treatment of itinerant electrons and the views that are based on their localized or atomlike states. Sometimes, we had no alternative. For example, the *d* electrons in Mott insulators or the 4*f* electrons in almost all rare-earth metals are *truly* localized. Sometimes we faced an alternative. For example, when one calculates the properties of the alkali metals, one may completely "take apart" the ionic core and analyze the core electrons as itinerant through the use of the density functional formalism. In most cases, however, it is *convenient* to treat them as purely "atomlike," that is, belonging to the ionic core, and to use the language of pseudopotential theory (see Ch. 2). Of course, the latter approach has a more limited applicability, and in considering large compressions, one has to "unfreeze" the core. Within its limits of applicability, however, it offers a way to calculate far more delicate characteristics of a metal. It may also occur that the same electrons in the same substances must be treated as itinerant in a narrow energy interval near the Fermi level and as localized on a larger energy scale (as is the case with the *f* electrons in heavy-fermion systems, Ch. 6). All of this demonstrates that the "itinerant" and the "localized" pictures of the electronic subsystem in a solid are mutually complementary; in fact, they come about owing to a simplification of the real, substantially many-particle picture. Before one can describe a quantum system in terms of "wave–particle" duality, one must reduce the many-particle quantum system to its single-particle equivalent because a wave in the multi-

dimensional space of all coordinates of all electrons is not a classical entity. In this single-particle description, the electron may turn out itinerant or atomlike, as the case may be. A convenient mathematical formalism in the former case is second quantization that involves the usual Fermi operators; in the latter, this will be the use of X operators with their substantially more sophisticated algebra (see Ch. 5).

In the quantum theory of condensed matter, there are, generally speaking, two fundamental problems. They are the ground-state problem and the excitation-spectrum problem. In dealing with them, the representation of electronic states as either purely itinerant or purely localized might be imperfect: it may adequately describe one of the properties of a many-electron system and fail to do so with the other properties of the same system. Here is an example that validates the truth of the above assertion with regard to the ground-state problem. An important characteristic for the ground state of a quantum system is its energy E_0 and its dependence on the density of particles, interaction constants, the masses of particles, the deformation constants of the crystal lattice, etc. Many physical properties can be found immediately from the expression for E_0, and one need not know the explicit form of the wave functions for the ground state, $|\Phi_0\rangle$, in order to do that. For example, by calculating E_0 for various deformations of the lattice, one can determine its elastic constants. Quite often, E_0 can be found by the direct variational method, whereby the wave function is sought in some trial form (see, for example, Sections 5.3, 5.5, and 6.4). Importantly, entirely different trial functions may yield close values of E_0. Moreover, a physically less accurate picture of the ground state can lead to a more accurate value of E_0.

An apt example is as follows [26]. In the one-dimensional Hubbard model with a number of electrons equal to that of lattice sites, the ground state is dielectric for any interaction constant U, and the exact solution [30] yields for $U \ll t = 1$ (where t is the transfer integral chosen equal to unity) an energy gap G defined by

$$G \sim \sqrt{U}\exp(-\frac{2\pi}{U}).$$

The trial function (5.34) corresponding to the self-consistent field approximation gives a qualitatively close result (5.38), which differs only in its pre-exponential factor. The Gutzwiller trial function (5.73) leads to the metallic state with any finite U and is inadequate in this sense. When, however, E_0 is estimated by this function [59], the behavior of $E_0(U)$ turns out to be closer to the exact result

$$E_0(U) \simeq -\frac{4}{\pi} + \frac{U}{4} - 0.017U^2 + \ldots,$$

than the estimate based on the function (5.34)

$$E_0(U) \simeq -\frac{4}{\pi} + \frac{U}{4} + O\left[\exp(-\frac{4\pi}{U})\right].$$

Thus, on the one hand, a qualitatively proper choice of the "localized" (dielectric) or "itinerant" (metallic) picture will not, generally, guarantee the best description of the ground-state energy and of the physical properties directly related to it. On the other hand, high accuracy in describing such properties is not a strong argument in favor of any choice of the picture.

We dwelt on this point at length because it often leads to a misunderstanding. For example, the Kohn–Sham theorem lying at the basis of the density-functional formalism (see Section 4.1) guarantees only the *potential* possibility of calculating E_0 exactly for a given density distribution $n(r)$ by this method. However, apart from the difficulty in finding the explicit form of the functional that implements this attractive possibility ("Which mouse specifically will put a bell on the cat's neck?"), there is one more stumbling bock. A good description of E_0 is a vital point. Among other things, it enables one to find equally good experimental values for elastic constants, etc. However, as we observed from reference to Gutzwiller's formalism, it does not safeguard that what we described as a metal is a metal, and as a dielectric is a dielectric.

This lack of a direct relation between a good description of elastic constants and the energy spectrum (there is or there is not a bandgap) in many-particle systems has, however, a "silver lining." If we limit ourselves from the outset to describing only the lattice properties of a metal, we may neglect some finer points, to put it mildly. For instance, in a heavy-fermion system (see Section 6.5), the f electrons behave in an intricate way in a very narrow layer (with a width of about the Kondo temperature $T_K \sim 10$ K) near the Fermi level E_F. The contribution of this layer to E_0 is $T_K/E_F \sim 0.001$, and the standard band-theoretic description, which neglects a most interesting thing about heavy-fermion systems – the existence of heavy fermions – is able, at least in theory, to describe most of their lattice properties quite well. A more elementary example along the same lines is the theory of alkali metals, based on the use of local pseudopotential (see Section 2.2). Being quite fruitful in describing the lattice properties, it is, however, unable (as follows from our calculations not included in this review) to describe the Fermi surfaces of these metals with reasonable accuracy.

We now turn to describing the excited states of solids. Almost all successes of many-particle physics, including solids, are associated with the concept of quasiparticles or elementary excitations. Even if the interaction is strong and the electrons are localized in the ground state, elementary excitations will be coupled loosely and itinerant. That is, in an ideal lattice, they are characterized by a certain dependence of energy on quasimomentum. This is the traditional view first stated, apparently, by Schubin and Vonsovskii in their works on the polar model of the crystal [6 - 9]. At present, it is formally validated by the Green's function method [71] and, we may say this with certainty, it still holds in overwhelming number of cases. There are, however, systems that cast doubt on the omnipotence of the quasiparticle description. An example of such systems described with sufficient detail in this review (see

Section 5.6 dealing with nonquasiparticle states in narrow-band Hubbard ferromagnets). Of greater interest in this respect are, however, low-dimensional systems existing in the Luttinger liquid state (see Section 5.8). In one-dimensional (and, possibly, two-dimensional?) systems of interacting electrons, single-particle excitations cannot be described in the language of quasiparticles even approximately, unless the interaction is vanishingly small [see, for example, equation (5.182)]. Indeed, here we run into a situation where no simplified (single-particle) descriptions, including those in the language of localized excitations, are feasible. Fortunately, many one-dimensional models are exactly solvable, and one can do without such simplifications.

In conclusion, we may say that the review was written in an attempt to look at the various approaches to describing metallic systems from a unified point of view. In doing so, we tried to demonstrate that even here "the opposites complement rather than exclude one another" (Niels Bohr).

REFERENCES

1. Vonsovskii, S.V. and Katsnel'son, M.I., *Quantum Solid-State Physics*, Berlin: Springer, 1989.
2. De Boer, J.H. and Verwey, E.J.W., Semiconductors with Partially and Completely Filled Bands, *Proc. Phys. Soc.*, 1937, vol. A49, pp. 59 - 67.
3. Mott, N.F., Metal–Insulator Transitions, London: Taylor and Francis, 1974; Mott, N.F., *Perekhod Metall–Izolyator*, Moscow: Nauka, 1979, Addenda of the Editor of the Translated Version.
4. Zel'dovich, Ya.B. and Landau, L.D., On the Relation between the Liquid and Gaseous States of Metals, *Zh. Eksp. Teor. Fiz.*, 1944, vol. 14, pp. 32 - 34.
5. Mott, N.F., The Basis of the Theory of Metals with Special Reference to the Transition Metals, *Proc. Phys. Soc.*, 1949, vol. A62, pp. 416 - 422.
6. Schubin, S.P. and Vonsovsky, S.V., On the Electron Theory of Metals, *Proc. Roy. Soc.*, 1934, vol. A145, pp. 159 - 180.
7. Schubin, S.P. and Wonsowsky, S.V., Zur Elektronentheorie der Metalle: I, *Phys. Z. UdSSR*, 1935, vol. 7, pp. 292 - 328.
8. Schubin, S.P. and Wonsowsky, S.V., Zur Elektronentheorie der Metalle: II, *Phys. Z. UdSSR*, 1936, vol. 10, pp. 348 - 377.
9. Shubin, S.P., *Izbrannye Trudy po Teoreticheskoi Fizike* (Selected Works on Theoretical Physics), Sverdlovsk, 1991.
10. Svirskii, M.S. and Vonsovskii, S.V., On the Possibility of the Spontaneous Ionization of Interacting Electrons in a Crystal, *Fiz. Met. Metalloved.*, 1957, vol. 4, pp. 392 - 399.
11. Vonsovskii, S.V., Svirskii, M.S., and Svirskaya, L.M., On the Theory of Spontaneous Ionization of a Crystal with Interacting Electrons: I. Polar Model: Hubbard I Approximation, *Phys. Met. Metallogr.*, 1992, vol. 74, no. 4, pp. 344 - 351.
12. Vonsovskii, S.V., Svirskii, M.S., and Svirskaya, L.M., On the Theory of Spontaneous Ionization of a Crystal with Interacting Electrons: II. The Polar Model: Allowance for the Effects of Transfer Processes, Electrostatic and Exchange Interaction of Electrons in Couples and in Neighboring Crystal Lattice Sites, *Phys. Met. Metallogr.*, 1992, vol. 74, no. 4, pp. 352 - 359.
13. Vonsovskii, S.V., Svirskii, M.S., and Svirskaya, L.M., On the Theory of Spontaneous Ionization of a Crystal with Interacting Electrons: III. Insulating and Conducting States, *Phys. Met. Metallogr.*, 1992, vol. 74, no. 6, pp. 565 - 572.
14. Slater, J.C., Magnetic Effects and the Hartree–Fock Equation, *Phys. Rev.*, 1951, vol. 82, pp. 538 - 541.
15. Slater, J.C., *The Self-Consistent Field for Molecules and Solids*, New York: McGraw-Hill, 1974.
16. Terakura, E., Oguchi, T., Williams, A.R., and Kübler, J., Band Theory of Insulating Transition Metal Monoxides: Band-Structure Calculations, *Phys. Rev. B*, 1984, vol. 30, pp. 4734 - 4748.
17. Anderson, P.W., The Resonating Valence Bond State in La_2CuO_4 and Superconductivity, *Science*, 1987, vol. 235, pp. 1186 - 1193.
18. Heitler, W. and London, F., Wechselwirking von neutral Atom und Homeopolaren Bindung in Quantum Mechanik, *Z. Phys.*, 1927, vol. 44, pp. 455 - 468.
19. Bogolyubov, N.N., *Lektsii po Kvanotovoi Statistike* (Lectures on Quantum Statistics), Kiev: Radyanska Shkola, 1949.
20. Hubbard, J., Electron Correlations in Narrow Energy Bands: IV. The Atomic Representation, *Proc. Roy. Soc.*, 1965, vol. A285, pp. 542 - 560.
21. Hirsh, J.E., Superconductivity and Hydromagnetism, *Physica B*, 1990, vol. 163, pp. 291 - 298.
22. Vonsovsky, S.V. and Katsnelson, M.I., Some Types of Instabilities in the Electron Energy Spectrum of the Polar Model of the Crystal: I. The Maximum Polarity State, *J. Phys. C*, 1979, vol. 12, pp. 2042 - 2053.
23. Anderson, P.W., Fifty Years of the Mott Phenomenon: Insulators, Magnets, Solids, and Superconductors as Aspects of Strong-Repulsion Theory, Varenna Summer School Lectures, *Frontiers and Borderlines in Many-Particle Physics*, Amsterdam: North-Holland, 1988.
24. Oertel, L., Zur Theorie des Ferromagnetismus: II. *Z. Phys.*, 1937, vol. 10, pp. 758 - 765.
25. Brandow, H., Electronic Structure of Mott Insulators, *Adv. Phys.*, 1977, vol. 26, pp. 651 - 808.
26. Katsnelson, M.I. and Irkhin, V.Yu., Metal–Insulator Transition and Antiferromagnetism in the Ground State of the Hubbard Model, *J. Phys. C*, 1984, vol. 17, pp. 4291 - 4308.
27. Anderson, P.W., Limits on the Energy of the Antiferromagnetic Ground State, *Phys. Rev.*, 1951, vol. 83, p. 1260.
28. Vonsovsky, S.V. and Katsnelson, M.I., Some Types of Instabilities in the Electron Energy Spectrum of the Polar Model of the Crystal: II. The Criterion of Stability of a Metallic State, *J. Phys. C*, 1979, vol. 12, pp. 2055 - 2064; Vonsovskii, S.V. and Katsnel'son, M.I. The Metal–Insulator Criterion and Exciton States in Metals in the Polar Model of Solids, *Problemy Sovremennoi Fiziki* (Problems of Modern Physics), Leningrad: Nauka, 1980, pp. 233 - 245.
29. Barentzen, H., Ivanov, C.I., and Girardeau, M.D., Pair Theory of the Hubbard Hamiltonian: Variational Approach, *J. Phys. C*, 1987, vol. 20, pp. 4801 - 4821.

30. Lieb, E.H. and Wu, F.Y., Absence of Mott Transition in an Exact Solution of the Short-Range, One-Band Model in One Dimension, *Phys. Rev. Lett.*, 1968, vol. 20, pp. 1445 - 1448.
31. Harary, F. and Palmer, E., *Graphical Enumeration*, New York: Academic, 1973.
32. Irkhin, V.Yu. and Katsnelson, M.I., On the Description of Antiferromagnetism without Anomalous Averages, *Z. Phys. B*, 1986, vol. 62, pp. 201 - 205.
33. Halperin, B.I. and Rice, T.M., The Electronic State of the Semiconductor Semimetal Transition, *Solid Sate Physics*, New York: Academic, 1968, vol. 21, pp. 116 - 192.
34. Peierls, R.E., *Quantum Theory of Solids*, Oxford: Clarendon, 1955.
35. Kotliar, G. and Ruckenstein, A.E., New Functional Integral Approach to Strongly Correlated Fermi Systems: The Gutzwiller Approximation as a Saddle Point, *Phys. Rev. Lett.*, 1986, vol. 57, pp. 1362 - 1365.
36. Svane, A. and Gunnarsson, O., Localization in the Self-Interaction-Corrected Density-Functional Formalism, *Phys. Rev. B*, 1988, vol. 37, pp. 9919 - 9922; Antiferromagnetic Moment Formation in the Self-Interaction-Corrected Density-Functional Formalism, *Europhys. Lett.*, 1988, vol. 7, pp. 171 - 175.
37. Svane, A. and Gunnarsson, O., Transition-Metal Oxides in the Self-Interaction-Corrected Density-Functional Formalism, *Phys. Rev. Lett.*, 1990, vol. 65, pp. 1148 - 1151.
38. Jones, R.O. and Gunnarsson, O., The Density-Functional Formalism, Its Applications and Prospects, *Rev. Mod. Phys.*, 1989, vol. 61, pp. 689 - 746.
39. Anisimov, V.I. and Gunnarsson, O., Density-Functional Calculations of Effective Coulomb Interactions in Metals, *Phys. Rev. B*, 1991, vol. 43, pp. 7570 - 7574.
40. Anisimov, V.I., Zaanen, J., and Andersen, O.K., Band Theory and Mott Insulators: Hubbard U instead of Stoner I, *Phys. Rev. B*, 1991, vol. 44, pp. 943 - 952.
41. Irkhin, V.Yu., Katsnel'son, M.I., and Trefilov, A.V., Nonquasiparticle States and the Character of the Electronic Spectrum in Iron and Nickel, *Pis'ma Zh. Eksp. Teor. Fiz.*, 1991, vol. 53, pp. 351 - 354.
42. Hermsmeier, B. Osterwalder, J., Friedman, D.J., and Fadley, C.S., Evidence for a High-Temperature Short-Range Magnetic-Order Transition in Mn (001), *Phys. Rev. Lett.*, 1989, vol. 62, pp. 478 - 481.
43. *Magnetic Properties of Layered Transition Metal Compounds*, De Jongh, J., Ed, Dordrecht: Kluver, 1990.
44. Izyumov, Yu.A. and Skryabin, Yu.N., *Statisticheskaya Mekhanika Magnitnykh Sistem* (Statistical Mechanics of Magnetic Systems), Moscow: Nauka, 1987.
45. Ruelle, D., *Statistical Mechanics: Rigorous Results*, New York: Benjamin, 1969.
46. Polyakov, A.M., Interaction of Goldstone Particles in Two Dimensions: Applications to Ferromagnets and Massive Yang-Mills Fields, *Phys. Lett. B*, 1975, vol. 59, pp. 79 - 81.
47. Chakravarty, S., Halperin, B.I., and Nelson, D.R., Two-Dimensional Quantum Heisenberg Antiferromagnets at Low Temperatures, *Phys. Rev. B*, 1989, vol. 39, pp. 2344 - 2371.
48. Arovas, P. and Auerbach, A., Functional Integral Theories of Low Dimensional Quantum Heisenberg Models, *Phys. Rev. B*, 1988, vol. 38, pp. 316 - 332.
49. Yoshioka, D., Boson Mean Field Theory of the Square Lattice Heisenberg Model, *J. Phys. Soc. Jpn.*, 1989, vol. 58, pp. 3733 - 3745.
50. Takahashi, M., Modified Spin-Wave Theory of a Square-Lattice Antiferromagnet, *Phys. Rev. B*, 1989, vol. 40, pp. 2494 - 2501.
51. Irkhin, V.Yu. and Katsnelson, M.I., Current Carriers in a Quantum Two-Dimensional Heisenberg Antiferromagnet, *J. Phys.: Condens. Matter*, 1991, vol. 3, pp. 6439 - 6453.
52. Irkhin, V.Yu., Katanin, A.A., and Katsnelson, M.I., Short-Range Order above T_N in Quasi-Two-Dimensional Heisenberg Antiferromagnet, *Phys. Lett. A*, 1991, vol. 157, pp. 295 - 298.
53. Irkhin, V.Yu., Katanin, A.A., and Katsnelson, M.I., On the Self-Consistent Spin-Wave Theory of Frustrated Heisenberg Antiferromagnets, *J. Phys.: Condens. Matter*, 1992, vol. 4, pp. 5227 - 5237.
54. Hubbard, J., Electron Correlations in Narrow Energy Bands: III. An Improved Solution, *Proc. Roy. Soc.*, 1964, vol. A281, pp. 401 - 419.
55. Cyrot, M., Phase Transition in Hubbard Model, *Phys. Rev. Lett.*, 1970 vol. 25, pp. 871 - 874.
56. Zaitsev, R.O., Mott Transition in the Multidimensional Hubbard Model, *Zh. Eksp. Teor. Fiz.*, 1978, vol. 75, pp. 2362 - 2374.
57. Arai, T. and Cohen, M.H., Functional-Derivative Study of the Hubbard Model: III. Fully Renormalized Green's Function, *Phys. Rev. B*, 1980, vol. 21, pp. 3300 - 3308; Stability of the Split-Band Solution and Energy Gap in the Narrow-Band Region of the Hubbard Model, *Phys. Rev. B*, 1980, vol. 21, pp. 3309 - 3319; Quasiparticle Excitations, the Relaxation and Transport Properties in the Narrow Band Region of the Hubbard Model, *Phys. Rev. B*, 1980, vol. 21, pp. 3320 - 3333.
58. Gutzwiller, M.B., Correlation of Electrons in a Narrow *s* Band, *Phys. Rev. A*, 1965, vol. 137, pp. 1726 - 1735.
59. Vollhardt, D., Normal ^{3}He: An Almost Localized Fermi Liquid, *Rev. Mod. Phys.*, 1984, vol. 56, pp. 99 - 120.
60. Florencio, J. and Chao, K.A., Theory of Itinerant Antiferromagnetism: Zero-Temperature Properties, *Phys. Rev. B*, 1976, vol. 14, pp. 3121 - 3129.
61. Hirsh, J.E., Renormalization-Group Study of the Hubbard Model, *Phys. Rev. B*, 1980, vol. 22, pp. 5259 - 5266.
62. Anokhin, A.O., Irkhin, V.Yu., and Katsnelson, M.I., On the Theory of Mott Transition in the Paramagnetic State, *J. Phys.: Condens. Matter*, 1991, vol. 3, pp. 1475 - 1491.
63. Hubbard, J., Electron Correlations in Narrow Energy Bands, *Proc. Roy. Soc.*, 1963, vol. A276, pp. 238 - 257.
64. Zubarev, D.N., Two-Time Green's Functions in Statistical Physics, *Sov. Phys. Usp. (Engl. Transl.)*, 1960, vol. 3, p. 320.
65. Elliott, R.J., Krumhansl, J.A., and Leath, P.L., The Theory and Properties of Randomly Disordered Crystals and Related Physical Systems, *Rev. Mod. Phys.*, 1974, vol. 46, pp. 465 - 544.
66. Edwards, D.M. and Hertz, J.A., The Breakdown of Fermi Liquid Theory in the Hubbard Model, *Physica B*, 1990, vol. 163, pp. 527 - 529; Edwards, D.M., The Breakdown of Fermi Liquid Theory in the Hubbard Model II, *J. Phys.: Condens. Matter*, 1993, vol. 5, pp. 161 - 170.
67. Brinkman, W.F. and Rice, T.M., Application of Gutzwiller's Variational Method to the Metal-Insulator Transition, *Phys. Rev. B*, 1970, vol. 2, pp. 4302 - 4304.
68. Chao, K.A. and Berggren, K.F., Gutzwiller Theory of Electron Correlation at Finite Temperature, *Phys. Rev. B*, 1977, vol. 15, pp. 1656 - 1668.
69. Ogawa, T. and Kanda, K., Lattice Statistical Aspects of Electron Correlation Problems, *Z. Phys. B*, 1978, vol. 30, pp. 355 - 366.
70. Takano, H. and Okiji, A., Magnetic Structure of the Ground State of the Hubbard Model, *J. Phys. Soc. Jpn.*, 1981, vol. 50, pp. 2891 - 2899.
71. Abrikosov, A.A., Gor'kov, L.P., and Dzyaloshinskii, I.E., *Metody Kvantovoi Teorii Polya v Statisticheskoi Fizike* (Methods of Quantum Field Theory in Statistical Physics), Moscow: Fizmatgiz, 1962.
72. March, N.H., Suzuki, M., and Parinello, M., Phenomenological Theory of First- and Second-Order Metal–Insulator Transitions at Absolute Zero, *Phys. Rev. B.*, 1979, vol. 19, pp. 2027 - 2029.
73. Landau, L.D., Fermi Liquid Theory, *Zh. Eksp. Teor. Fiz.*, 1956, vol. 30, pp. 1058 - 1068; Vibrations of Fermi Liquid, *Zh. Eksp. Teor. Fiz.*, 1958, vol. 32, pp. 59 - 66.
74. Jarrett, H.S., Cioud, W.H., Bouchard, H.J., *et al.*, Evidence for Itinerant *d* Electron Ferromagnetism, *Phys. Rev. Lett.*, 1968, vol. 21, pp. 617 - 620.
75. Nagaoka, Y., Ferromagnetism in a Narrow, Almost Half-Filled Band, *Phys. Rev.*, 1966, vol. 147, pp. 392 - 405.
76. Irkhin, V.Yu. and Katsnel'son, M.I., Charge Carriers in a Narrow-Band Hubbard Ferromagnetic in the Spin-Wave Temperature Range, *Fiz. Tverd. Tela*, 1983, vol. 25, pp. 3383 - 3388; Spin Waves in Narrow-Band Ferromagnets, *J. Phys. C.*, 1985, vol. 18, pp. 4173 - 4188.
77. Kittel, C., *Quantum Theory of Solids*, New York: J. Wiley & Sons, 1963.
78. Vonsovskii, S.V. and Katsnel'son, M.I., The One-Electron Density Matrix and the Metal-Nonmetal Criterion for Crystalline Solids, *Sov. Phys. Usp. (Engl. Trans.)*, 1989, vol. 32(8), pp. 720 - 722.
79. Edwards, D.M. and Hertz, J.A., Electron–Magnon Interactions in Itinerant Ferromagnetism: 2. Strong Ferromagnetism, *J. Phys. F: Metal Phys.*, 1973, vol. 3, pp. 2191 - 2205.
80. Irkhin, V.Yu. and Katsnelson, M.I., Ground State and Electron-Magnon Interactions in Itinerant Ferromagnets: Half-Metallic Ferromagnets, *J. Phys.: Condens. Matter*, 1990, vol. 2, pp. 7151 - 7171.
81. Auslender, M.I., Irkhin, V.Yu., and Katsnelson, M.I., Itinerant Electron Ferromagnetism in Narrow Energy Bands, *J. Phys. C*, 1988, vol. 21, pp. 5521 - 5571.
82. Folkerts, W., Sawatzky, G.A., Hass, C., de Groot, R.A., and Hillebrecht, F.V., Electronic Structure of Some 3*d* Transition-Metal Pyrites, *J. Phys. C.*, 1987, vol. 20, pp. 4135 - 4144.
83. Kanamori, J., Electron Correlation and Ferromagnetism of Transition Metals, *Prog. Theor. Phys.*, 1963, vol. 30, pp. 275 - 289.
84. Tyablikov, S.V., *Metody Kvantovoi Teorii Magnetizma* (Methods of Quantum Magnetism Theory), Moscow: Nauka, 1965.
85. Visscher, P.B., High-Temperature Thermodynamics of the Hubbard Model: An Exact Numerical Solution, *Phys. Rev. B*, 1974, vol. 10, pp. 932 - 942; Phase Separation Instability in the Hubbard Model, *Phys. Rev. B*, 1974, vol. 10, pp. 943 - 945.
86. Auslender, M.I. and Katsnel'son, M.I., The Effective Spin Hamiltonian and Phase Separation in the Almost Half-Filled Hubbard Model and the Narrow-Band Model, *Teor. Mat. Fiz.*, 1982, vol. 51, pp. 436 - 444.
87. Krivoglaz, M.A., Fluctuon States of Electrons, *Usp. Fiz. Nauk*, 1973, vol. 111, pp. 617 - 654.
88. Nagaev, E.L., *Fizika Magnitnykh Poluprovodnikov* (Physics of Magnetic Semiconductors), Moscow: Nauka, 1979.
89. Nagaev, E.L., Heavily Doped Magnetic Semiconductors, *Redkozemel'nye Poluprovodniki* (Rare-Earth Semiconductors), Leningrad: Nauka, 1977, pp. 48 - 81.
90. Auslender, M.I. and Katsnel'son, M.I., Interaction of a Conduction Electron with Critical Spin Density Fluctuations in the *s–f* Exchange Model of Magnetic Semiconductors: An Estimate of Free Energy and Static Conductivity, *Teor. Mat. Fiz.*, 1980, vol. 24, pp. 261 - 272; Magnetic Susceptibility of the Spin Polaron States in the *s–f* Exchange Model above Curie Temperature, *J. Magn. Magn. Mater.*, 1981, vol. 24, pp. 117 - 124; Asymptotics of the Density of States for Electrons Interacting with Critical Order Parameter Fluctuations, *Dokl. Akad. Nauk SSSR*, 1982, vol. 265, pp. 601 - 604.
91. Khomskii, D.I., Electronic Correlations in Narrow Bands: The Hubbard Model, *Fiz. Met. Metalloved.*, 1970, vol. 29, pp. 31 - 57.
92. Vonsovskii, S.V., On the Quantum Theory of Ferromagnetism, *Izv. Akad. Nauk SSSR, Ser. Fiz.*, 1952, vol. 16, pp. 387 - 398.
93. Ziman, J.M., *Models of Disorder: The Theoretical Physics of Homogeneously Disordered Systems*, Cambridge: Cambridge University, 1979.
94. Abu-Chacra, R., Anderson, P.W., and Thouless, D.J., A Self-Consistent Theory of Localization, *J. Phys. C.*, 1973, vol. 6, pp. 1734 - 1752.
95. Katsnel'son, M.I., The Coupled State of an "Excess" Electron and a Spin Wave in a Ferromagnetic Chain, *Fiz. Met. Metalloved.*, 1982, vol. 54, pp. 396 - 398.
96. Kane, C.L., Lee, P.A., and Read, N., Motion of a Single Hole in a Quantum Antiferromagnet, *Phys. Rev. B*, 1989, vol. 39, pp. 6880 - 6897.
97. Von Szczepanski, K.J., Horsch, P., Stephan, W., and Ziegler, M., Single-Particle Excitations in a Quantum Antiferromagnet, *Phys. Rev. B*, 1990, vol. 41, pp. 2017 - 2026; Martinez, G. and Horsch, P., Spin Polarons in the *t–J* Model, *Phys. Rev. B*, 1990, vol. 44, pp. 317 - 331.
98. Schulz, H.J., Correlation Exponents and the Metal-Insulator Transition in the One-Dimensional Hubbard Model, *Phys. Rev. Lett.*, 1990, vol. 64, pp. 2831 - 2834.
99. Anderson, P.W., "Luttinger-Liquid" Behavior of the Normal Metallic State in the 2D Hubbard Model, *Phys. Rev. Lett.*, 1990, vol. 64, pp. 1839 - 1841.

100. Mahan, G., *Many-Particle Physics*, New York: Plenum, 1981.
101. Wen, X.G., Metallic Non-Fermi Liquid Fixed Point in Two and Higher Dimensions, *Phys. Rev. B*, 1990, vol. 42, pp. 6623 - 6627; Anderson, P.W., Confinement in the One-Dimensional Hubbard Model: Irrelevance of Single-Particle Hopping, *Phys. Rev. Lett.*, 1991, vol. 67, pp. 3844 - 3847.
102. Fukuyama, H., Narikiya, O., and Hasegawa, Y., Non-Fermi Liquid State in Two-Dimensional Hubbard State, *Tech. Rep. ISSP A*, 1990, no. 234.
103. Anokhin, A.O., Irkhin, V.Yu., and Katsnelson, M.I., On the Effect of Strong Electron Correlations on Various Superconductivity Mechanisms, *Physica C*, 1991, vol. 179, pp. 167 - 175.
104. Anderson, P.W., *Theory of the Excitation Spectrum of the "Normal" Metal in Cuprate Superconductors: Fit to Experiment and Demonstration of Enhanced Pair Susceptibility*, Princeton (Preprint), 1990.
105. Massido, S., Posternak, M., and Baldereschi, A., Unrestricted Hartree–Fock Approach to the Insulating Behavior of Antiferromagnetic $CaCuO_2$, *Phys. Rev. B*, 1992, vol. 46, pp. 11705 - 11708.
106. Brooks, M.S.S., Johansson, B., and Skriver, H.L., Electronic Structure and Bulk Ground-State Properties of the Actinides, *Handbook on the Physics and Chemistry of the Actinides*, Freeman, A.J. and Lander, G.H., Eds., Amsterdam: North-Holland, 1984, vol. 1, ch. 3.
107. Katsnel'son, M.I., Solov'ev, I.V., and Trefilov, A.V., Alpha–Delta Transition in Plutonium as a Mott Transition in the *f* Subsystem, *Pis'ma Zh. Eksp. Teor. Fiz.*, 1992, vol. 56, pp. 276 - 279.
108. Vonsovskii, S.V., *Magnetizm* (Magnetism), Moscow: Nauka, 1971; Vonsovskii, S.V., *Magnetism*, New York: J. Wiley & Sons, 1974, vol. II.
109. Fulde, P. and Loewenhaupt, M., Magnetic Excitations in Crystal-Field Split 4*f* Systems, *Adv. Phys.*, 1985, vol. 34, pp. 589 - 662.
110. Gurtovoi, K.G. and Levitin, R.Z., Magnetism of the Actinides and Their Compounds, *Usp. Fiz. Nauk*, 1987, vol. 153, pp. 193 - 232.
111. Khomskii, D.I., The Problem of Intermediate Valence, *Usp. Fiz. Nauk*, 1979, vol. 129, pp. 443 - 485.
112. Lawrence, J.M., Riseborough, P.S., and Parks, R.D., Valence Fluctuation Phenomena, *Rep. Prog. Phys.*, 1981, vol. 44, pp. 1 - 84.
113. Moruzzi, V.L., Janak, J.F., and Williams, A.R., *Calculated Electronic Properties of Metals*, New York: Plenum, 1978.
114. Papacostantopoules, D.A., *Handbook of Band Structure of Elemental Solids*, New York: Plenum, 1986.
115. Johansson, B., The α–γ Transition in Cerium is a Mott Transition, *Philos. Mag. A*, 1974, vol. 30, pp. 469 - 482.
116. Lipkin, H., *Quantum Mechanics: New Approaches to Selected Topics*, Amsterdam: North-Holland, 1973, Ch. 8.
117. Kasuya, T., Takegahara, K., Fujita, T., Tanaka, T., and Bannai, E., Valence Fluctuating State in SmB_6, *J. Phys., Colloq. C5*, 1979, vol. 40, pp. 308 - 313.
118. Travaglini, G. and Wachter, P., Intermediate-Valent SmB_6 and the Hybridization Model: An Optical Study, *Phys. Rev. B*, 1984, vol. 30, pp. 893 - 898.
119. Travaglini, G. and Wachter, P., Low-Energy Electronic Structure of Intermediate-Valence "Golden" SmS, *Phys. Rev. B*, 1984, vol. 30, pp. 5877 - 5883.
120. Wachter, P., TmSe and Its Alloys, *J. Magn. Magn. Mater.*, 1985, vols. 31 - 34, pp. 439 - 442.
121. Amato, A. and Sierro, J., Magneto-Thermopower of TmS and TmSe, *J. Magn. Magn. Mater.*, 1985, vols. 47 - 48, pp. 475 - 477.
122. Kasaya, M., Ida, F., Nagishi, K., Nakai, S., and Kasuya, T., A New and Typical Valence Fluctuating System YbB_{12}, *J. Magn. Magn. Mater.* 1985, vols. 31 - 34, pp. 437 - 438.
123. Kasaya, M., Ida, F., Takigawa, M., and Kasuya, T., Mixed Valence Properties of YbB_{12}, *J. Magn. Magn. Mater.*, 1985, vols. 47 - 48, pp. 429 - 435.
124. Wachter, P., Marabelli, F., and Bucher, B., Plutonium Chalcogenides: Intermediate Valence and Electronic Structure, *Phys. Rev. B*, 1991, vol. 43, pp. 11136 - 11143.
125. Wachter, P. and Travaglini, G., Intermediate Valence and the Hybridization Model: A Study of SmB_6, "Gold" SmS, and YbB_{12}, *J. Magn. Magn. Mater.*, 1985, vols. 47 - 48, pp. 423 - 428.
126. Al'tshuler, T.S., Mironov, V.N., Khaliullin, G.G., and Khomskii, D.I., EPR Detection of the Temperature Dependence of the Energy Gap in SmB_6, *Pis'ma Zh. Eksp. Teor. Fiz.*, 1984, vol. 40, pp. 28 - 30.
127. Sugiyama, K., Ohya, A., Date, M., *et al.*, Magnetic and Electron Properties of YbB_{12} under High Magnetic Field, *J. Magn. Magn. Mater.*, 1985, vol. 52, pp. 283 - 285.
128. Tsidil'kovskii, I.M., *Zonnaya Struktura Poluprovodnikov* (The Band Structure of Semiconductors), Moscow: Nauka, 1978.
129. Irkhin, V.Yu. and Katsnel'son, M.I., On the Theory of Intermediate-Valence Semiconductors, *Zh. Eksp. Teor. Fiz.*, 1986, vol. 90, pp. 1080 - 1084; Intermediate-Valence Semiconductors in a Magnetic Field, *Fiz. Tverd. Tela*, 1987, vol. 29, pp. 1461 - 1466.
130. Liu, S.H. and Ho, K.M., Effects of *d*–*f* Correlation on the Mixed-Valence Properties of Cerium Systems. The *f*-Band Problem, *Phys. Rev. B*, 1984, vol. 30, pp. 3039 - 3046.
131. Bardeen, J., Cooper, L.M., and Schrieffer, J., Theory of Superconductivity, *Phys. Rev.*, 1957, vol. 108, pp. 1175 - 1204.
132. Schlottmann, P., Simple Spinless Mixed-Valence Model: I. Coherent Hybridization States versus Virtual Bond States, *Phys. Rev. B*, 1980, vol. 22, pp. 613 - 621.
133. Berton, A., Chassy, Y., Cornut, B., *et al.*, Specific Heat Measurements of TmSe, *Phys. Rev. B*, 1981, vol. 23, pp. 3504 - 3510.
134. Irkhin, Yu.P., On the Possibility of Ferromagnetism in a Limited Temperature Range in Paramagnets with a Maximum $\chi(I)$, *Pis'ma Zh. Eksp. Teor. Fiz.*, 1981, vol. 33, pp. 122 - 125.
135. Lee, P.A., Rice, T.M., Serene, J.W., *et al.*, Theory of Heavy-Electron Systems, *Commun. Condens. Matter Phys.*, 1986, vol. 12, pp. 99 - 161.
136. Bassani, J.F. and Paravicini, P., *Electronic States and Optical Transitions in Solids*, Ballinger, R.A., Ed., Oxford: Pergamon, 1975.
137. Bader, S.D., Philips, N.E., and McWhan, D.B., Heat Capacity and Resistivity of Metallic SmS at High Pressure, *Phys. Rev. B*, 1973, vol. 7, pp. 4686 - 4688.
138. Stewart, G.R., Heavy-Fermion Systems, *Rev. Mod. Phys.*, 1984, vol. 56, pp. 755 - 787.

139. Fulde, P., Introduction to the Theory of Heavy Fermions, *J. Phys. F*, 1988, vol. 18, pp. 601 - 639.
140. Proc. of the Int. Conf. on Anomalous Rare Earths and Actinides, Grenoble, *J. Magn. Magn. Mater.*, 1987, vols. 63 - 64.
141. Marabelli, F. and Wachter, P., Electronic Structure and Magnetic Properties of Heavy Fermions, *J. Magn. Magn. Mater.*, 1987, vol. 70, pp. 364 - 368.
142. Zwicknagl, G., Quasiparticles in Heavy-Fermion Systems, *Adv. Phys.*, 1992, vol. 41, pp. 203 - 302.
143. Gunnarsson, O. and Schönhammer, K., Electron Spectroscopies for Ce Compounds in the Impurity Model, *Phys. Rev. B*, 1983, vol. 28, no. 8, pp. 4315 - 4321.
144. Lenz, D., Schmidt, H., Ewert, S., *et al.*, The Anomalous Bulk Modulus of $CeBe_{13}$, *Solid State Commun.*, 1984, vol. 52, pp. 759 - 763.
145. Brovman, E.T. and Kagan, Yu.M., Phonons in Nontransition Metals, *Usp. Fiz. Nauk*, 1974, vol. 112, pp. 369 - 387.
146. Geilikman, B.T., *Issledovaniya po Fizike Nizkikh Temperatur* (Studies in Low-Temperature Physics), Moscow: Atomizdat, 1979.
147. Kondo, J., Theory of Dilute Magnetic Alloys, *Solid State Phys.*, 1969, vol. 23, pp. 184 - 283.
148. Grüner, G. and Zawadowski, A., Magnetic Impurities in Nonmagnetic Metals, *Rep. Progr. Phys.*, 1974, vol. 37, pp. 1497 - 1583.
149. Tsvelick, A.M. and Wiegman, P.B., Exact Results in the Theory of Magnetic Alloys, *Adv. Phys.*, 1983, vol. 32, pp. 453 - 471.
150. Nozieres, P., A "Fermi-Liquid" Description of the Kondo Problem at Low Temperatures, *J. Low-Temp. Phys.*, 1974, vol. 17, pp. 31 - 42.
151. Coleman, P., Mixed Valence as an Almost Broken Symmetry, *Phys. Rev. B*, 1987, vol. 35, pp. 5072 - 5116.
152. Vonsovskii, S.V., On Exchange Interaction of Outer- and Inner-Shell Electrons in Ferromagnetic (Transition) Metals, *Zh. Eksp. Teor. Fiz.*, 1946, vol. 16, pp. 981 - 996.
153. Vonsovskii, S.V. and Turov, E.A., On Exchange Interaction of Outer- and Inner-Shell Electrons in the Crystal (the *s*–*d* Exchange Model of the Transition Metals), *Zh. Eksp. Teor. Fiz.*, 1953, vol. 24, pp. 419 - 428.
154. Coleman, P. and Andrew, N., Kondo-Stabilized Spin Liquids and Heavy-Fermion Superconductivity, *J. Phys.: Condens. Matter*, 1987, vol. 1, pp. 4057- 4080.
155. Moshchalkov, V.V. and Brandt, N.V., Nonmagnetic Kondo Lattices, *Usp. Fiz. Nauk*, vol. 149, pp. 585 - 634.
156. Irkhin, V.Yu. and Katsnel'son, M.I., The Problem of Kondo Magnets, *Fiz. Met. Metalloved.*, 1991, no. 1, pp. 16 - 33.
157. Aeppli, G., Bucher, E., Broholm, C., *et al.*, Magnetic Order and Fluctuations in Superconducting UPt_3, *Phys. Rev. Lett.*, 1988, vol. 60, pp. 615 - 618.
158. Proc. of the 6th Int. Conf. on Crystal-Field Effects and Heavy-Fermion Physics, Frankfurt, *J. Magn. Magn. Mater.*, 1988, vols. 76 - 77.
159. Jaccard, D., Sierro, J., Brison, J.P., and Floquet, J., Transport Properties of Heavy Electron Metals, *J. de Phys., C8*, 1988, vol. 49, pp. 741 - 746.
160. Kleiman, R.N., Bishop, D.J., Ott, K.H., *et al.*, Observation of Magnetic Order in the Heavy-Fermion Superconductor UBe_{13}, *Phys. Rev. Lett.*, 1990, vol. 64, pp. 1975 - 1978.
161. Gangopadhayay, A.K., Schilling, J.S., Schubert, E., *et al.*, Incipient Magnetic Order in $CeCu_6$, *Phys. Rev. B*, vol. 38, pp. 2603 - 2607.
162. Mori, H., Yashima, H., and Sato, N., A New Dense Kondo System $Ce_yLa_{1-y}Ge_2$: Resistivity, Specific Heat, and Susceptibility, *J. Low-Temp. Phys.*, 1985, vol. 58, pp. 513 - 532.
163. Nieva, G.L., Serene, J.C., Afyoni, M., *et al.*, From Ferromagnetic to Nonmagnetic Ground State in $CePd_{1-x}Ni_x$, *Z. Phys. B*, 1987, vol. 70, pp. 181 - 186.
164. Thompson, J.B., Fisk, Z., and Ott, H.R., Response of Uranium-Based Heavy-Fermion Magnets to Hydrostatic Pressure, *J. Magn. Magn. Mater.*, 1986, vols. 54 - 57, pp. 393 - 399.
165. Gignoux, D., Schmits, D., Zerguine, M., *et al.*, Magnetic Properties and Magnetic Structures of $CeAl_2Ga_2$, *J. Magn. Magn. Mater.*, 1988, vol. 74, pp. 1 - 6.
166. Broholm, G., Kjeme, J.K., Aeppli, G., *et al.*, Spin Fluctuations in the Antiferromagnetic Heavy-Fermion System, *Phys. Rev. Lett.*, 1987, vol. 58, pp. 917 - 920.
167. Irkhin, V.Yu. and Katsnelson, M.I., Kondo Effect, Spin Dynamics, and Magnetism in Anomalous Rare-Earth and Actinide Compounds, *Z. Phys. B*, 1989, vol. 75, pp. 67 - 76.
168. Irkhin, Yu.P., The *s*–*d* Hybridization and Paramagnetic Susceptibility of the Transition Metals, *Pis'ma Zh. Eksp. Teor. Fiz.*, 1986, vol. 32, pp. 205 - 209.
169. Dhar, S.K., Gschneidner, K.A. Jr, and Lee, W.H., Spin-Fluctuation Effects in $CeSi_x$ Alloys: High-Field Heat Capacity, Magnetic Susceptibility, and Electric Resistivity Studies and a Comment on $TiBe_2$, *Phys. Rev. B*, 1987, vol. 36, pp. 341 - 345.
170. Desclaux, J.P. and Freeman, A.J., *Handbook on the Physics and Chemistry of the Actinides*, Amsterdam: North- Holland, Freeman, A.J. and Lander, G.H., Eds., 1984, vol. 1, ch. 1.
171. Irkhin, V.Yu. and Katsnel'son., M.I., Electron-Magnon Interaction in Itinerant Ferromagnets, *Fiz. Met. Metalloved.*, 1988, vol. 66, no. 1, pp. 41 - 52.
172. Irkhin, V.Yu. and Katsnelson, M.I., On the Mean-Field Theory of Magnetically Ordered Kondo Lattices, *J. Phys.: Condens. Matter*, 1991, vol. 3, pp. 8715 - 8720.
173. Irkhin, V.Yu. and Katsnelson, M.I., Kondo Effect, Spin Dynamics, and Magnetism in Anomalous Rare-Earth and Actinide Compounds: II. The Problem of the Ground State, *Z. Phys. B*, 1991, vol. 82, pp. 77 - 86.
174. Ochiai, A., Suzuki, T., and Kasuya, T., Kondo State in Sm_4X_3 (X = Bi, Se, and As), *J. Magn. Magn. Mater.*, 1985, vol. 52, pp. 13 - 17.
175. Vonsovsky, S.V., Irkhin, Yu.P., Irkhin, V.Yu., and Katsnelson, M.I., Temperature-Induced Ferromagnetism: Pyromagnetism, *J. de Phys., C8*, 1988, vol. 49, pp. 253 - 254.
176. Tsvyashchenko, A.V. and Krylov, V.I., The Mixed-Valence Magnetic Ground State of Eu Ions in the High-Pressure Synthesized Compound EuNi with the Laves Phase Structure, *J. Phys.: Condens. Matter*, 1990, vol. 2, pp. 4507 - 4512.
177. Anderson, P.W., Baskaran, G., Zou, Z., and Hsu, T., Resonating-Valence-Bond Theory of Phase Transitions and Superconductivity in La_2CuO_4-Based Compounds, *Phys. Rev. Lett.*, 1987, vol. 58, pp. 2790 - 2793.

178. Coleman, P., Some New Perspectives on Two-Dimensional Antiferromagnetism, *J. Magn. Magn. Mater.*, 1989, vol. 82, p. 168.

179. Sera, M., Fujita, T., Suzuki, T., and Kasuya, T., The Thermal Expansion and Magnetostriction in $Ce_{1-x}La_xBi$, *Valence Instabilities*, Amsterdam: North-Holland, 1982, pp. 435 - 438.

180. Shiga, M., Wada, H., and Nakamura, Y., Giant Spin Fluctuations in YMn_2 and Related Compounds, *J. de Phys., C8*, 1988, vol. 49, pp. 241 - 246.

181. Furuno, T., Ando, K., and Kunii, S., Physical Properties of Sm_3Se_4 at Low Temperature, *J. Magn. Magn. Mater.*, 1988, vols. 76 - 77, pp. 110 - 118.

182. Irkhin, V.Yu. and Katsnel'son, M.I., The RVB State in the Sm_3Se_4 System with Charge Degrees of Freedom, *Pis'ma Zh. Eksp. Teor. Fiz.*, 1989, vol. 49, pp. 500 - 502.

183. Nakamura, O., Oyamada, A., and Ochiai, A., Magnetic and Transport Properties in $Yb_4As_{2.7}P_{0.3}$, *J. Magn. Magn. Mater.*, 1988, vols. 76 - 77, pp. 293 - 254.

184. Irkhin, V.Yu. and Katsnelson, M.I., A Scaling Approach to the Theory of Magnetic Kondo Lattices, *J. Phys.: Condens. Matter*, 1992, vol. 4, pp. 9661 - 9672.

185. Anderson, P.W., A Poor Man's Derivation of Scaling Laws for the Kondo Problem, *J. Phys. C.*, 1970, vol. 3, pp. 2436 - 2441.

186. Gaudin, M., *La fonction d'onde de Bethe*, Paris: Masson, 1983.

187. Kagan, Yu.M., Kikoin, K.A., and Prokof'ev, N.V., Renormalization of the Effective Mass and the de Haas–Von Alphen Effect in Heavy-Fermion Systems, *Pis'ma Zh. Eksp. Teor. Fiz.*, 1992, vol. 56, pp. 221 - 232.

188. Katsnelson, M.I. and Vonsovsky, S.V., Possible Effect of Exciton Condensation on Properties of Ferromagnetic Materials, *J. Magn. Magn. Mater.*, 1980, vols. 15 - 18, pp. 275 - 276.

The Physics of Metals and Metallography, Vol. 76, No. 4, 1993.

THEORY OF METALS

Molecular-Dynamics Calculations of Phase Transitions in the Pd–D System and Cold Nuclear Fusion

S. A. Tsvetkov, N. B. Bondarenko, I. L. Bel'tyukov, A. N. Varaksin, and A. A. Zhivoderov

Ural Polytechnical Institute, Ekaterinburg, 620002 Russia

Received November 13, 1992

Abstract – This work is a continuation of the molecular-dynamics calculations that were performed earlier with the aim to validate the influence of the phase transitions in metal–deuterium systems on the course of the cold fusion reactions [1]. An attempt was made to determine the region in the phase diagram of the Pd–D system that is most "favorable" for cold nuclear fusion.

INTRODUCTION

A theoretical verification of the hypothesis [2] assuming the relation between the cold nuclear fusion (CNF) and phase transitions in palladium deuteride was performed earlier [1]. To validate the hypothesis by the molecular-dynamics method (MD), the phase transition in the Pd–D system was simulated at one temperature for a particular composition.

When modeling the phase transition at different temperatures and Pd–D compositions, the intensity of cold nuclear fusion is clearly determined by several competing factors. For example, the amplitude of thermal vibrations of Pd and D atoms increases with temperature, which must lead to a continuous enhancement of the intensity of CNF. However, according to [1], this intensity also depends on the difference between the Pd–D interaction potentials in α and β phases. As the temperature increases, this difference decreases and disappears completely at $T = T_{cr}$, which causes a decrease in the CNF intensity. In addition, the intensity of CNF is obviously dependent on the deuterium concentration n in palladium deuteride because the chance of close D–D approach is proportional to n. The search for optimum conditions (sufficient amplitude of atomic vibrations and sufficient difference in the interaction potentials) is the subject of this paper.

COMPUTATIONAL METHOD, RESULTS, AND DISCUSSION

We adapted the program for the calculations of the behavior of D atoms in Pd in phase transitions [1] to perform the calculations on personal computers; the results presented in this work were realized on an IBM PC/AT-286 computer.

Of the phase transition models realized in [1], we chose the β–α transition in a microcrystallite, one half of which consists of pure Pd and the second half, of palladium deuteride PdD_n (Fig. 1). The model was chosen on the basis of the previous calculations because, in this case, one of the MD calculations led to the maximum deuteron kinetic energy (>10 eV) and to the minimum D–D separation (0.7 Å).

Using this model, we carried out four MD calculations for the palladium microcrystallite with free boundaries, containing 10 × 10 × 10 Pd atoms, under the following conditions: the temperatures were taken to be 300, 350, 400, and 450 K; the [D]/[Pd] ratio in the

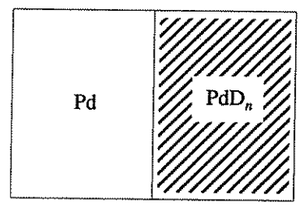

Fig. 1. Model microcrystallite used in calculations.

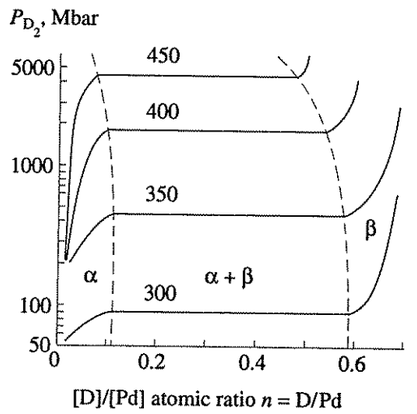

Fig. 2. Pressure-concentration phase diagram of the Pd–D system [3].